UNIVERSITÀ DEGLI STUDI DI MESSINA

DIPARTIMENTO DI SCIENZE CHIMICHE, BIOLOGICHE,

FARMACEUTICHE ED AMBIENTALI

DOTTORATO DI RICERCA IN SCIENZE CHIMICHE

DOCTOR OF PHILOSOPHY IN CHEMICAL SCIENCES

S.S.D. CHIM/10 CHIMICA DEGLI ALIMENTI

ADVANCED ANALYTICAL TECHNIQUES FOR THE CHARACTERIZATION OF COMPLEX FOOD PRODUCTS

PhD thesis of:
Yassine Oulad El Majdoub

Tutor:
Prof. Francesco Cacciola

Coordinator:
Prof. Concetta De Stefano

XXXV CICLO (2019-2022)

Preface

The present PhD thesis comprises the results of the accomplished research based on the development and application of conventional and innovative chromatographic techniques, and ambient mass spectrometry on different food matrices.

The herein applied analytical chemistry techniques have shown their efficiency to provide potentially advantageous information regarding traceability, authenticity and salubrity due to the presence of potentially beneficial compounds for human health in the studied matrices.

In particular, conventional liquid and gas chromatography were initially employed in a low-scale study in 2018, focused on the evaluation of the relationship between the geographic origin of virgin olive oils (VOOs) from 5 different Moroccan regions and their content in phenolic compounds, vitamin E, and fatty acid methyl esters (FAMEs). In 2018 and 2019, a similar study was conducted on extra virgin olive oils (EVOOs) in 19 Moroccan regions, including pedoclimatic factors. The achieved results were assessed through different chemometric analyses performed on both studies to discriminate olive oil, bioactive compounds, and different studied regions by clusters. The biological compounds (phenolic compounds, vitamin E, and fatty acid methyl esters) in EVOOs highlighted by different analytical techniques, may be considered as markers for the traceability and the salubrity of EVOOs in the studied Moroccan regions.

High-performance liquid chromatography coupled to mass spectrometry was also applied for the analysis of bioaccessible polyphenols of *Hibiscus sabdariffa* L. in simulated *in vitro* human digestion.

Finally, a chemical characterization of *Brassica juncea* L. extracts was also carried out by the employment of liquid and gas chromatography coupled with mass spectrometry.

The last part of the thesis shed light on the employment of ambient mass spectrometry, where rapid evaporative ionization mass spectrometry (REIMS) was employed, along with conventional liquid chromatography, for the discrimination of Moroccan *Lamiaceae* species.

I would like to acknowledge the National Operational Program on Research and Innovation (PON) for the valuable sustainment and funding of the research works and scientific contributions.

Yassine Oulad El Majdoub

Table of contents

CHAPTER 1

Advanced food analytical methods based on chromatographic and mass spectroscopic techniques

1.1 Hyphenated techniques in food analysis

The hyphenated techniques are derived from the combination between separation techniques and on-line spectroscopic detection system. During the recent past decades, hyphenated analytical methods have undergone remarkable improvements which have considerably enlarged their employments in the analysis of biological materials, particularly natural products, which are considered very complex matrices. Food matrices contain in addition to major constituents such as proteins, lipids, and carbohydrates, a comprehensive minor component including phenolic compounds, vitamins, pigments, and volatile compounds. Furthermore, food matrices may contain contaminants and other hazardous compounds under certain conditions. To acquire a thorough profile regarding the chemical composition of a complex food product, the following hyphenated techniques (**Figure 1.1**) e.g., CE-MS, GC-MS, LC-MS, and LC-NMR are largely employed.

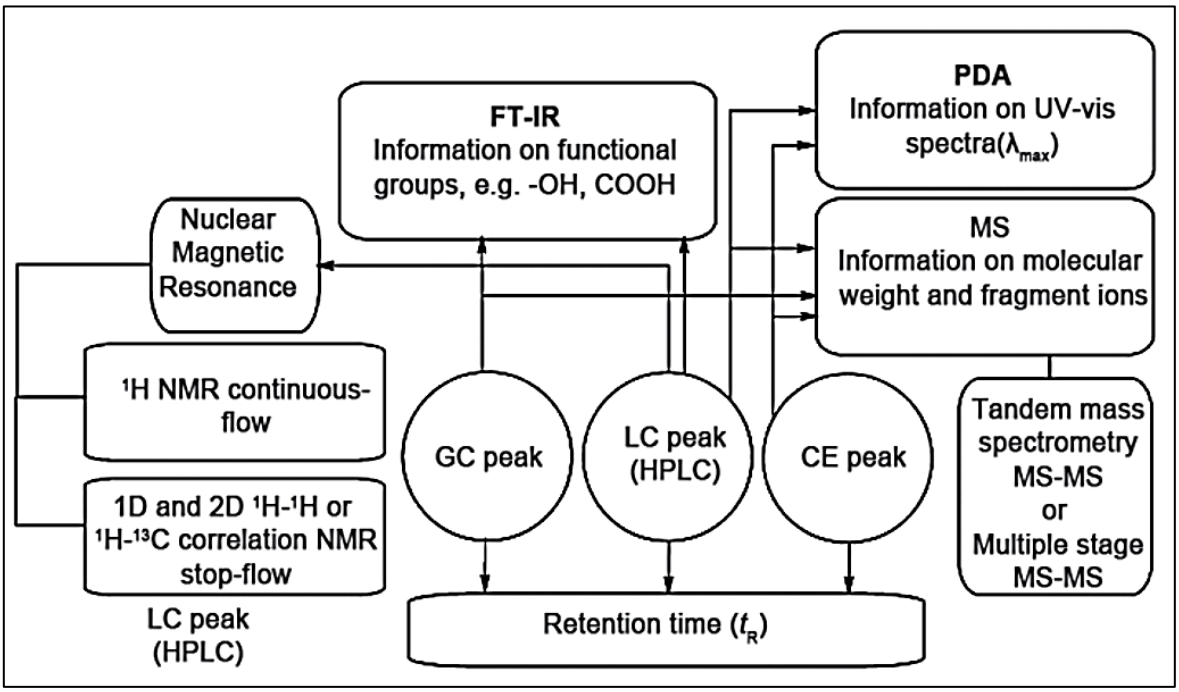

Figure 1.1. Hyphenated analytical techniques employed in food complex matrix [1].

HPLC is most employed separation technique for quantitative and qualitative characterization of unknown compounds in complex extracts or fractions of food products. Related

hyphenated techniques such as HPLC-MS and HPLC-NMR improve the sensitivity and specificity of the system resulting in a great capability of unknown compounds determination. Particularly, LC-MS technique allows the analysis of a wide range of polar and nonpolar constituents of food products, besides its application on a large scale of molecular weight, including proteins, oligosaccharides, and tannins. Recently, the multiple hyphenated technique LC-PDA-NMR-MS has also shown an increasing interest in the analysis of food product matrices.

There is no requirement that the hyphenation always occurs between only two techniques; in some instances, the coupling of separation and detection techniques may involve more than one separation or detection technique, such as, LC-PDA-MS, LC-MS-MS, LC-NMR-MS, and LC-PDA-NMR-MS. The on-line coupling of solid phase extraction (SPE) with solid-phase microextraction can be incorporated to create a more powerful integrated system, e.g., SPE-LC-MS, for trace analysis and analyte enrichment [1]. Nevertheless, when it comes to analyzing the most important natural and contaminant substances in food, the sample preparation process plays an important role in obtaining required parameters.

Regarding the analysis of lipids, it has been demonstrated that both LC–APCI-MS and LC–APPI-MS can be applied to the analysis of mixtures of neutral lipids, such as triacylglycerols and sterols. Where an appropriate choice of ionization source plays a powerful role in the analysis of large neutral lipids, which have turned out to be problematic by employing other techniques such as GC–MS and LC–ESI-MS [2,3]. On the other hand, LC–ESI-MS and LC–APCI-MS are the most suitable techniques for polar lipids analysis such as phospholipids. Whereas GC–EI-MS is chosen mainly for the analysis of acylglycerol and sterol fractions of lipids [2,3,4]. As regards the characterization of peptides and proteins, the prevalent hyphenated approaches appropriate proteomics include MALDI-TOF-MS and LC–ESI-MS. Where MALDI-TOF-MS represent an accurate and rapid technique allowing the acquirement of a fingerprint of the protein composition obtained from different food products. Moreover, tandem hyphenated techniques such as MALDI-TOF-TOF or LC–ESI-MS-MS allow the analysis of low-molecular mass peptides for the purpose of interpretation of the protein structure [5]. Hyphenated techniques are also applied in the analysis of saccharides. Where MALDI-TOF-MS MS techniques employing different ionization modes and the hyphenated techniques is of great importance to elucidate the structure of sugars. In addition, LC–MS supplied with fast atom bombardment (FAB) interface, has proven effective for accurate determination of saccharides isotopes and for their structural elucidation. GC-MS was also employed for the analysis of mono- and oligosaccharides after a required derivatization procedure to rend the compounds amenable with GC analysis [2]. GC–MS has shown a

substantial capacity in the analysis and determination of food volatile compounds. The ability of this method can be improved by the employment of solid phase microextraction (SPME) which stands for a sample preparation technique that extract and concentrate the volatile compounds. Over the last few years, GC–MS supplied with several analyzers, such as quadrupole and ion trap, consented the acquirement of information on volatile compounds [6]. In addition, the application of high-speed TOF mass analyzer combined with comprehensive two-dimensional (GCxGC) has been used as a tool for rapid and comprehensive analysis of these compounds [7,8]. Typically, Electron impact (EI) is favored for the analysis of volatile compounds, since it allows library searching based on the EI mass spectra. Chemical ionization (CI) is used mostly to confirm molecular weight (MW) of the compounds of interest. Worth noting that under certain conditions, the use of retention indexes is important for identification and confirmation of aroma and flavor compounds.

1.2 Multidimensional liquid chromatography

The development of liquid chromatography (LC) over many decades has led to recent technological advances (e.g., sub-2 μm and core−shell particles, high pressure, and lower dispersion instrumentation). However, one-dimensional liquid chromatography (1D-LC) often is unable to rapidly separate mixtures of interest, despite decades of development. Failures of 1D-LC typically involve two distinct types of problems: (A) mixtures that are excessively complex in a general sense (such as thousands of metabolites present in biological samples) and thus beyond the ability of 1D-LC to separate the mixture into distinct components (i.e., singlet peaks) (B) The mixtures do not necessarily contain complex compounds per se but contain several species of interest that are extremely difficult to resolve due to either the presence of too many compounds or the presence of closely related compounds (for example, enantiomers and structural isomers).

Two-dimensional liquid chromatography is an important addition to the family of liquid chromatography techniques, which includes one-dimensional isocratic and gradient elution LC. A multidimensional separation can offer a great improvement in resolving power over conventional one-dimensional liquid chromatography (1D-LC) when used appropriately.

Figure 1.1 shows the operational setup of a 2D-LC system and its relation to a 1D-LC system. The first dimension (^{1}D) column is used for conventional separations, which may be performed in an isocratic separation or a gradient elution separation. The effluent from the ^{1}D column is then transferred to a ^{2}D column with a very different separation selectivity than the 1D column in order to have any real impact on the overall chromatographic resolution of the samples.

In practice, the ^{2}D separation column and its associated detector perform chemical analysis on the effluent from the ^{1}D column. Due to the different selectivity of the second column from the first, there is a greater likelihood that peaks that are partially or totally overlapping neighbors on the ^{1}D column will separate on the ^{2}D column. The resolving power of the second dimension does not simply add to that of the first dimension, but actually multiplies it so long as there is no (or minimal) alteration of the compounds separated in the ^{1}D column during the sampling process.

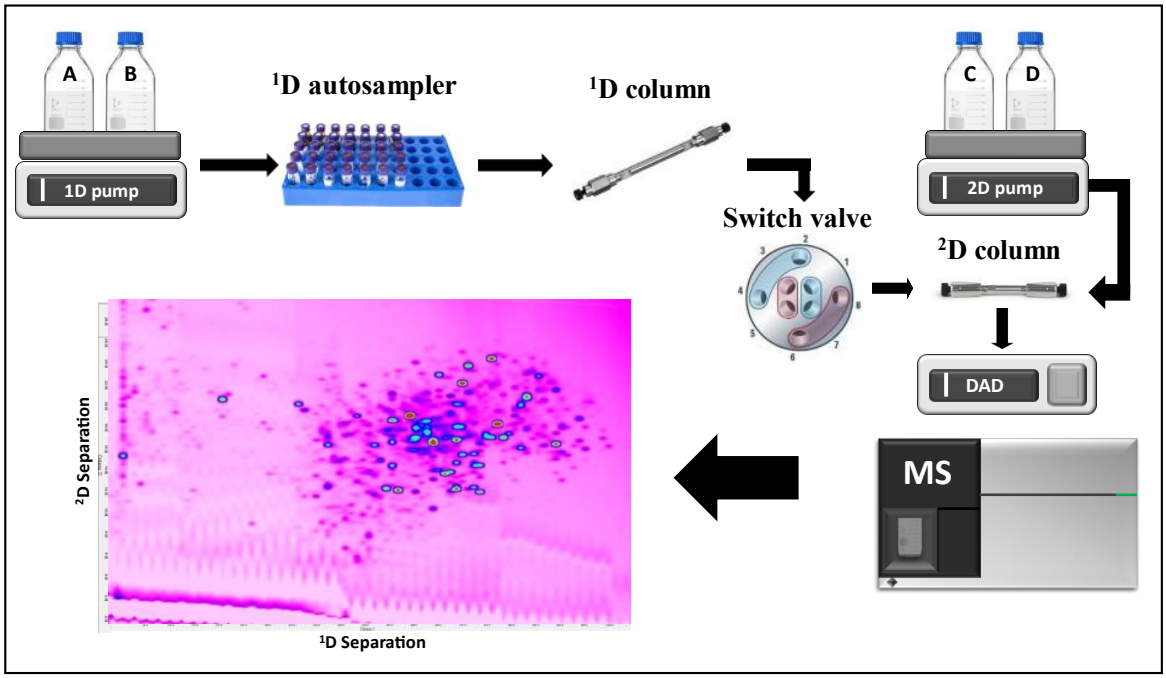

Figure 1.1. Schematic representation of two-dimensional liquid chromatography (2D-LC) technique.

1.2.1 Classification of 2D-LC

Temporal application

Based on temporal application 2D-LC can be classified in online and off-line forms. An online 2D-LC procedure consists of injecting effluent from the ^{1}D column into the ^{2}D column as soon as it is collected. In this form of 2D-LC, the process is fully automated and does not require any operator intervention at least until all of the data has been collected. Using an autosampler in the first dimension enables the analysis of multiple samples. The main limitation of online 2D-LC is that the theoretical maximum resolution is not as high as it would be in an offline mode. Nevertheless, the resolving power per unit run time is usually higher with online LCxLC than with offline LCxLC. As fractions of the ^{1}D effluent are immediately transferred from one column to another in online LCxLC, the analysis time of

the ^{2}D fraction must be equal to the sampling time. In order to keep the total 2D LC analysis time reasonable, this means that samples must be collected frequently and each 2D separation performed on a fast time scale. This in turn severely limits the resolution of any 2D separation. In the offline form of 2D-LC, fractions of the ^{1}D effluent are collected and stored before undergoing ^{2}D separation. This naturally leads to a longer total analysis time than with online chromatography; However, the 2D analysis time no longer needs to equal the sampling time and is usually much greater. As a result, a higher resolving power in the second dimension and thus an overall increase in the resolving power of the two-dimensional methodology can be achieved.

Since the ^{1}D separation in offline 2D-LC is in continuous run, storing samples until they undergo ^{2}D separation can result in the loss of some trace species in the collection vessel and the possibility of contamination or degradation, or both. Eluent may be removed in part or in whole depending on the operation. It is a much more tedious method than online LCxLC and frequently requires considerable operator attention. Hence, the manual steps required make it prone to errors.

There is an intermediate mode known as stop-flow. Usually, there is no sampling loop in this mode, as the fractions are directly transferred from the ^{1}D column to the head of the ^{2}D column. Fractions injected to the 2D column are analyzed while the flow in the 1D column is paused. As the 2D analysis time is not limited, the peak capacity of this approach is significantly increased. This method suffers from solvent compatibility issues as well as being more time consuming than the on-line approach.

Number of targeted peaks

The 2D-LC approach can be further divided into two forms: comprehensive (LC×LC) and heart cutting (LC-LC). A comprehensive LC×LC separation entails the separation of all effluent from the first column by a second column. The second column has a limited analysis time as each fraction must be removed from the column before the next fraction is injected to avoid mixing. This means that the second column is usually operated under ultra-high pressure (UHPLC) conditions, which can complicate the subsequent MS coupling. However, it allows full characterization of complex samples and is very popular for such applications.

In heart-cutting chromatography, peaks are selectively targeted, and a fraction of a given peak is collected and injected onto a second column. Heart-cutting 2D-LC is very useful for not too complex samples containing compounds with very similar retention behavior. The system and method set-up are typically less complex, and the cost of operation is lower compared to full 2D-LC. In addition, multiple peaks can be sampled from the first dimension for further separation in the second dimension, depending on the analysis time in the second dimension.

Multiple heart-cutting (mLC-LC) setups that employ more than one sampling loop might be recommended in order to sample more peaks from the first dimension without causing temporary overlap with the second-dimension analysis (**Figure 1.2**).

1.2.2 Theoretical aspects

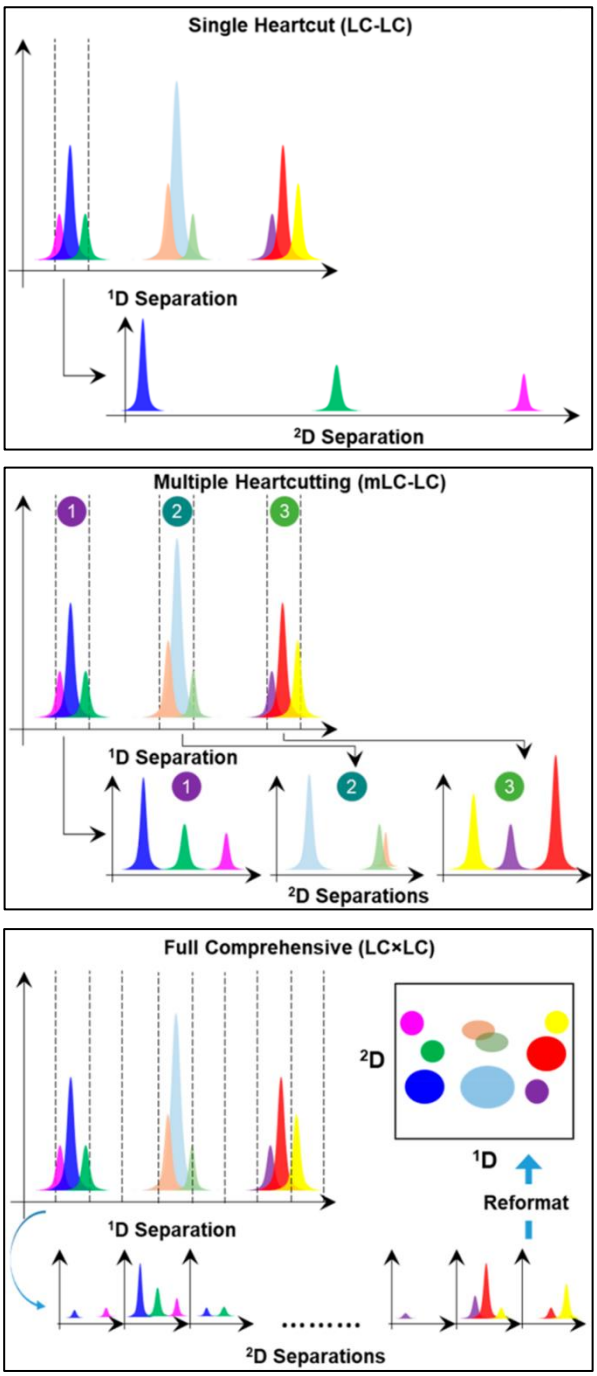

Figure 1.2. Different modalities of 2D LC analyses [9].

The separation efficiency of liquid chromatography under gradient conditions is well described by a peak capacity, which refers to the maximum number of peaks that can fit

within the separation window based on the time between the latest eluting peak and the earliest eluting peak [10]. According to Giddings, the two-dimensional comprehensive technique yields better results in terms of resolving power; in fact, he highlighted that the peak capacity can be considerably increased by coupling columns with different retention mechanisms (i.e., orthogonality) [11,12]. Ideally, for totally orthogonal systems, the total peak capacity is equal to the product of the peak capacity in the first and second dimensions (**Figure 1.3**):

$$n_{c,2D} = n_{c1} x\ n_{c2} \qquad \text{[Eq. 1]}$$

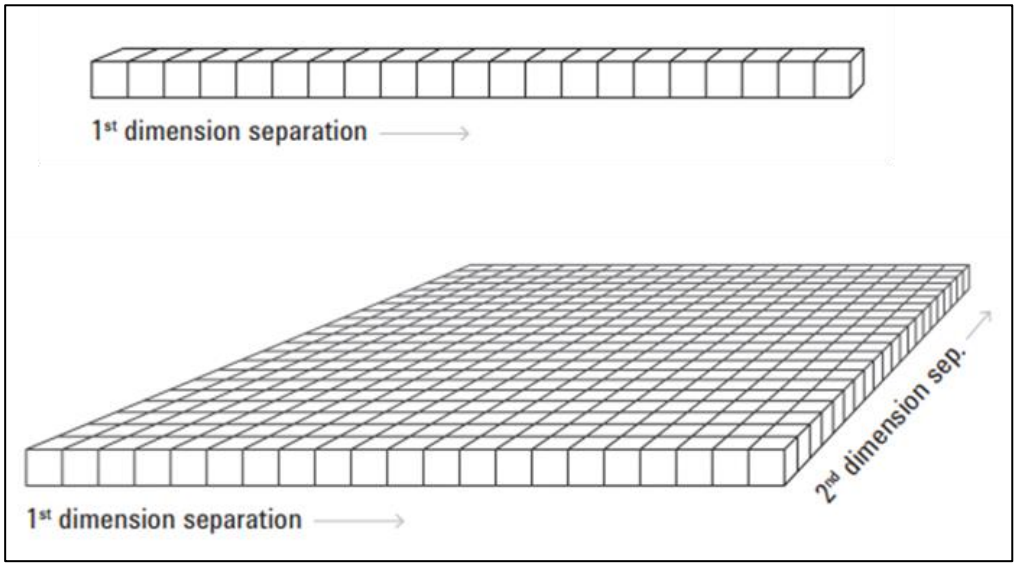

Figure 1.3. Schematic illustration of peak capacity in 2D-LC [13].

High resolution systems have a n_c value of several hundred, indicating the separation of about 100 peaks. To achieve a maximum resolving power, the separation of the peaks should occur at their maximum density, but in complex real samples it is a rare event considering the different coelutions and the random distribution of the peaks in the chromatogram; for this reason, the number of separate compounds is largely lower than the theoretical peak capacity. As it has been highlighted by Giddings, the peak capacity can be increased using multidimensional techniques and this is of considerable utility for samples consisting of complex mixtures.

The effective area occupied by the analytes or their 2D space, should be considered. In theory, peak capacity equations assume that peaks from the samples under investigation cover the entirety of the ^{2}D separation space (100% surface coverage). This is seldom the case, however, with real LC×LC systems. The distribution of peaks in the ^{2}D separation space is

influenced by a wide range of factors, including the sample composition, the method used, the gradient time, plate count, initial and final compositions of the mobile phase, and the flow rate. In practice, some parts of the ^{2}D separation space are not occupied by analytes, which effectively decreases the peak capacity of this dimension. For this reason, instead of the theoretical peak capacity, the practical peak capacity was introduced to evaluate well the performance of 2D-LC separations, since it takes into account both the effects of orthogonality (effective surface coverage (f_c) and ^{1}D undersampling [14].

The practical peak capacity is determined by equation 2 as follows:

$$n'_{c,2D} = \frac{{}^{1}n^{c} \times {}^{2}n^{c} \times f_c}{\beta} \qquad \text{[Eq. 2]}$$

Where:

f_c refers to the orthogonality.

${}^{1}n^{c}$ refers to the theoretical peak capacities of first dimensions.

${}^{2}n^{c}$ refers to the theoretical peak capacities of second dimension.

The β parameter accounts for ^{1}D undersampling and is defined by equation 3.

$$\beta = \sqrt{1 + 3.35\left(\frac{{}^{1}t_{s} \times {}^{1}n^{c}}{{}^{1}t_{g}}\right)^{2}} \qquad \text{[Eq. 3]}$$

Where:

${}^{1}t_{s}$ refers to the sampling time.

1.2.3 Application of 2D-LC in complex food products

The use of two-dimensional liquid chromatography can significantly improve the amount of compounds that can be analyzed, separated, and quantified within a single analytical procedure. The potential of 2D-LC is elevated, and it can be applied in both academic and industrial fields to solve several real analytical problems and achieve outstanding results. The areas of application include pharmaceuticals, natural products, polymers, forensic, and omics (lipidomics, metabolomics, and proteomics). Since 2D-LC has an increased peak capacity, simple pretreatment, and good separation efficiency, it resulted suitable for the analysis of complex food samples. Considering its high sensitivity, it is able to separate target substances

more effectively in samples with complex matrices, particularly samples containing a greater amount of proteins [15]. 2D-LC was also used to separate protein from soybean samples by using a stop-flow method combined with a dual-switching valve system and a short C4 analytical column [16]. By using this method, the incompatibility of the solvent composition and pH value is overcome, and the analytical performance of the second chromatographic column is improved. Besides entire protein separation, 2D-LC was also employed for the detection of milk peptides which present the result of milk protein degradation, thus generating large number of peptides. Identifying and characterizing these complex samples requires effective analytical techniques. An online integrated LC×LC technique was applied to analyze the soluble peptides in milk, which was equipped with two sub-columns to evaluate their performance and behavior by using two different pH responses [17]. Consequently, a great 2D-LC separation and high peak capacity were achieved.

2D-LC was further applied in oil matrix, which is considered a fundamental part for most foods, with important economic and nutritional impact. Natural samples contain a large number of fatty acids, which results in a variety of labels [18]. Generally, oil samples contain complex compositions with variations in their fatty acyl chains, the number of double bonds, their positions, and their cis/trans configurations, all of which have a significant effect on their biological and nutritional characteristics [19]. Hence, it represents a complex matrix and difficult to analyze the composition of triacylglycerides (TAGs). Furthermore, to distinguish adulterated oil, it is necessary to identify the source of edible oil. In order to accomplish this, a novel 2D-LC technique was developed by combining the features of a silver-ion packed column with those of a C8 column [20]. It has also demonstrated and improved efficiency and selectivity towards TAGs. As a result of this method, biomarkers in peanut oil, corn oil, and soybean oil can be quickly characterized and quantified, thereby providing an efficient and convenient chromatographic technique. To complete the quantitative analysis of TAGs, Wei et al. combined 2D-LC and atmospheric pressure chemical ionization mass spectrometry (APCI-MS) [21]. As a consequence, this method has potential for routine quality control of edible oils as well as for tagging other fats, foods with a high lipid content, and even biological samples containing a high amount of fats.

2D-LC was also largely applied in the analysis of bioactive compounds such as phenolic compounds, which are omnipresent in the plant kingdom. Comprehensive (LC×LC) technique was applied for the analysis of polyphenolic contents in 4 samples of pistachio kernels from various geographic regions [22]. In the ^{1}D separation a cyano column was employed, whereas a C18 silica column was used in ^{2}D separation. A shift gradient elution was employed in the second dimension in order to increase the orthogonality the peak

capacity, resulting in the achievement of good linearity, sensitivity, accuracy and precision, and detection of 51 different polyphenolic compounds, where 18 of them are reported here for the first time.

Since 2D-LC technology is relatively easy to operate today and the high-pressure capability of modern instruments enables high flow rates and correspondingly fast analyses, the number of applications in this field is likely to continue to grow.

1.3 Ambient mass spectrometry

Mass spectrometry has been widely used as a detector when combined with separation techniques due to its high sensitivity and ability to provide a large amount of structural information. Therefore, it lends itself to both qualitative and quantitative analyses. Although several MS ionization sources have been developed, the use of these traditional techniques for some applications is sometimes limited by certain problems, such as low ionization efficiency, incompatibility with buffers commonly used in liquid chromatography mobile phases and possible contamination of the sources.

The approach of ambient ionization for mass spectrometry (MS) was established in 2004 by Cooks and co-workers [23], which refers to the handling of samples directly for mass spectral analysis without the need to prepare or pre-treat the samples before analysis. Ambient ionization refers to both desorption and ionization procedures that are conducted at atmospheric pressure.

Ambient ionization MS has first introduced with the solvent-based desorption electrospray ionization (DESI) technique [23], immediately followed by the publication of the plasma-based direct analysis in real-time (DART) technique [24]. Consequently, improvements have been made in the analytical performance and design of both methods in order to enable their use in a variety of applications. Alongside, in recent years, there have been tens of new ambient ionization MS techniques developed which employ other physical-chemical processes such as laser ablation, thermal desorption, and vibrational excitation to directly probe and/or ionize several samples in their natural environment. Since this field has diversified to include a wide range of methodologies, ambient ionization MS has evolved to include the analysis of samples which have been subjected to offline preparation before being directly analyzed by ambient ionization MS [25,26].

Since ambient ionization techniques in mass spectrometry include all those ionization methods that occur under ambient pressure and temperature conditions, with minimal or no sample preparation, nor chromatographic separation, they represent an ideal means to study tissue samples in their native form without any chemical modification, ideally *in vivo*, giving exceptional significance to these methods in the biological and above all medical fields [27].

Applications beyond the biomedical field include food safety [28,29], bacterial species analysis [30], environmental and chemical contaminant characterization [31], including agrochemicals [32] and drugs of abuse [33].

Mass ambient techniques can be classified into three groups according to their ionization mechanism:

• Spray or jet ionization techniques such as DESI where the charges are produced by a high-voltage electrospray needle;

• Ambient ionization techniques with electrical discharge, such as DART (Direct Analysis in Real Time) where metastable ions, electrons and atoms are produced using He/N_2 and a corona discharge;

• Gas, heat or laser-assisted desorption/ionization techniques such as REIMS (Rapid Evaporative Ionization Mass Spectrometry) where a solid or liquid sample is ionized at atmospheric pressure between 300° and 500° C [34].

Briefly, only two ambient mass spectrometry DART and REIMS techniques are described in greater detail.

1.3.1 Direct Analysis in Real Time (DART)

DART is a technique in which the use of solvents is not expected to support the ionization process. Hence, it is considered a "dry" technique because no traces of liquids are detected on the surfaces at the end of the analysis. The process of DART depends on the collision of a gas stream with the surface to be ionized which usually flows at a speed of 1 L/min and this gas carries species activated by an electric glow discharge, causing desorption and ionization of the analytes of interest. The DART source consists of multiple compartments through which nitrogen or helium flows. The voltage applied in the first compartment between the needle electrode and the first perforated disk electrode caused the electric glow discharge which leads to the production of excited ions, electrons and neutral atoms [35,36]. However, as the gas flows to subsequent compartments, separate electrodes within the DART source filter cations to the second compartment and anions and electrodes to the third compartment and allow only the excited neutral species across. The passage of the excited neutral gas through

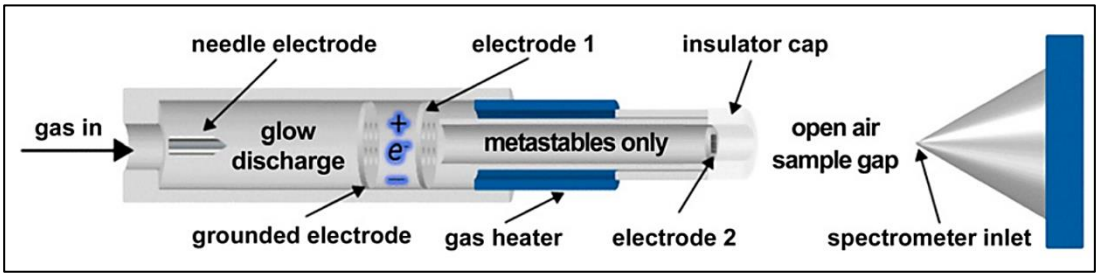

Figure 1.1. Diagram illustrating the DART technique [37].

the third compartment can optionally be heated as it passes through the electrode grid before being directed to the sample surface and the inlet of the mass spectrometer (**Figure 1.1**).
Different ionization mechanisms have been proposed in DART and these depend on the type of carrier gas, the concentration, and the polarity of the analytes.
The first theory tends that the atoms or molecule of excited neutral gas (metastable species (N*)) act according to Penning ionization, in which their energy is transmitted to the analytes (M), leading to the formation of molecular ions (Eq. 1). This occurs when the analyte molecule has ionization energy (IE) to a lesser extent than the internal energy of the excited gaseous molecules. The use of nitrogen is limited since its excited state is at very low energy, insufficient for the ionization of the analytes.

$$N^{*} + M \rightarrow N + M^{+\cdot} + e^{-} \qquad \text{[Eq. 1]}$$

On the other hand, helium, which is the most widely used gas, mainly produces the metastable 2^3S electronic excited state which has higher internal energy than the IE of atmospheric gases such as nitrogen, oxygen, or water. Consequently, the ionization of neutral water molecules in a cascade leads to the formation of clusters of protonated water molecules. Finally, the protons are transferred to analytes of higher proton affinity forming the protonated molecules (Eq. 2 and 3).

$$He(2^3S) + nH_2O \rightarrow [(H_2O_{n-1})H]^{+} + OH^{-} + He(1^1S) \qquad \text{[Eq. 2]}$$

$$[(H_2O_{n-1})H]^{+} + M \rightarrow [M + H]^{+} + nH_2O \qquad \text{[Eq. 3]}$$

DART mainly produces charged species $[M+H]^+$ from polar analytes and $[M^{+\cdot}]$ from non-polar analytes. However, unlike DESI, it requires the sample to have a certain degree of volatility and is unable to ionize larger molecules such as proteins. Additionally, the formation of metal adducts or multi-charged ions is not normally observed with DART. However, the DART failed to detect disaccharides such as lactose and sucrose, which were detected by the DESI. Differences in ionization mechanisms could justify this observation. The DART source was also combined with a quadrupole analyzer and its performance in analyzing small drug molecules was compared with that of LC/UV/ESI/MS [38]. The same compounds were ionized with both techniques in both positive and negative ionization modes, generating nearly identical spectra. In general, the signal intensities for the ions produced by

the ESI were about one to two orders of magnitude higher than that of the DART. Although it is a faster technique than ESI, DART could not ionize β-estradiol and terbutaline in negative ionization mode. In general, the use of DART for the quantification of liquid samples holds more promise than solid matrices despite the irreproducibility in liquid sample placement. The most accessible tactic for accurate and precise quantification is the use of internal standards with or without sample preconcentration allowing to achieve a sensitivity between nanograms per millimeter and micrograms per milliliter (ppb to ppm). Other improvements have been introduced to enable current sample placement and a reproducible desorption/ionization process, including the introduction of different sampling devices to choose from depending on sample type (solid or liquid), required sensitivity and the purpose (for the application of statistical analyzes and the construction of spectral databases it is necessary to use devices which allow the greatest number of analyzes to be carried out in the most automatic way possible).

Application of DART in food products

DART has demonstrated its advantages when it is applied to food products for the purpose of determining authenticity and adulteration. There are several parameters that affect the quality and safety of food. One of the most important parameters is authenticity, which indicates whether or not there has been fraud in the production of the food. A food quality grade is inherently labelled as a means of characterizing food authenticity, but most food safety issues result from intentional mislabeling or adulteration. Moreover, a number of food additives have been introduced, both natural and synthetic. There are several reasons why food additives can be added to foods, such as improving taste and appearance, protecting food from contamination by microbes or enzymes, and preventing the oxidation of oil that contains unsaturated fatty acids. As a result, overdoses or off-label usage of food additives and adulterants may constitute intended food contaminants.

DART technique was employed to discover the adulteration of extra virgin olive oil (EVOO), which is considered to be the most valuable of all kinds of olive oil due to its unique taste and flavour. There is the possibility, however, of adulteration with hazelnut oil or lower-quality grade olive oil, which requires the development of a suitable method of differentiation. The DART-TOF-MS was used to obtain comprehensive profiles of non-polar TAGs diluted in toluene and polar compounds extracted in a methanol-water mixture.

When TAGs are subjected to the DART ionization, insource fragmentation occurs, leading to DAG fragment ions $[M+H-R_i-CO_2-H]^+$, monoacylglycerol fragment ions $[M+H-R_i-CO_2-R_i-CO]^+$, and acylium ions $[RCO]^+$. In addition to distinguishing diverse products of olive oil (EVOO, olive oil pomace, olive oil), as well as revealing EVOO adulteration with hazelnut

oil at 6% and 15% (v/v), the use of linear discriminant analysis (LDA) allowed evaluating profiles of polar compounds and TAGs [39].

Furthermore, DART was also applied in dairy products to reveal suspected adulteration of mixing milk obtained from various farm animals (cow, goat, and sheep) and the supplement of dairy products (sot cheese) with vegetable oil. Based on the obtained label profiles, two simple procedures were assessed, namely milk dilution with methanol and milk extraction with toluene. In addition to TAGs, low molecular weight compounds such as lactic acid and FFAs were detected as negative [M-H]- ions. Despite a low sensitivity in the detection of doped milk from different species, the DART-orbitrap-MS method was able to distinguish milk mixtures at a level of adulteration of 50% (*v/v*). In light of the significant differences between TAGs in milk fat and vegetable oil, relative intensities can serve as a reliable authenticity detection indicator, as evidenced by the fact that soft cheese was adulterated with vegetable oils (rapeseed, sunflower, and soybean) at levels of up to 1% (*w/w*) [40].

1.3.2 Rapid Evaporative Ionization Mass Spectrometry (REIMS)

Rapid evaporative ionization mass spectrometry (REIMS) was first described in 2009 as a direct use of surgical diathermy for the ionization of biological tissue constituents *in vivo* [41]. Surgical diathermy is a tool universally used for the dissection of tissues and hemostasis of vessels through the use of radiofrequency alternating electric current, which determines the heating and thermal ablation of the tissues during surgical dissection. In the course of diathermic manipulation (also known as electrosurgery), the patient becomes part of the electrical circuit and the electrical current flowing through the tissue induces heat dissipation due to the high impedance of biological tissue (impedance measures the ease with which an alternating current pass in an electric circuit). Surgical diathermy is used in two different ways. In the case of the so-called monopolar electrosurgery, the patient lies on a large surface electrode, while the surgeon operates with a sharp handpiece which acts as another electrode for the section. When the circuit closes, the current density reaches its maximum value at the point of contact of the handpiece with the tissue surface, becoming sufficiently high for abrasion and thermal evaporation of analytes desorbed from the surface of the sample. The REIMS instrumental set-up is based precisely on the detection of the molecular vapors produced during the diathermic process (**Figure 1.2**).

Surgical diathermy has shown a physicochemical analogy with some ionization methods in mass spectrometry (with particular attention to laser desorption and thermospray ionization), has been tested as a potential source of ions in mass spectrometry and has been found capable to produce organic ions associated with the structural lipid content of the tissues.

The molecular vapors are then introduced thanks to a venturi pump. Aerosol sampling was implemented using an orthogonal MS inlet tube to exert a certain level of momentum for the sampled particles and keep the lipid droplets out of the vacuum air of the instrument. It has been discovered that the ion formation detected by the mass spectrometer takes place in the ambient interface of the instruments through a collision phenomenon on the surface of the droplet, consequently, a further refinement of the technique has been made which led to the introduction of a heated collision surface in the system, which is an integral part of the model commercialized by Waters Corporation (Milford, USA). This has led to greater reproducibility and sensitivity by lowering the detection limits of the technique.

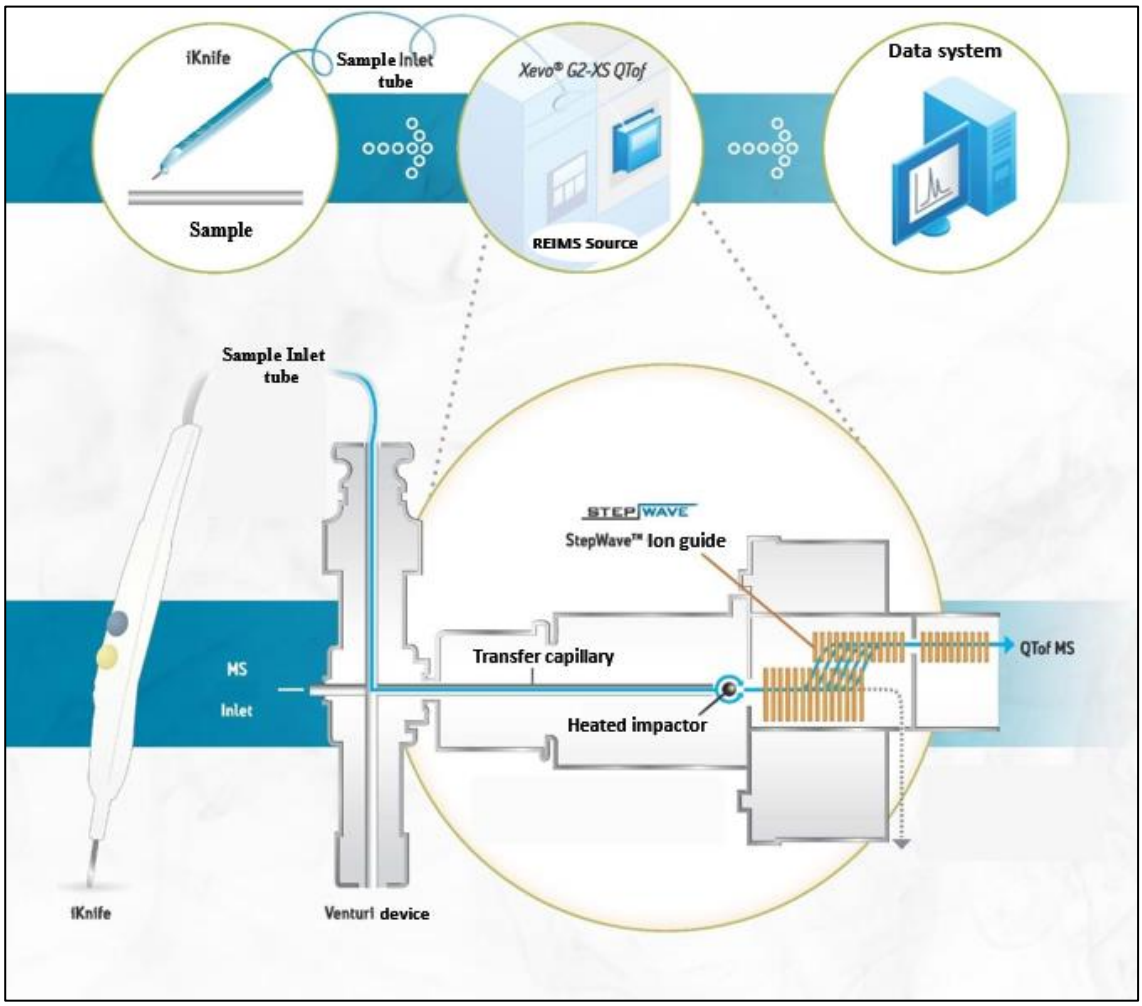

Figure 1.2. Schematic illustration of REIMS technique [42].

The coupling of the electrosurgical pencil with REIMS technology is often referred to as an "iKnife" or intelligent surgical device.

Surgical applications are mainly focused on neoplastic specimens in the strict sense, for the purpose of identifying unknown tissues for diagnostic purposes. During *in vivo* and *ex vivo*

applications, operators use an electrosurgical pencil (also known as a "pencil") equipped with an aerosol evacuation line, which is connected to the mass spectrometer via a (PTFE) tube remote from the operating table about 2-3 cm. At the time of tissue dissection, the aerosol is aspirated by the instrument and subsequently analyzed. The resulting mass spectra are recalibrated, background subtracted, normalized, and subjected to multivariate statistical analysis. The last step involves the localization of the data with respect to a previously constructed statistical model, which in the surgical field could translate into the immediate distinction between healthy tissue and tumor tissue or into a precise histological classification of the type and degree of cancer. Although REIMS technology was originally developed for intraoperative tissue identification, other laboratory applications have more recently been introduced. These applications include the analysis of *ex vivo* tissue samples from surgical dissections and the analysis of *in vitro* tumour tissue models. The main rationale is to create a database containing reference data for *in vivo* tissue identification; however, the same approach can also be used for the rapid diagnosis of specimens obtained from tissue dissection.

Application of REIMS in food products

REIMS technology has also found a place recently for application in the food sector, in particular for identifying animal species or meat quality [28,43,44] and fish products [29]. The application of meat and fish samples was successful because the samples were solid and easy to cut. Moreover, they are juicy and conductors of electricity. REIMS has several advantages as a valid direct analysis technique for determining food authenticity. As a result, the analysis can be completed within two seconds, significantly reducing the time scale. With REIMS and high-resolution mass spectrometry (HRMS), a wide variety of food products can be characterized with in situ samples while untargeted mass spectral profiles can be generated. Using multivariate statistical analysis algorithms, it is possible to train and validate chemometric models using the spectral profiles of authentic food samples. By comparing the spectral profiles of "unknown" samples with the validated model via similarity scoring, it is possible to make near-instantaneous classification decisions (**Figure 1.3**). Moreover, this technique was recently also applied to extra virgin olive oils and pistachio, the common objective, in this case, was to be able to extend the applicability and advantages of this technique as a useful means against fraudulent activities to the detriment of producers operating in the food chain and consumers. Italy, in particular, represents one of the countries most subject to such phenomena which aim, for example, to imitate some of the prestigious Made in Italy products, and this is above all linked to the significant number of PDO (Protected Designation of Origin), PGI (Protected Geographical Indication), and DOCG

(*Denominazione di Origine Controllata e Garantita*) present in the area. REIMS was employed for the evaluation of the authenticity and geographical origin of pistachio samples, in order to safeguard the PDO Bronte pistachio, subject to adulteration given its high cost on the market [45].

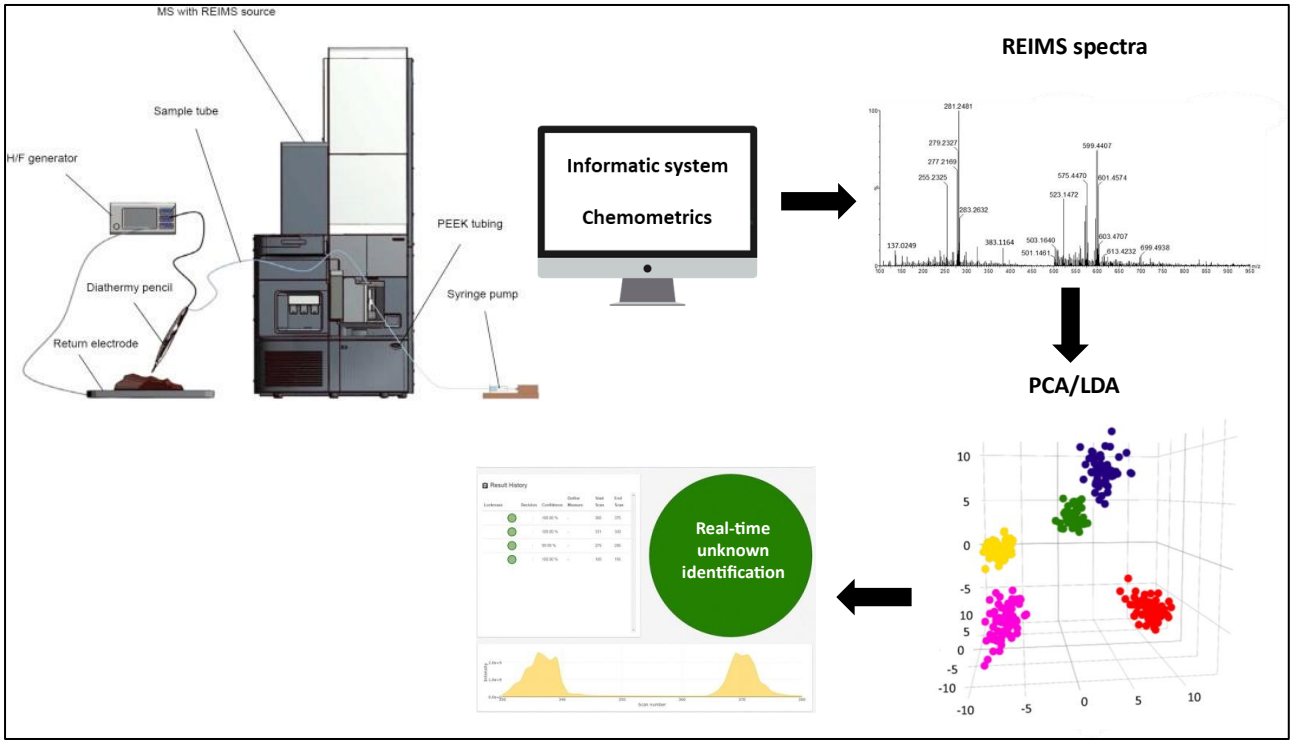

Figure 1.3. Workflow diagram of REIMS combined with integrative chemometrics.

Furthermore, discrimination at the level of Italian olive oil was also carried out by REIMS. Despite the great variability within the same class (different cultivars, different producers) and the close geographical proximity of all classes, the results demonstrated very promising discrimination of EVOOs. Particularly, the PDO model required an expanded sample set including all possible variables (harvest year, producer and production lot, production and harvest area, cultivars employed), in contrast to the mono cultivar model, which had higher correctness scores after a limited number of analyses. Consequently, the olive cultivar may play a significant role in the discrimination process. The combination of a suitable sampling device with MS and chemometrics provided a powerful and unified tool for authenticating products and tracing them even within the same country, as well as preserving consumers as well as the competitiveness, namely, the global market [46].

REIMS was also employed for the authentication of honey samples from different botanical species. The technique has been shown to be able to discriminate between monofloral and polyfloral honey and to detect adulterations due to the preparation of mixtures of high-quality honey with a low-quality product up and about 5% of poor-quality honey [47]. An even more

recent use of the technique has involved the elucidation of the majority of components of the fruit of the *Kigelia africana*, thus extending the applicability of this technique to the study of phytochemical components, such as phenolic compounds [48]. By exploiting the coupling of the REIMS source with a high-resolution hybrid analyzer, a detailed screening of this botanical species has been obtained, thanks to accurate mass data that have been compared with metabolomics and lipidomics databases also available online and with MS experiments /MS for the elucidation of the chemical structure of isobaric species. Also, in the latter case, it is possible to compare the experimental spectra obtained with those present in some databases accessible for free online (Humane metabolome database). The characterization of this species is particularly interesting in light of its use in traditional African medicine and the growing interest of pharmaceutical companies in the use of these botanical species for therapeutic purposes or for the isolation and purification of their active ingredients. In particular, the native lipid composition of *Kigelia africana* was characterized for the first time using the iknife technique, opening up potential practical implications in the evaluation of therapeutic activity [48].

1.4 References

1. Patel, KalpeshN, JayvadanK Patel, ManishP Patel, GaneshC Rajput, and HiteshA Patel. 2010. “Introduction to Hyphenated Techniques and Their Applications in Pharmacy.” Pharmaceutical Methods 1 (1): 2.
2. Careri, M, F Bianchi, and C Corradini. 2002. “Recent Advances in the Application of Mass Spectrometry in Food-Related Analysis.” Journal of Chromatography A 970 (1–2): 3–64.
3. Cai, Sheng-Suan, and Jack A. Syage. 2006. “Atmospheric Pressure Photoionization Mass Spectrometry for Analysis of Fatty Acid and Acylglycerol Lipids.” Journal of Chromatography A 1110 (1–2): 15–26.
4. Canabatediaz, B, A Seguracarretero, A Fernandezgutierrez, A Belmontevega, A Garridofrenich, J Martinezvidal, and J Duranmartos. 2007. “Separation and Determination of Sterols in Olive Oil by HPLC-MS.” Food Chemistry 102 (3): 593–98.
5. Careri, M, and A Mangia. 2003. “Analysis of Food Proteins and Peptides by Chromatography and Mass Spectrometry.” Journal of Chromatography A 1000 (1–2): 609–35.
6. Kataoka, Hiroyuki, Heather L Lord, and Janusz Pawliszyn. 2000. “Applications of Solid-Phase Microextraction in Food Analysis.” Journal of Chromatography A 880 (1–2): 35–62.
7. Adahchour, Mohamed, Leo L.P van Stee, Jan Beens, René J.J Vreuls, Max A Batenburg, and Udo A.Th Brinkman. 2003. “Comprehensive Two-Dimensional Gas Chromatography with Time-of-Flight Mass Spectrometric Detection for the Trace Analysis of Flavour Compounds in Food.” Journal of Chromatography A 1019 (1–2): 157–72.
8. Čajka, Tomáš, Jana Hajšlová, Jack Cochran, Kateřina Holadová, and Eva Klimánková. 2007. “Solid Phase Microextraction–Comprehensive Two-Dimensional Gas Chromatography–Time-of-Flight Mass Spectrometry for the Analysis of Honey Volatiles.” Journal of Separation Science 30 (4): 534–46.
9. Pirok, Bob W. J., Dwight R. Stoll, and Peter J. Schoenmakers. 2019. “Recent Developments in Two-Dimensional Liquid Chromatography: Fundamental Improvements for Practical Applications.” Analytical Chemistry 91 (1): 240–63.
10. Giddings, J. Calvin. 1967. “Maximum Number of Components Resolvable by Gel Filtration and Other Elution Chromatographic Methods.” Analytical Chemistry 39 (8): 1027–28.

11. Giddings, J. C. 1987. “Concepts and Comparisons in Multidimensional Separation.” Journal of High Resolution Chromatography 10 (5): 319–23.
12. McCoy, Benjamin J. 1990. “Multidimensional Chromatography—Techniques and Applications. Edited by H. J. Cortes, Marcel Dekker, New York, NY, 1990, 424, AIChE Journal 36 (12): 1933–1933.
13. Stoll, Dwight R., and Peter W. Carr. 2022. “Theoretical Guiding Principles for Two-Dimensional Liquid Chromatography.” In *Multi-Dimensional Liquid Chromatography*, by Dwight R. Stoll and Peter W. Carr, 1st ed., 103–14. Boca Raton: CRC Press.
14. Rutan, Sarah C., Joe M. Davis, and Peter W. Carr. 2012. “Fractional Coverage Metrics Based on Ecological Home Range for Calculation of the Effective Peak Capacity in Comprehensive Two-Dimensional Separations.” Journal of Chromatography A 1255 (September): 267–76.
15. Melfi, Maria Teresa, Donatella Nardiello, Anna Natale, Maurizio Quinto, and Diego Centonze. 2019. “An Automated Food Protein Isolation Approach on Preparative Scale by Two-dimensional Liquid Chromatography with Active Modulation Interface.” ELECTROPHORESIS 40 (7): 1096–1106.
16. Nardiello, Donatella, Maria Teresa Melfi, Carla Pignatelli, and Diego Centonze. 2020. “Enhancing Online Protein Isolation as Intact Species from Soy Flour Samples by Actively Modulated Two-Dimensional Liquid Chromatography (2D-LC).” Journal of Pharmaceutical and Biomedical Analysis 179 (February): 112976.
17. Sommella, Eduardo, Giacomo Pepe, Giovanni Ventre, Francesco Pagano, Michele Manfra, Giuseppe Pierri, Omar Ismail, Alessia Ciogli, and Pietro Campiglia. 2015. “Evaluation of Two Sub-2μm Stationary Phases, Core–Shell and Totally Porous Monodisperse, in the Second Dimension of on-Line Comprehensive Two Dimensional Liquid Chromatography, a Case Study: Separation of Milk Peptides after Expiration Date.” Journal of Chromatography A 1375 (January): 54–61.
18. Li, Wen-Kui, and Yan-Ping Shi. 2020. “Recent Advances of Magnetic Extractants in Food Analysis.” TrAC Trends in Analytical Chemistry 129 (August): 115951.
19. Řezanka, Tomáš, Jaromír Lukavský, Milada Vítová, Linda Nedbalová, and Karel Sigler. 2018. “Lipidomic Analysis of Botryococcus (Trebouxiophyceae, Chlorophyta) - Identification of Lipid Classes Containing Very Long Chain Fatty Acids by Offline Two-Dimensional LC-Tandem MS.” Phytochemistry 148 (April): 29–38.
20. Wei, Fang, Shu-Xian Ji, Na Hu, Xin Lv, Xu-Yan Dong, Yu-Qi Feng, and Hong Chen. 2013. “Online Profiling of Triacylglycerols in Plant Oils by Two-Dimensional Liquid

Chromatography Using a Single Column Coupled with Atmospheric Pressure Chemical Ionization Mass Spectrometry." Journal of Chromatography A 1312 (October): 69–79.

21. Wei, Fang, Na Hu, Xin Lv, Xu-Yan Dong, and Hong Chen. 2015. "Quantitation of Triacylglycerols in Edible Oils by Off-Line Comprehensive Two-Dimensional Liquid Chromatography–Atmospheric Pressure Chemical Ionization Mass Spectrometry Using a Single Column." Journal of Chromatography A 1404 (July): 60–71.
22. Arena, Katia, Francesco Cacciola, Domenica Mangraviti, Mariosimone Zoccali, Francesca Rigano, Nino Marino, Paola Dugo, and Luigi Mondello. 2019. "Determination of the Polyphenolic Fraction of Pistacia Vera L. Kernel Extracts by Comprehensive Two-Dimensional Liquid Chromatography Coupled to Mass Spectrometry Detection." Analytical and Bioanalytical Chemistry 411 (19): 4819–29.
23. Takáts, Zoltán, Justin M. Wiseman, Bogdan Gologan, and R. Graham Cooks. 2004. "Mass Spectrometry Sampling Under Ambient Conditions with Desorption Electrospray Ionization." Science 306 (5695): 471–73.
24. Cody, Robert B., James A. Laramée, and H. Dupont Durst. 2005. "Versatile New Ion Source for the Analysis of Materials in Open Air under Ambient Conditions." Analytical Chemistry 77 (8): 2297–2302.
25. Venter, Andre, Marcela Nefliu, and R. Graham Cooks. 2008. "Ambient Desorption Ionization Mass Spectrometry." TrAC Trends in Analytical Chemistry 27 (4): 284–90.
26. Venter, Andre R., Kevin A. Douglass, Jacob T. Shelley, Gregg Hasman, and Elahe Honarvar. 2014. "Mechanisms of Real-Time, Proximal Sample Processing during Ambient Ionization Mass Spectrometry." Analytical Chemistry 86 (1): 233–49.
27. Wu, Chunping, Allison L. Dill, Livia S. Eberlin, R. Graham Cooks, and Demian R. Ifa. 2013. "Mass Spectrometry Imaging under Ambient Conditions: MASS SPECTROMETRY IMAGING UNDER AMBIENT CONDITIONS." Mass Spectrometry Reviews 32 (3): 218–43.
28. Balog, Julia, Dora Perenyi, Cristina Guallar-Hoyas, Attila Egri, Steven D. Pringle, Sara Stead, Olivier P. Chevallier, Chris T. Elliott, and Zoltan Takats. 2016. "Identification of the Species of Origin for Meat Products by Rapid Evaporative Ionization Mass Spectrometry." Journal of Agricultural and Food Chemistry 64 (23): 4793–4800.
29. Black, Connor, Olivier P. Chevallier, Simon A. Haughey, Julia Balog, Sara Stead, Steven D. Pringle, Maria V. Riina, et al. 2017. "A Real Time Metabolomic Profiling Approach to Detecting Fish Fraud Using Rapid Evaporative Ionisation Mass Spectrometry." Metabolomics 13 (12): 153.

30. Cameron, Simon J. S., Frances Bolt, Alvaro Perdones-Montero, Tony Rickards, Kate Hardiman, Alireza Abdolrasouli, Adam Burke, et al. 2016. “Rapid Evaporative Ionisation Mass Spectrometry (REIMS) Provides Accurate Direct from Culture Species Identification within the Genus Candida.” Scientific Reports 6 (1): 36788.
31. Ifa, Demian R., Nicholas E. Manicke, Allison L. Dill, and R. Graham Cooks. 2008. “Latent Fingerprint Chemical Imaging by Mass Spectrometry.” Science 321 (5890): 805–805.
32. García-Reyes, Juan F., Ayanna U. Jackson, Antonio Molina-Díaz, and R. Graham Cooks. 2009. “Desorption Electrospray Ionization Mass Spectrometry for Trace Analysis of Agrochemicals in Food.” Analytical Chemistry 81 (2): 820–29.
33. Bailey, Melanie J., Elizabeth C. Randall, Catia Costa, Tara L. Salter, Alan M. Race, Marcel de Puit, Mattijs Koeberg, Mark Baumert, and Josephine Bunch. 2016. “Analysis of Urine, Oral Fluid and Fingerprints by Liquid Extraction Surface Analysis Coupled to High Resolution MS and MS/MS – Opportunities for Forensic and Biomedical Science.” Analytical Methods 8 (16): 3373–82.
34. Li, Li-Ping, Bao-Sheng Feng, Jian-Wang Yang, Cui-Lan Chang, Yu Bai, and Hu-Wei Liu. 2013. “Applications of Ambient Mass Spectrometry in High-Throughput Screening.” The Analyst 138 (11): 3097.
35. Li, Mei, Hong Chen, Xin Yang, Jianmin Chen, and Chunlei Li. 2009. “Direct Quantification of Organic Acids in Aerosols by Desorption Electrospray Ionization Mass Spectrometry.” Atmospheric Environment 43 (17): 2717–20.
36. Cotte-Rodríguez, Ismael, Zoltán Takáts, Nari Talaty, Huanwen Chen, and R. Graham Cooks. 2005. “Desorption Electrospray Ionization of Explosives on Surfaces: Sensitivity and Selectivity Enhancement by Reactive Desorption Electrospray Ionization.” Analytical Chemistry 77 (21): 6755–64.
37. DART ion source schematio. http://en.wikipedia.org/wiki/File:DART_ion_source_schematic.gif.
38. Petucci, Chris, Jason Diffendal, David Kaufman, Belew Mekonnen, Gene Terefenko, and Brian Musselman. 2007. “Direct Analysis in Real Time for Reaction Monitoring in Drug Discovery.” Analytical Chemistry 79 (13): 5064–70.
39. Vaclavik, Lukas, Tomas Cajka, Vojtech Hrbek, and Jana Hajslova. 2009. “Ambient Mass Spectrometry Employing Direct Analysis in Real Time (DART) Ion Source for Olive Oil Quality and Authenticity Assessment.” Analytica Chimica Acta 645 (1–2): 56–63.
40. Hrbek, Vojtech, Lukas Vaclavik, Ondrej Elich, and Jana Hajslova. 2014. “Authentication of Milk and Milk-Based Foods by Direct Analysis in Real Time Ionization–High

Resolution Mass Spectrometry (DART–HRMS) Technique: A Critical Assessment." Food Control 36 (1): 138–45.

41. Schäfer, Karl-Christian, Júlia Dénes, Katalin Albrecht, Tamás Szaniszló, Júlia Balog, Réka Skoumal, Mária Katona, Miklós Tóth, Lajos Balogh, and Zoltán Takáts. 2009. "In Vivo, In Situ Tissue Analysis Using Rapid Evaporative Ionization Mass Spectrometry." Angewandte Chemie International Edition 48 (44): 8240–42.
42. WATERS. 2015. REIMS research system with iKnife sampling: Direct molecular profiling in seconds [Online]. Available: http://www.waters.com/webassets/cms/library/docs/720005418en.pdf [Accessed 16 November 2022].
43. Guitton, Yann, Gaud Dervilly-Pinel, Renata Jandova, Sara Stead, Zoltan Takats, and Bruno Le Bizec. 2018. "Rapid Evaporative Ionisation Mass Spectrometry and Chemometrics for High-Throughput Screening of Growth Promoters in Meat Producing Animals." Food Additives & Contaminants: Part A 35 (5): 900–910.
44. Verplanken, Kaat, Sara Stead, Renata Jandova, Christof Van Poucke, Jan Claereboudt, Julie Vanden Bussche, Sarah De Saeger, Zoltan Takats, Jella Wauters, and Lynn Vanhaecke. 2017. "Rapid Evaporative Ionization Mass Spectrometry for High-Throughput Screening in Food Analysis: The Case of Boar Taint." Talanta 169 (July): 30–36.
45. Rigano, Francesca, Sara Stead, Domenica Mangraviti, Renata Jandova, Davy Petit, Nino Marino, and Luigi Mondello. 2019. "Use of an 'Intelligent Knife' (Iknife), Based on the Rapid Evaporative Ionization Mass Spectrometry Technology, for Authenticity Assessment of Pistachio Samples." Food Analytical Methods 12 (2): 558–68.
46. Mangraviti, Domenica, Francesca Rigano, Adriana Arigò, Paola Dugo, and Luigi Mondello. 2021. "Differentiation of Italian Extra Virgin Olive Oils by Rapid Evaporative Ionization Mass Spectrometry." LWT 138 (March): 110715.
47. Wang, Huijun, Xueli Cao, Tian Han, Hairun Pei, Hong Ren, and Sara Stead. 2019. "A Novel Methodology for Real-Time Identification of the Botanical Origins and Adulteration of Honey by Rapid Evaporative Ionization Mass Spectrometry." Food Control 106 (December): 106753.
48. Arena, Katia, Francesca Rigano, Domenica Mangraviti, Francesco Cacciola, Francesco Occhiuto, Laura Dugo, Paola Dugo, and Luigi Mondello. 2020. "Exploration of Rapid Evaporative-Ionization Mass Spectrometry as a Shotgun Approach for the Comprehensive Characterization of Kigelia Africana (Lam) Benth. Fruit." Molecules 25 (4): 962.

CHAPTER 2

Characterization of phenolic compounds, vitamin E and fatty acids in monovarietal extra virgin and virgin olive oils "*Picholine marocaine*" by Liquid and Gas Chromatography coupled to Mass Spectrometry

2.1 Introduction

Moroccan olive cultivation accounts for 5% of the agricultural gross domestic product and 15 % of its agricultural food exports [1]. In terms of tree-growing areas, olive trees cover 65% (1,045,186 ha), of which 37% (384,528 ha) are irrigated and 63% (660,658 ha) are not irrigated. The majority of olives produced are pressed, 25% are canned, and 10% are lost or consumed locally. In 2017, Morocco exported over 76% of its table olives (70,000 tons), 14% of its olive pomace (128 tons) and 10% of its olive oil (88 tons) 2017 [2]. Additionally, Moroccan olive oil is mainly exported to Spain, Portugal, Holland, Italy, the USA, and Asia [2]. However, olive oil quality and composition are not adequately represented in a database. Noncompliance with the international olive oil council requirements could have adverse consequences for the commercialization of Moroccan olive oils [2]. Three extraction processes are employed to extract olive oil: the traditional discontinuous press process, the two-phase decanter process, and the three-phase decanter process.

The traditional discontinuous olive pressing involves picking olives, removing leaves, washing, crushing, kneading (paste) with warm water (38°C) and pressing (pomace and wastewater from olive mills) [3]. The olive pomace is then centrifuged vertically or decanted after centrifugation to obtain the olive oil. In a two-phase decanter process, naturally occurring olive water is used to create both olive oil and olive mill waste (liquids and solids). In a three-phase decanter process, three different products are obtained, after beating and the addition of the water during the centrifugation process, olive oil, olive mill wastewater and olive solid mill wastes (olive cakes) [3,4]. The two-phase decanter extraction process is primarily used in Morocco for olive oil extraction. The north-central region of Morocco is well-known for several major olive-growing areas: Fes-Meknes (346,000 ha), Marrakech-Safi (215,000 ha), Tanger-Tetouan Al-Hoceima (163,000 ha), Oriental (122,000 ha), Beni Mellal-Khenifra (80,000 ha), Rabat-Salé-Kenitra (66,135 ha), Souss-Massa (19,455 ha), Darâa-Tafilalet (16,000 ha), Casablanca-Settat (15,000 ha), and Guelmim-Oued noun (2000 ha) [2]. Furthermore, within these regions, the provinces of Touanate, Taza, Chefchaouen,

Beni Mellal and Errachidia have a stronger vocation to olive cultivation, occupying productive olive areas of 131,000 ha, 55,000 ha, 43,000, 14,000 ha and 3,000 ha respectively [5].

Olive cultivation is dominated by the *Picholine marocaine* variety (up to 96%), due to its high adaptability to bioclimatic stages (plains, mountains, aridity, and Sahara), organoleptic characteristics (medium-green fruitiness, bitterness, and balanced spiciness), the richness of the chemical and aromatic profiles and dual purpose (production of olive oil and preserved olives).

Moreover, as a part of the Green Moroccan Plan, cultivar diversification is encouraged, which includes Dahbia, Haouzia and Menara varieties, as well as Spanish and Italian-introduced cultivars (Picual, Frantoio, Manzanilla, Gordal, Arbequina, etc.).

Functional foods such as olive oil include several components that contribute to its overall sensory properties and health benefits. Many bioactive substances in olive oil contribute to its nutritional value, such as phenolic compounds, vitamin E, fatty acids, carotenoids, and phytosterols [6].

Polyphenols are among a wide variety of secondary metabolites which are produced in plants, including flavonoids, isoflavonoids, phenolic acids, proanthocyanidins, tannins, and lignans [7]. Phenolic compounds are naturally distributed in drupes, basically during the extraction of olive oil around 90% of such polyphenols, which present hydrophilic properties, are finished into pomace and mill wastewater [8–10]. The main phenolic compounds which occur in olive oil are phenolic acids (e.g., hydroxytyrosol and tyrosol), secoiridoids (e.g., oleuropein) and lignans (e.g., pinoresinol) [11–13]. The health benefits of phenolic compounds have been widely acknowledged due to the claims about their protection against low-density lipoproteins (LDL), maintenance of normal blood pressure and healthy high-density lipoproteins (HDL) concentration, anti-inflammatory properties, contribution to the upper respiratory system health, and upkeep of normal function of the gastrointestinal system [14].

Phenolic compounds play an important role in the stability of olive oils against autooxidation as well as their involvement in organoleptic characteristics such as bitterness, pungency, and astringency [15–18]. In addition, lipophilic bioactive compounds such as vitamin E occur naturally in olive oil, comprising four different forms of tocopherols (α, β, γ, δ) and four different forms of tocotrienols (α, β, γ, δ), along with α-tocopherol as the major powerful antioxidant component of vitamin E. α-tocopherol is the dominant antioxidant component of vitamin E; its antioxidant capacity is attributed to its scavenging ability towards reactive oxygen species (ROS) generated by the endogenous system, thus contributing to the body's

defences. Moreover, α-tocopherol contributes as well to the protection against the oxidation of polyunsaturated fatty acids (PUFAs) within membrane phospholipids (preserving membrane integrity and stability of the erythrocytes and the conductibility of nerves, preventing haemolytic anaemia, neurological symptoms, ataxia, peripheral neuropathy, myopathy, and pigmented retinopathy) and plasma lipoproteins [19].

Olive oil contains a high percentage of triacylglycerol (99%), which is composed of monounsaturated fatty acids such as oleic and palmitoleic acids, saturated fatty acids such as palmitic acids, and polyunsaturated fatty acids such as linoleic acids.

Compared to other vegetable oils, olive oil contains a reduced amount of free fatty acids (1%), monoglycerides, diglycerides, phosphatides, waxes, and sterol esters [20]. It is important to note that olive oil's chemical composition is influenced by several factors, including the olive cultivar, agronomics (irrigation and fertilization), cultivation practices (harvesting and maturity), technological specifications (storage and extraction system), and geographical features (altitude, latitude, edaphology characteristics) [21–25].

The present study aimed to investigate initially, through a small-scale study performed on the following studied regions Chefchaouen, Taounate, Errachidia, Beni Mellal, and Taza in 2018, the relationship between the chemical composition of the virgin olive oils (VOOs) of *Picholine marocaine*. The investigation aims to analyze phenolic compounds, vitamin E, and fatty acids using reversed-phase liquid chromatography coupled with photodiode arrays and electrospray ionization mass spectrometry (HPLC-PDA/ESI-MS), a normal-phase liquid chromatography coupled to a fluorescence detector (NP-HPLC/FLD), and gas chromatography coupled with flame ionization detection and with mass spectrometry (GC-FID/MS), respectively. As part of the investigation objective, a large-scale study was sequentially conducted on 38 samples of EVOO collected from 19 Moroccan regions during two successive years 2018 and 2019. This later study, besides the analysis of polyphenols and vitamin E in EVOO, has also implemented the study of the influence of the crop year and pedoclimatic conditions on the quality of EVOO.

2.2 Materials and methods

2.2.1 Chemicals and reagents

Polyphenol commercial standards such as caffeic acid (≥98%), gallic acid (≥97.5%), ethyl gallate (≥96%), oleuropein aglycone (3,4-DHPEAEA) (≥98%), luteolin (≥97%), vanillic acid (≥95%), apigenin (≥99%), tyrosol (p-HPEA) (≥95%) and hydroxytyrosol (3,4-DHPEA) (≥90%) were obtained from (Merck KGaA, Darmstadt, Germany). The employed formic acid and organic solvents such as acetonitrile, water, *n*-hexane, ethanol, and methanol were all

HPLC grade and were obtained from Merck Life Science (Merck KGaA, Darmstadt, Germany). Diethyl ether, sodium hydroxide, sodium methanolate methanol, boron trifluoride, *n*-heptane and phenolphthalein were purchased from (Merck KGaA, Darmstadt, Germany). Tocopherols (α, β, γ, δ) and tocotrienol (α, β, γ, δ) standards were acquired from Extrasynthese (GenayCedex, France).

2.2.2 Sample collection and preparation

In the low-scale study, VOO samples were purchased from local markets in four different Northern Moroccan regions: Fes-Meknes (Taounate and Taza), Drâa-Tafilalet (Errachidia), Tanger-Tetouan-Al Hoceima (Chefchaouen), and Beni Mellal-Khenifra (Beni Mellal) [26]. VOO were obtained from olives of *Picholine marocaine* cultivar which were harvested between October and December 2018.

In the large-scale study, thirty-eight Moroccan EVOO samples of *Picholine marocaine* cultivar were obtained from nineteen Moroccan mills located in the regions of EVOO production (**Figure 2.1**). The collection was carried out during two consecutive productive seasons 2018 and 2019. During the productive season of 2018, 19 EVOO samples were collected from 19 olive oil mills in the North-Center-West Moroccan area as follows: 2 samples from Tangier-Tetouan-Al Hoceima (Sp1, Sp2), 1 sample from Rabat-Sale-Kenitra (Sp3), 7 samples from Fes-Meknes (Sp4-Sp10), 4 samples from Beni Mellal-Khenifra (Sp11–Sp14) and 5 samples from Marrakech-Safi region (Sp15-Sp19). In the successive crop year of 2019, EVOO samples were collected from the same previous mills. The collected EVOO samples were well stored in ambered and tightly closed bottles, in order to protect the oil from oxygen and light. Soil sampling was performed in November 2018 with the means of Edelman's Auger equipment, on the earth depth range of (0–60 cm).

Determination of acidity

A mixture of diethyl ether and ethanol was used to dissolve five grams of each olive oil (VOO or EVOO) (50:50, *v*/*v*). Subsequently, an indicator of phenolphthalein was added to 50 mL of titrated sodium hydroxide 0.1M [27]. Acidity is expressed as follows:

$$\text{Acidity } (\%) = \left(\frac{\mathrm{M} \times \mathrm{V} \times \mathrm{M}'}{\mathrm{m}}\right) \times 100$$

where: M: molarity of NaOH solution (0.1 M); V: volume of titrated NaOH (mL), m: the weight of olive oil (g); M': the molar weight of oleic acid (282 g/mol).

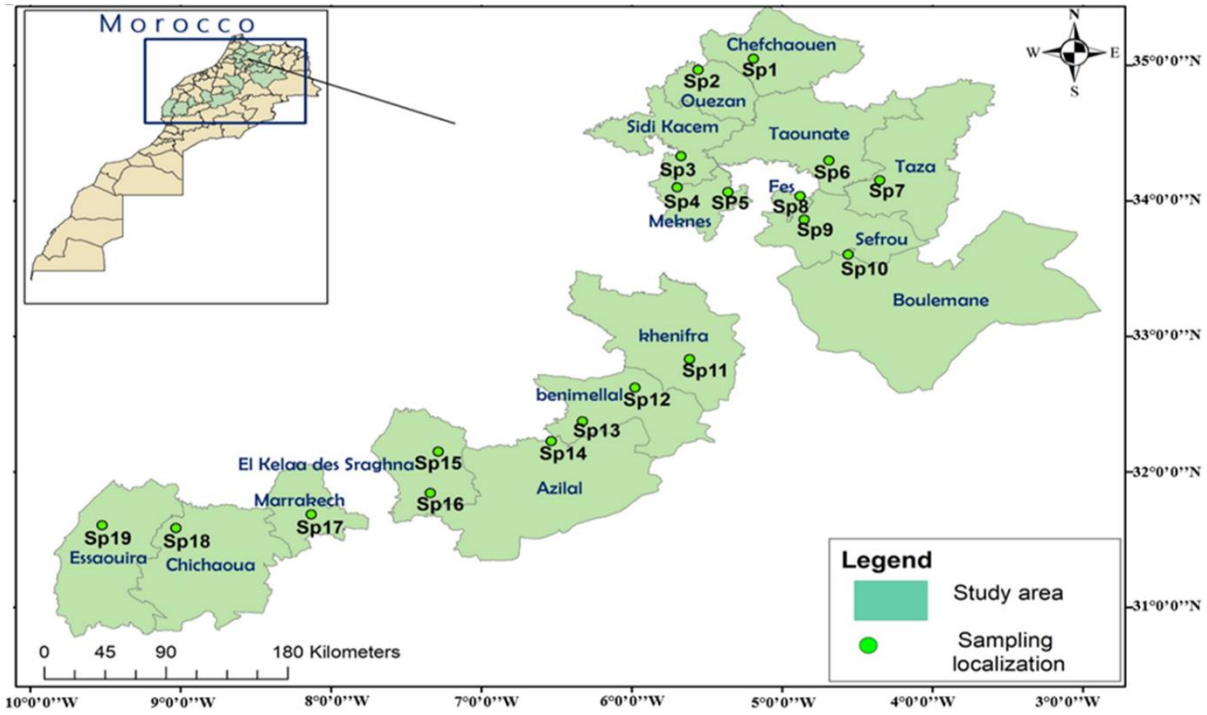

Figure 2.1. The geographic distribution with information about longitude and latitude of the studied sampling sites of EVOO in Morocco, green polygons represent the province of origin and small spots correspond to the 19 locations with ordered distribution from north to south, Sp1 to Sp19.

2.2.3 Chromatographic analyses of chemical compounds in olive oil

Phenolic compounds extraction

Phenolic compounds were extracted from VOO following a protocol described previously [26,28,29]. In brief, an amount of one gram of each olive oil (VOO or EVOO) was dissolved in one mL of n-hexane, followed by the addition of 1 mL of methanol:water (60:40, *v*/*v*), the mixture is then vortexed for 5 min, sonicated in an ultrasound bath (60 W, 25 ◦C, 37 Hz) for 2 min, and centrifuged for 10 min at 3000 rpm. The aqueous phase of 1 mL was collected and washed with 1 mL of *n*-hexane to discard the remained oil fraction. A volume of 20 µL (1000 ppm) of ethyl gallate was added to each extract prior to the injection to HPLC-PDA-ESI-MS.

HPLC-PDA-ESI-MS analysis of phenolic compounds

HPLC analysis was conducted on a Shimadzu instrument (Kyoto, Japan), which consisted of binary solvent pumps (LC-20AD), SPD-M20A photodiode array, and LCMS-2020 mass spectrometry (MS) detector. The instrument was equipped with an electrospray ionization

(ESI) source and conducted in negative ionization mode. In order to acquire data, Shimadzu LabSolution Ver. 5.91 software was employed (Kyoto, Japan).

Separation of phenolic compounds was performed on an analytical column Ascentis Express C18 (150 x 4.6 mm, 2.7 µm) (Merck Life Science, Merck KGaA, Darmstadt, Germany).

The employed mobile phases were as follows: A (H_2O) and B (acetonitrile) both acidified with 0.1% HCOOH; with a flow rate of 1 mL/min. The elution gradient was: 0.1 min 10% B, 4 min 35% B, 12 min 47% B, 12.5 min% B, min 60% B,16 min 75% B, 21 min 100% B and the injection volume was 5 µL. ESI-MS was performed with the optimized conditions as follows: capillary temperature 400 °C, capillary voltage 3500 V, nebulizer N_2 pressure 45 psi, drying N_2 flow rate 12 L/min, mass scan range (*m/z* 100–1000); the volume injection was 200 µL.

Validation of the chromatographic method included determination of the linearity, repeatability and recovery of the extraction at two levels of fortification; limits of detection (LODs) and limits of quantification (LOQs) were assessed based on 3:1 and 10:1 (signal-to-noise ratio). All the analyses and the calibration curves of the following compounds were acquired in single ion monitoring (SIM): gallic acid, hydroxytyrosol, tyrosol, caffeic acid, oleuropein, luteolin and apigenin. Their calibration curves were established at four different concentrations (1 mg/L, 25 mg/L, 50 mg/L and 100 mg/L), with 5 repetitions for each standard. Oleuropein calibration curve was provided for the quantification of the following compounds: derivatives and isomers of oleuropein, elenolic acid and oleacein. Hydroxytyrosol was employed for the quantification of verbascoside isomers and acetoxypinoresinol. Tyrosol and ligstroside aglycone were quantified with the calibration curve of tyrosol.

NP-HPLC/FLD analysis of tocopherols and tocotrienols

HPLC analyses were performed on a Shimadzu Nexera-X2 system (Shimadzu, Kyoto, Japan) composed of an online degasser (DGU-20ASR), an autosampler (SIL-30 AC), two dual-plunger parallel-flow pumps (LC-30AD), a column oven (CTO-20AC), and a fluorescence detector (RF-20AXS). Separation of tocopherols (α, β, γ, δ) and tocotrienols (α, β, γ, δ) was carried out on an Ascentis Si column (250 × 4.6 mm I.D., particle sizes of 5 µm, Merck KGaA, Darmstadt, Germany). VOOs samples were diluted in *n*-hexane (1:15 or 1:50) before their injection (5 µL) into the normal phase high-performance liquid chromatography (NP-HPLC) system coupled to a fluorescence detector with the following excitation and emission wavelengths of 290 and 330 nm, respectively. The employed mobile phase *n*-hexane-

isopropanol was run in isocratic mode (99:1, *v*:*v*), with a flow rate of 1.7 mL/min. Generated data were acquired through LabSolution Ver. 5.85 software (Shimadzu, Kyoto, Japan).

Fatty Acid Methyl Esters Extraction (FAMEs)

10 mg of virgin olive oil was mixed with 500 µl of sodium methoxide-methanol (0.5%, *w/v*). The solution was then stirred at 2000 rpm for 2 min and heated to 95°C for 15 min. Successively, 50 µL of boron trifluoride diluted in methanol (14% *w/v*) was added to the reaction mixture and the solution was mixed for 2 min at 2000 rpm and heated to 95°C for 15 min. After cooling, 350 µL of n-heptane and 300 µL of a saturated NaCl solution were added to the solution and vortexed at 2000 rpm for 2 min. Finally, the *n*-heptane FAME layer was extracted and injected into the gas chromatographic systems.

GC–MS/FID Analysis of FAMEs

FAMEs analysis was performed by GC–MS using a GCMS-QP2010 (Shimadzu, Duisburg, Germany) supplied with a split/splitless injector and AOC-20i autosampler. A SLBII60i capillary column (30 m × 0.25 mm id, 0.20 µm film thickness) was employed for chromatographic separation (Merck KGaA, Darmstadt, Germany). The column oven temperature was programmed in the range of 50 to 280 ˚C with a rate of 3 ˚C/min. The temperature of injection was 280 ˚C/min, with an injection volume of 0.2 µL, using a split ratio of 1:50. The employed carrier gas was helium with a linear velocity of 30 ˚C/cm and an inlet pressure of 26.6 kPa. The mass spectrometry conditions were set as follows: mass range of 40–550 *m/z*, electron ionization of 70 eV, ion source temperature of 250 ˚C, interface temperature of 200 ˚C, and detector voltage of 0.98 kV. FAMEs identification was facilitated by the employment of linear retention indices (LRIs) calculation, using C4–C24 standard solution. Peak assignments were accomplished by the means of MS similarity spectra (over 90%) and the comparison of LRI to the database values of lipids (LIPIDS Mass Spectral Library, Shimadzu, Kyoto, Japan).

GC-FID analyses were performed using a GC-2010 instrument (Shimadzu, Duisburg, Germany) equipped with a split/splitless injector, AOC-20i autosampler and FID detector. The utilized column and temperature program have remained the same as described for the GC-MS analysis. The FID parameters were as follows: FID temperature at 280°C, hydrogen flow at 40 mL/min, makeup flow (N_2) at 30 mL/min, and air flow at 400 mL/min. All experiments were performed in triplicate.

2.2.4 Characterization of soil physicochemical properties

The collected soil samples were dried in the open air to restrain microbial activity. Dried samples were subsequently ground to separate soil from gravel and pebbles prior to being

reduced into a homogeneous powder. After that, soil powder was sieved manually with 0.2 and 2 mm mesh, respectively. The active soil acidity (pH water) was determined using a pH meter according to the soil:water ratio of (1:2.5), and the conductivity by employing a conductivity meter. Total limestone ($CaCO_3$) was evaluated using Bernard's Calcimeter Method, total organic carbon and organic matter by the Walkley and Black method. Total nitrogen was also assessed using the Kjeldahl method. Furthermore, the available potassium was extracted with standard ammonium acetate and then quantified with a flame photometer. Each sample was analyzed in duplicate.

2.2.5 Statistical analysis

The obtained results of both low and large-scale studies were expressed as mean values ± standard deviation (SD). All data were subjected to principal component analysis (PCA) and were included in a heat map. Geographical origins of olive oils and pedoclimate were considered as the variables in these plots and the different biological compounds (phenolic compounds, vitamin E, and fatty acids), as treatments. PCA was applied to examine the relationship between the studied geographical origins, pedoclimatic conditions and different biological compounds.

2.3 Results and discussion

2.3.1 Study of VOOs of Picholine marocaine in 5 Moroccan provinces

A variety of phenolic compounds, vitamin E, and fatty acids were identified and quantified in the VOOs of *Picholine marocaine* obtained from samples collected from five Moroccan provinces (Taounate, Errachidia, Chefchaouen, Beni Mellal and Taza), as indicated in **Tables 2.1 and 2.2**. Since the investigated VOOs were commercial samples, their acidity was assessed in accordance with [27]. All 5 studied olive oils were classified as virgin olive oils according to the obtained acidity range from 1.1 to 2.0%.

The most abundant vitamin E was α-tocopherol in all analyzed EVOO samples (ranging from 38.38 mg/kg to 100.36 mg/kg), whereas δ-tocopherol has shown a lower content below the limit of quantification (LOQ) in all EVOO samples. The VOO obtained from Taounate (Fes-Meknes region) represented the richest value of vitamin E (107.63 mg/kg); on the other hand, the poorest sample was denoted in Taza, which belongs to the same region (46.07 mg/kg). Beni Mellal VOO has presented the highest content of α-tocotrienol with (7.60 mg/kg); on the other hand, α-tocotrienol content in Taounate and Errachidia was below the LOQ. A similarity in the qualitative and quantitative profiles of vitamin E in Errachidia and Chefchaouen was revealed.

The present results are consistence with Zarrouk et al. findings [33] conducted on Moroccan, Tunisian and Spanish olive oils, where α-tocopherol and γ-tocopherol were presented at levels of 30 mg/kg and 5 mg/kg, respectively. Moreover, α-tocopherol content in the studied VOO samples corresponds to the average content recommended by the United States Department of Agriculture (USDA) [34].

VOO were characterized by the presence of different classes of phenolic compounds, including phenolic alcohols (tyrosol and hydroxytyrosol), phenolic acids (caffeic acid, ferulic acid and elenolic acid), secoiridoids (oleuropein aglycone, 10-hydroxy-oleuropein aglycone and ligstroside aglycone, oleocanthal and oleacein) and flavonoids (luteolin, luteolin glucoside, apigenin). As reported in **Table 2.1**, VOO from Chefchaouen was found to have the highest phenolic content (723.47 mg/kg), in contrast, the lowest phenolic content was represented by the Errachidia (17.99 mg/kg). The content of different classes of bioactive compounds in VOO from the five studied regions was distributed as follows: phenolic alcohols (<LOQ-340.6 mg/kg), phenolic acids (13.06–89.55 mg/kg), secoiridoids (3.86–314.04 mg/kg) and flavonoids (1.07–17.96 mg/kg). As regards secoiridoids, the highest content was obtained from Taounate (314.04 mg/kg) and Chefchaouen VOOs (285.39 mg/kg). Whereas the highest amount of phenolic acid was attained in VOOs from Chefchaouen with 89.55 mg/kg, while the highest flavonoid content was noticed in VOO from Beni Mellal (17.96 mg/kg) followed by Taza (11.69 mg/kg). VOOs collected from the same region of Fes-Meknes, have shown an interesting difference in terms of bioactive molecules content. The vitamin E content in Taounate VOO was more than double that in Taza VOO, while the phenol content was seven times higher. This could be due to bottling or storage conditions that may have affected the VOO acidity level and consequently the level of bioactive molecules.

Table 2.1. Determination of phenolic compounds and vitamin E content in virgin olive oils (VOOs) of *Picholine marocaine* cultivar from five studied provinces. Results are expressed as average (mean ± SD) in mg/kg.

Compounds\Region (Provinces)	Fes-Meknes (Taounate)	Drâa-Tafilalet (Errachidia)	Tanger-Tetouan-Al Hoceïma (Chefchaouen)	Fes-Meknes (Taza)	Beni Mellal-Khenifra (Beni Mellal)
α-tocopherol	100.4 ± 0.14	55.8 ± 0.10	55.3 ± 0.27	38.4 ± 0.10	39.9 ± 0.24
α-tocotrienol	<LOQ	<LOQ	2.92 ± 0.07	1.97 ± 0.05	7.60 ± 0.04
β-tocopherol	2.1 ± 0.07	1.9 ± 0.07	2.1 ± 0.06	1.6 ± 0.07	1.7 ± 0.05
γ-tocopherol	5.2 ± 0.06	4.2 ± 0.05	4.5 ± 0.08	4.1 ± 0.10	4.3 ± 0.06
δ-tocopherol	<LOD	<LOD	<LOD	<LOD	<LOD
Tyrosol	<LOD	<LOD	300.6 ± 11.26	<LOD	186.2 ± 2.58
Hydroxytyrosol	6.4 ± 0.54	<LOD	40.0 ± 1.46	2.8 ± 0.15	4.6 ± 0.07
Caffeic acid	<LOQ	<LOD	<LOD	<LOD	3.5 ± 0.06
Ferulic acid	<LOD	4.4 ± 0.43	3.9 ± 0.07	2.0 ± 0.03	0.8 ± 0.04
10-hydroxy-oleuropein aglycone [a]	25.4 ± 0.09	1.2 ± 0.18	65.7 ± 3.81	0.3 ± 0.00	1.4 ± 0.24
Oleocanthal [a]	<LOD	<LOD	<LOQ	<LOQ	0.8 ± 0.00
Luteolin	<LOQ	<LOQ	6.4 ± 0.19	7.8 ± 0.72	6.3 ± 0.13
Oleacein	3.1 ± 0.15	0.2 ± 0.02	33.3 ± 1.91	2.3 ± 0.01	3.5 ± 0.17
Apigenin	<LOQ	<LOQ	<LOQ	<LOQ	6.1 ± 0.00
Oleuropein aglycone [a]	231.3 ± 4.45	1.9 ± 0.00	198.3 ± 13.17	18.6 ± 0.00	20.6 ± 1.24
Luteolin glucoside	2.5 ± 0.03	1.1 ± 0.51	1.5 ± 0.03	3.9 ± 0.22	5.5 ± 1.79
Elenolic acid	31.3 ± 2.00	8.7 ± 0.81	85.6 ± 2.67	13.7 ± 0.26	19.6 ± 1.63
Ligstroside aglycone [b]	57.3 ± 2.92	0.7 ± 0.04	21.4 ± 0.39	1.2 ± 0.07	3.9 ± 0.19
Acidity%	1.3%	2.0%	2.0%	2.0%	1.1%
Σ Vitamin E	107.6 *	61.9	64.8	46.1	53.5
Σ Phenolic alcohols	6.4	<LOD	340.6	2.8	190.8
Σ Phenolic acids	31.3	13.1	89.5	15.8	24.0
Σ Secoiridoids	314.0	3.9	285.4	20.1	26.6
Σ Flavonoids	2.5	1.1	7.9	11.7	18.0
Σ Phenols	354.2 **	18.1	723.4 **	50.4	259.4 **

Quantitative determination was carried out according to the following standard compounds: [a] oleuropein; [b] verbascoside; * values reported are above 90 mg/kg complying with Regulation 432/2012 of European Union [30]; ** values reported are above 250 mg/kg complying with the EU Health Claim [31].

Table 2.2. Average of relative quantification of fatty acid methyl ester extractions (FAMEs) in *Picholine marocaine* VOOs collected from five studied regions.

Fatty Acid	Mass Spectral Similarity (%)	Experimental LRI	Tabulated LRI	Taounate (%)	Errachidia (%)	Chefchaouen (%)	Taza (%)	Beni Mellal (%)
Palmitic acid (C16:0)	95	1600	1600	9.99	9.63	8.60	7.66	7.75
Hypogeic acid (C16:1n9)	91	1605	1605	0.31	0.33	0.32	0.32	0.37
Palmitoleic acid (C16:1n7)	96	1615	1616	0.65	0.61	0.47	0.32	0.33
Margaric acid (C17:0)	90	1694	1694	0.03	0.04	0.04	0.04	0.04
Margaleic acid (C17:1n7)	91	1707	1711	0.05	0.05	0.05	0.06	0.06
Stearic acid (C18:0)	95	1802	1801	2.08	2.95	2.42	2.35	2.49
Oleic acid (C18:1n9)	91	1812	1808	75.89	69.79	76.94	79.39	78.15
Cis-vaccenic acid (C18:1n7)	96	1816	1816	2.80	2.33	2.32	2.31	2.19
linoleic acid (C18:2n6)	95	1839	1838	6.71	12.67	7.41	6.25	7.29
α-linolenic acid (C18:3n3)	96	1883	1883	0.83	0.93	0.80	0.67	0.69
Arachidic acid (C20:0)	94	1999	2000	0.27	0.28	0.27	0.26	0.26
Eicosenoic acid (C20:1n9)	91	2014	2015	0.26	0.31	0.28	0.28	0.30
Behenic acid (C22:0)	92	2199	2201	0.07	0.06	0.06	0.07	0.06
Legnoceric acid (C24:0)	90	2400	2400	0.04	0.03	0.03	0.02	0.03

Quantitative variations in phenolic compounds can be attributed to various factors including environmental conditions (temperature, pH, moisture, soil, microorganisms etc.), harvesting method, fruit ripeness, extraction, or storage processes [35-37]. Results of the present study are in agreement with findings reported by Bajoub et al. [38], where secoiridoid content was present in high concentration with respect to the low concentration presented by flavonoid and phenolic alcohol (except Taounate province). The amount of tyrosol obtained in Chefchaouen VOOs (300.57 mg/kg) and Beni Mellal (186.17 mg/kg) is much higher compared to the average content in commercial extra virgin olive oils (EVOOs) present on the Italian and European markets (56 mg/kg) [28], This can be explained by the hydrolysis of oleuropein and oleacin [13]. The obtained values are not in agreement with the reported ones by Bajoub et al., where the concentration of tyrosol in VOOs of *Picholine marocaine* from Chefchaouen, Taounate and Taza varied from 4.43 mg/kg to 7.46 mg/kg [38]. Similarly, in terms of hydroxytyrosol Bajoub et al. have reported an amount that ranges from 5.10 to 5.86 mg/kg, which is different from the values attained in the present study (<LOQ-40.03 mg/kg). Regarding secoiridoids, oleuropein aglycone (1.94–231.34 mg/kg), ligstroside aglycone (0.72–57.27 mg/kg) and 10-hydroxy-oleuropein (0.26–65.73 mg/kg) were obtained in the highest amount, while the lowest amount was achieved for oleacein (0.20–33.27 mg/kg) and oleocanthal (<LOQ-0.76 mg/kg). In comparison to the study led by Bajoub et al., the amount value of secoiridoids in VOOs of *Picholine marocaine* obtained from Meknes ranged from 504.12 to 1106.96 mg/kg for the crop season of 2011–2013 [39]. Moreover, oleuropein aglycone has shown the highest amount in VOO of *Picholine marocaine* from Chefchaouen and Taounate, where the lowest amount was found in Errachidia VOO. Similarly, ligstroside aglycone amount was very low in VOO from Errachidia, while the maximum amount was achieved in VOO from Taounate [38]. Elenolic acid was the most abundant phenolic acids in VOO with an average range from 8.7 to 85.6 mg/kg; where the highest amount was found in VOO from Chefchaouen (85.61 mg/kg), followed by Taounate (31.28 mg/kg) and Beni Mellal province (19.65 mg/kg). According to a study performed on *Picholine marocaine* VOO collected during the crop season (2011/2012), phenolic acids ranged from 0.13 to 0.22 mg/kg [40]. In contrast Bajoub et al. who have reported the highest amount of elenolic acid in VOO from Taounate, whereas Chefchaouen and Taza VOOs represented the lowest amount [38]. Regarding flavonoids, the average content of luteolin and apigenin in VOOs was in the range of (<LOQ - 7.80 mg/kg) and (<LOQ - 6.09 mg/kg), respectively. The achieved data on flavonoids are consistent with recently reported data through studies performed on *Picholine marocaine* VOOs,

where average contents of luteolin and apigenin varied between 3.20 mg/kg in Errachidia and 7.5 mg/kg in Meknes, respectively [33,40].

Regarding fatty acid methyl esters (FAMEs), which were analyzed only in the low-scale study on VOOs, 14 FAMEs were identified using GC-FID/MS. Qualitatively all the VOOs presented an equivalent profile in **Table 2.2**, whereas some distinctions were discovered at the quantitative level in the percentage composition of FAMEs. Where, the most abundant FAMEs were represented by oleic acid with a range of 69.79%–79.39%, followed by palmitic acid (7.76–9.99%), and linoleic acid (6.25–12.67%). In terms of oleic acid, the highest content was found in Taza (79.39%), followed by Beni Mellal (78.15%), Chefchaouen (76.94%), Taounate (75.89%) and Errachidia (69.79%). According to a previous study led on *Picholine marocaine* VOOs, Errachidia and Marrakech VOOs have presented the lowest percentage of oleic acid, while the highest content was found at the level of palmitic acid and linoleic acid [41]. Based on the results of the present study, the VOO from the Errachidia province showed a slightly different content of oleic and linoleic acids.

The concentration of linoleic acid exhibited a value of 12.67%, which is approximately double the concentration of the other studied VOOs; however, the concentration of oleic acid was 10% lower than the VOO with the highest content, viz. Taza. The reasons for such variations across regions could be largely related to the crop season (climate), the stage of maturity, and the geographic location, e.g., the desert area where olive trees grow [42].

To provide better visualization of the correlation of VOO chemical composition with the five different studied provinces, a heat map was drawn up (**Figure 2.2**). The relationships found between VOOs chemical compounds and geographic origins are presented in the form of clusters. Tyrosol, hydroxytyrosol, oleacein, elenolic acid, and 10-hydroxy-oleuropein aglycone distinguish the VOO from Chefchaouen, where α- and β-tocopherols, fatty acids, e.g., palmitic (C16:0), cis-vaccenic acid (C18:1n7), behenic (C22:0) and lignoceric (C24:0) are the characteristic compounds of Taounate province. Errachidia can be distinguished by the following compounds: hypogeic (C16:1n9), stearic (C18:0), eicosenoic (C20:1n9), linoleic (C18:2n6), arachidic (C20:0) and α-linoleic (C18:3n3) acids, beside the ferulic acid. The characteristic bioactive compounds of Beni Mellal province comprise apigenin, caffeic acid, oleocanthal, luteolin glucoside and α-tocotrienol. Lastly, Taza province is characterized by the presence of luteolin and luteolin glucoside, oleic (C18:1n9) and margaric acids (C17:0).

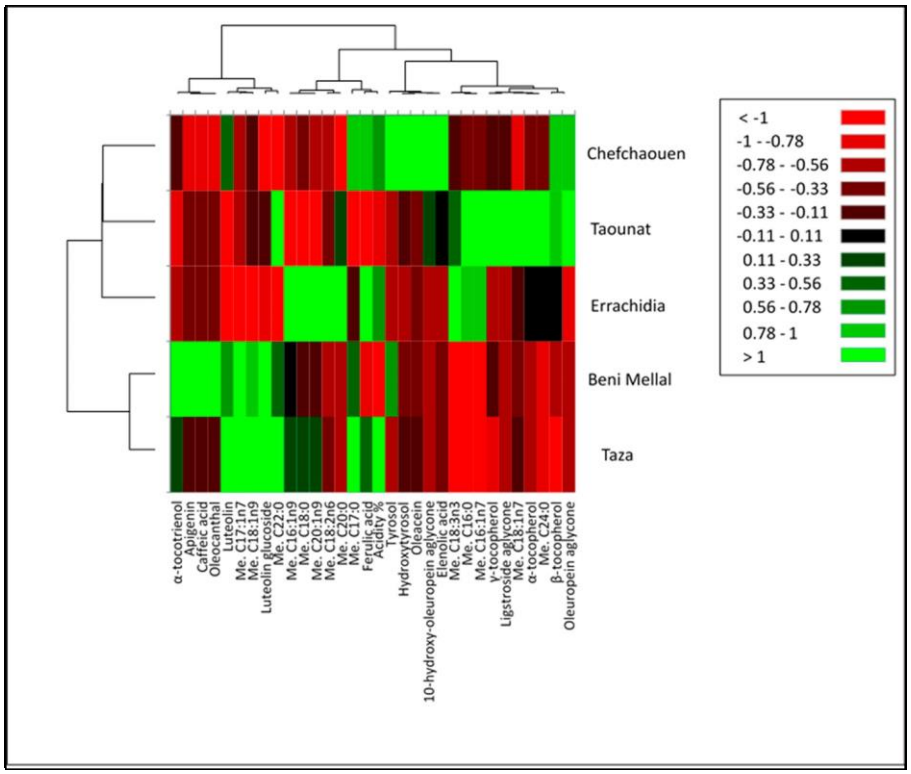

Figure 2.2. Heat-map and dendrogram visualization of different bioactive compounds; phenolic compounds, fatty acids, and vitamin E in *Picholine marocaine* VOOs from five Moroccan provinces. Green boxes refer to a higher concentration than the mean value among the studied samples. Red boxes refer lower concentrations.

The principal component analysis (PCA) approach was applied in the present study, in order to approve the relationships between the descriptive variables, phenolic compounds, vitamin E and fatty acids, and the studied VOOs from the five provinces.

A value of 71.2% was explained by the first two principal components (F1 and F2), whereas a value of 60.8% was explained by F1 and F3. PCA yielded results similar to those obtained by the heat-map. As it is shown in **Figure 2.3a**, a positive correlation was attended between Taza and Beni Mellal; on the other hand, in both **Figures 2.3a, and b**, a negative correlation between Beni Mellal and Taounate was observed. Furthermore, a negative correlation was highlighted between the following provinces: Errachidia–Beni Mellal, Chefchaouen–Tauonate, and Chefchaouen–Beni Mellal. Also, as shown in **Figure 2.3a**, no correlation was established between Errachidia and Taounate.

(a)

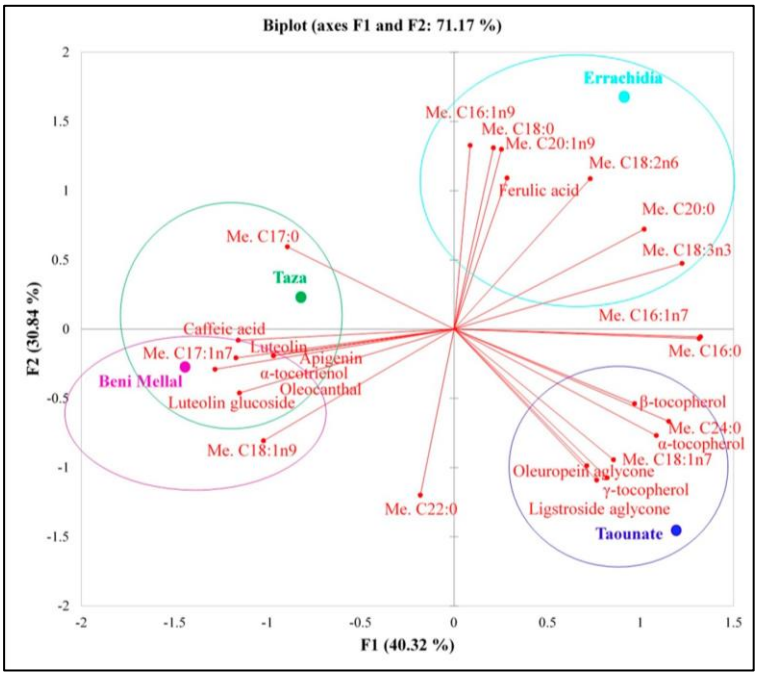

(b)

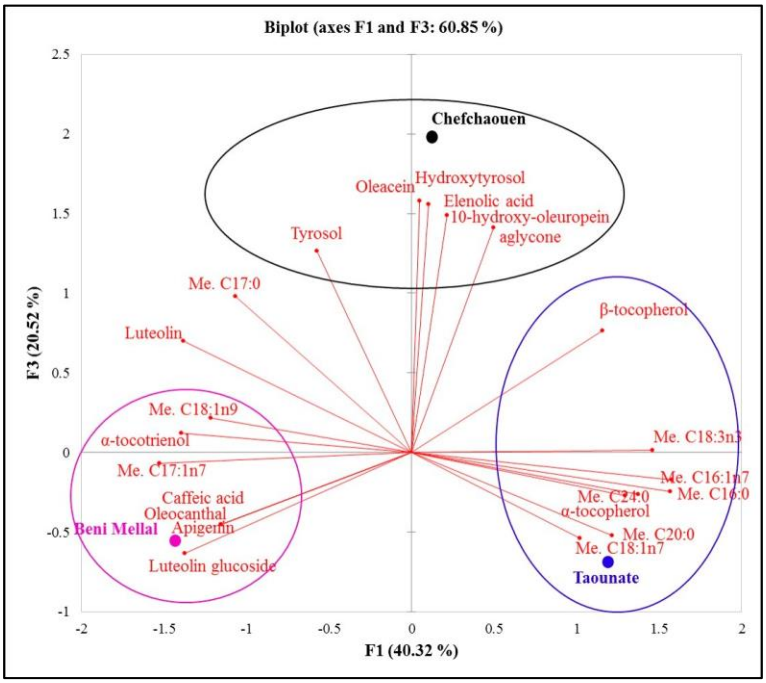

Figure 2.3. Principal component analysis (PCA) between phenolic compounds, vitamin E and fatty acids in VOO of *Picholine marocaine* and five provinces studied. (**a**) The first and second discriminant function; (**b**) the first and third discriminant function.

2.3.2 Study of EVOOs of Picholine marocaine in 19 Moroccan provinces

In the large-scale study executed in Morocco during 2018 and 2019 on *Picholine marocaine* EVOO, 23 hydrophilic polyphenols classified into four major classes were ascertained: phenolic acids, phenolic alcohols, flavonoids, and secoiridoids and derivates. **Table S2.1** shows that total phenol content ranges from 110.1 mg/kg (Sp6) to 4105.7 mg/kg (Sp2) and from 52.8 mg/kg (Sp10) to 1420.8 mg/kg (Sp5) for both crop seasons 2018 and 2019, respectively. Essentially, almost all the analyzed EVOO samples present an amount of phenolic compounds that falls within the average (250 mg/kg), which is recommended by the European Commission Regulation [43]. A similar range (50-1000 mg/kg) for the levels of total polar phenols in EVOO is reported in the book of Boskou [44].

In an investigation conducted by Diamantakos et al. [45] for 11 years, 5764 samples of olive oil from Greece of more than 30 varieties were analyzed by qNMR for their phenolic content.

A maximum amount of 4003 mg/kg of total phenols was achieved in oils produced in September 2017 from the variety *Kalamon*, indicating a significant correlation between the crop year and phenols. Another study investigated 44 varieties of olive oil throughout 3 years, and has shown a range (260 - 4497 mg/kg) of total phenolic compounds content during the 2017–2018 crop season [46].

Concerning the main represented classes of phenolic compounds in olive oils, secoiridoids and derivates represent the main class with an average of 1112.3 (for 2018) and of 705.85 mg/kg (for 2019), followed by the class of phenolic alcohols with a total average of 86.69 and 20.45 mg/kg for 2018 and 2019, respectively. The penultimate class is represented by phenolic acids in the range from 6.00 (Sp3) to 48.10 (Sp1) mg/kg for 2018, and from 3.54 (Sp18) to 34.33 (Sp3) for 2019. Flavonoids represent the minor class in the studied EVOOs with an average of 10.25 and 9.54 mg/kg for 2018 and 2019, respectively.

The exceptional resistance to oxidation of EVOOs is primarily due to the dialdehydic form of elenolic acid linked to 3,4-DHPEA (3,4-DHPEAEDA), decarboxymethyl 3,4-DHPEAEA, and 3,4-DHPEA. However, p-HPEA, lignans, and p-HPEA-EA were proved as weaker antioxidants [44]. According to Tuck and Hayball [47], oleuropein glycoside (heteroside of elenolic acid), 3,4-DHPEA and p-HPEA represent the highest amount (around 90%) of phenolic compounds in EVOO. As confirmed in the present study, 3,4-DHPEAEA appeared in good quantities with an average of 615.83 and 367.01 mg/kg, followed by elenolic acid 166.66 and 184.49 mg/kg and p-

HPEA-EA with a total average of 136.92 and 89.90 mg/kg in EVOO for 2018 and 2019, respectively.

In agreement with Moroccan findings [39,48], our analysis of the two crop years indicated higher levels of p-HPEA than 3,4-DHPEA as phenolic alcohols.

Generally, such an aspect is related to the storage period of olive oil [49], this results in the formation of hydrophilic compounds from secoiridoids.

In terms of flavonoids, luteolin was the most abundant compound (7.06 and 9.32 mg/kg for 2018 and 2019, respectively), followed by luteolin glucoside (4.32 and 1.12 mg/kg, respectively for 2018 and 2019).

Tocopherols (Vitamin E)

Five vitamin E isomers (α, β, γ, δ tocopherol and α-tocotrienol) were characterized in the EVOO samples examined in this work. The total content of vitamin E varied between 38.4 (Sp10) and 213.0 mg/kg (Sp14) in the crop year of 2018 and between 48.4 (Sp2) and 147.3 (Sp7) in the crop year of 2019, with a total average of 139.8 ± 36.46 and 92.60 ± 30.00 mg/kg, respectively. α-tocopherol was the most abundant isoform (91.5% and 87% of total vitamin E, respectively for 2018 and 2019) with an average of 122.7 ± 36.84 and 80.39 ± 27.68 mg/kg, a range of 32.9 ± 0.4 (Sp10)-201.1 ± 0.08 (Sp14) and 33.9 ± 0.4 (Sp10)-129.2 ± 0.4 (Sp7). It was followed by γ-tocopherol (7 and 6.5%) with a total content average of 6.6 ± 1.46 and 6.06 ± 2.48 mg/kg, for 2018 and 2019, respectively. On the other hand, the abundance of β-tocopherol and α-tocotrienol was different between the 2 successive crop years; in 2018 β-tocopherol content was more abundant than α-tocotrienol (1%). Whereas the abundance of both vitamin E was inverted in 2019, δ-tocopherol was found in trace, with an average of 0.66 ± 0.15 and 0.47 ± 0.34 mg/kg for 2018 and 2019, respectively.

The attained results regarding the average content of α-tocopherol are consistent with the recommended amount by USDA [50]. Moreover, a wide range of α-tocopherol content has been reported in different Mediterranean olive oils, such as Italian, Spanish, and Greek oils, with typical content values that range from 100 to 250 mg/kg oil [44]. The obtained results are consistent with those performed on Italian EVOO by Różańska et al. [28], where the total content of vitamin E was in the range of 70.2 and 232.2 mg/kg, with an average of 169.0 ± 37.7 mg/kg, as well, α-tocopherol was the main and abundant tocopherol isomer. Additionally, δ-tocopherol content appears to agree with that of the "*Picholine marocaine*" [51], where the content of δ-tocopherol was reported as 0.5 mg/kg. As well, Bedbabis et al. [52] have reported similar content

of δ-tocopherol in olives irrigated with well water and treated wastewater of 0.42 and 0.35 mg/kg in oils, respectively. Whereas, in Greek VOO, Psomiadou et al. [53] have reported an average content of δ-tocopherol of 4 mg/kg.

Pedoclimatic conditions

Climatic and edaphic information regarding the studied geographic sites is reported in **Table S2.2**. EVOO Sp10 was collected from a heavy rainfall site (639 mm); whereas, Sp18 received the lowest value of precipitation (145 mm). The yearly temperature average was between 14.04 and 18.22 °C and the wind speed was within 1.7–4.34 m/s.

Particle size is a key variable in agriculture. The percentage of sand in the studied samples ranged between 1.64% (Sp2) and 57.19% (Sp11), which is within the values (≤ 75%) established by the IOC [54], while silt and clay fractions were above the standard values. Thoroughly, 53% of the samples were silt loam, 21% are silty clay loam, 16% were clay loam, and about 5% were sandy loam and silty clay textures. Olive trees' growth appears to be favoured by such balanced proportions.

Results regarding soil physicochemical parameters have shown important reliability to olive tree growth, in particular, pH (except for Sp1), electrical conductivity (EC) and limestone, were within the optimal values for olive-growing areas [54], where pH varied in a range between 5.43 (Sp1) and 8.84 (Sp16) and the EC values did not exceed 2 dS/m. In addition, organic matter ranged from 0.57 to 3.29% with 84% of samples >1% (the optimum). Potassium levels ranged from 40.68 to 393.32 ppm, and C/N ratios from 5.35 to 32.38 indicating large variation between sampling sites.

The influence of geographical origin

Three main parameters comprise geographical origin; location (latitude, longitude, and altitude), soil composition, and climate which encompasses temperature, rainfall, humidity, and wind speed. The soil provides plants and microorganisms with organic and mineral components that they need to grow and thrive. Since the latter plays a prominent role in the nutrition of plants, its texture is essential for tree roots and water infiltration.

Hence, variability in soil composition could affect the olive tree, fruit and thus EVOO quality. Taking into account the variability of all these parameters, we attempted to study their impact on the bioactive profile of VOO by the correlation test and the PCA.

In effect, a thorough study including the impact of pedo-climatic factors, requires an accurate collection of EVOOs samples from different geographical sites characterized by the distinct location and climates, the same cultivar *Picholine marocaine*, and during the same period (November 2018). Fruit ripeness and geographic origin's climate present a tight relationship according to Bajoub and his co-authors [55,38] who disregarded the ripening index while examining the geographic origin discrimination in EVOOs from "*Picholine marocaine*" in a large Northern Moroccan area.

Principal component analysis (PCA)

Five main components were extracted because their cumulative variance was 54.4% PC1× PC2 and PC1 × PC3 were plotted as they were sufficient for the interpretability of the main correlative links between the variables studied. The first two eigenvectors carry 43.8% of the dataset information, dimensions 1 and 2 had 26.2 and 17.6% of affinity between EVOO phytochemical compounds, soil, climate and geographic origin parameters, respectively. Together, Dim 1 (26.2%) and Dim 3 (10.6%) carried 36.8% of the information. The relatively small fluctuations in the data described by PC1 and PC2 could be caused by the low variability of the parameters.

The two first components PC1 and PC2 have shown a good distribution of the studied variables, with a negative correlation between the following pedoclimatic parameters; latitude, rainfall, longitude, and bioactive compounds; α-tocotrienol and flavonoids (luteolin, apigenin, and luteolin glucoside) **Figure 2.4**. on the other hand, these latter bioactive compounds were correlated positively with conductivity. According to an investigation led by Guerfel et al. regarding the effect of three different geographic origins on two Tunisian VOO cultivars "Chemlali" and "Chétoui" [56], a considerable difference in EVOO characteristics were highlighted in the three studied locations. Likewise, Romero et al. have concluded that Latitude reinforces the effect of geographic origin [57]. Other studies performed on other matrices have confirmed the relationship between salinity (conductivity) and phenolic compounds, particularly flavonoids [58]. Moreover, Talhaoui et al. have confirmed that salinity stress combined with high sunlight exposes the plant to an overproduction of phenolic compounds, particularly flavonoids [59].

Furthermore, relative humidity, wind speed, and C/N ratio have shown a positive correlation with flavonoids and α-tocotrienol, as well, as with methyl 3,4-DHPEA-EA. Whereas a negative relationship was observed with the following compounds: hydroxy decarboxymethyl 3,4-DHPEA-EA, α, β, and γ-tocopherol. Through the study of PC1 × PC3 components, a negative

impact of the percentage of soil limestone ($CaCO_3$) on the δ-tocopherol amount was detected. Similarly, soil parameters (pHwater and available potassium) have shown a negative relationship towards hydro decarboxymethyl elenolic acid and gallic acid. Fundamentally, soil pH is the most significant factor since it affects almost all parameters of soil [60]. An investigation on the impact of soil pH on the stability of phenolic compounds was led by Friedman and Jürgens, where gallic acid was unstable in an alkaline medium [61], thus a high concentration of gallic acid in VOO sample from Sp1 was explained by the slight acidity of the soil (5.43 ± 0.13).

Considering climatic factors, according to the obtained results in this present study, rainfall occurs to affect considerably the content of phenolic compounds, which was consistent with the literature [62]. Furthermore, different phenolic profiles were detected in a study led on olive tree cultivation areas, where it was supposed to be affected by the climate condition, particularly rainfall [56]. On the other hand, Proietti et al. have stated that EVOO phenols content was greatly influenced by olives produced in high temperatures during summer and autumn with respect to olives growth in the cold atmosphere [63], whereas, Romero et al. have reported the influence of low temperatures during the harvest period on α-tocopherol yield [62]. Though, no relationship was observed between temperature and bioactive compounds.

In addition to PCA, and according to the correlation matrix a positive impact was observed ($r = 0.51$, $p < 0.05$) and ($r = 0.53$, $p < 0.05$) between the percentage of slit and α and β-tocopherol, respectively. Conversely, the slit percentage has shown a negative correlation ($r = -0.58$, $p < 0.01$) with decarboxymethyl elenolic acid dialdehyde (DEDA). The obtained results on the effect of soil parameters on the quality of EVOO reflect literature findings, where Rouas et al. have suggested that the variation in soil limestone percentage has had an impact on total EVOO bioactive content [64]. Whereas Rached et al. have observed the impact of soil type on the total content of phenolic compounds in EVOO [65].

Furthermore, the PCA results have shown a considerable positive correlation ($r = 0.61$, $p < 0.01$) between dehydro 3,4-DHPEA-EA and altitude. To some extent, the obtained results agree with literature findings where phenolic compounds are positively correlated with the altitude of the olive tree [66]. On the other hand, “Mastoides” olives have shown a negative correlation between phenol compounds and altitude [67].

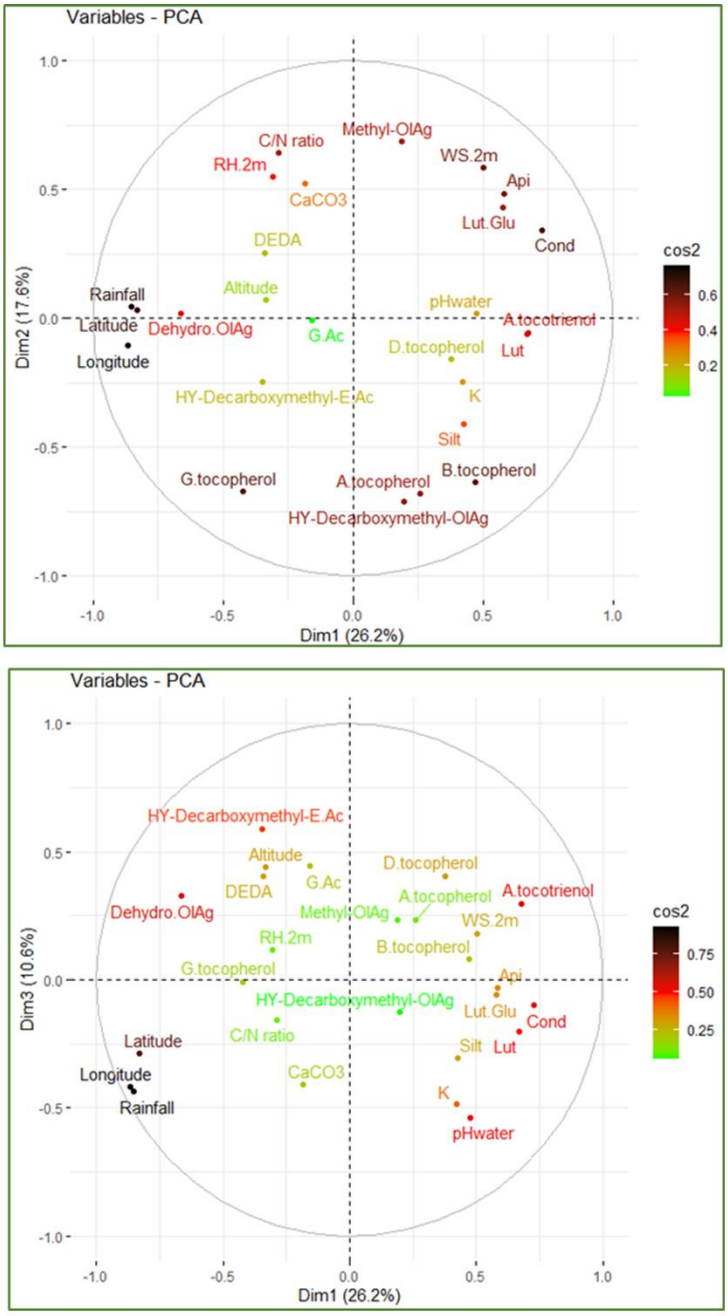

Figure 2.4. PCA principal component analysis of EVOO variable components; phenolic compounds, vitamin E, and pedo-climate parameters. Top (PC1 x PC2) and bottom (PC1 x PC3).

Elenolic acid, Lut: luteolin, Api: apigenin, HY-Decarboxymethyl-Ol.Ag: hydroxy decarboxymethyl 3,4-DHPEAEA, Dehydro. Ol.Ag: Dehydro 3,4-DHPEA-EA, DEDA: decarboxymethyl elenolic acid dialdehyde, Methyl-Ol.Ag: Methyl 3,4-DHPEA-EA, A-tocopherol: α-tocopherol, B-tocopherol: β-tocopherol, G-tocopherol:ϒ-tocopherol, D-tocopherol: δ-tocopherol. Cond: conductivity, $CaCO_3$: limestone, K: available potassium, WS.2 M: wind speed at 2 m, RH.2 M: Relative humidity at 2 m.

In summary, several correlations were observed through PCA: all vitamin E and isomers, two phenolic acids (gallic acid and hydroxydecarboxymethylelenolic acid), flavonoids (luteolin, apigenin, luteolin glucoside), and four secoiridoids and derivatives (dehydro 3,4- DHPEA-EA, methyl-3,4-DHPEA-EA, Hydroxydecarboxymethyl-3,4-DHPEA-EA, Decarboxymethylelenolic acid dialdehyde (DEDA) were correlated with geographic parameters (latitude, longitude and altitude), climate (except for temperature) and some soil parameters: texture (amount of silt), water pH, conductivity, available soil potassium, limestone ($CaCO_3$) and C/N ratio. However, phenolic alcohols have shown no correlation with other studied variables.

Hierarchical cluster analysis of principal components (HCPC)

To categorize the sampling sites, a cluster dendrogram was employed to characterize EVOO samples which share similarities at the level of bioactive compounds as well as geographic parameters. 5 clusters were distinguished based on the dendrogram (**Figure 2.5**). The first cluster consists of one sampling site (Sp10), characterized by the highest content of C/N ratio, methyl 3,4-DHPEA-EA, and limestone ($CaCO_3$), as well the lowest quantities of α, β and γ-tocopherol. Where cluster 2 which includes (Sp1, Sp9, and Sp11) was characterized

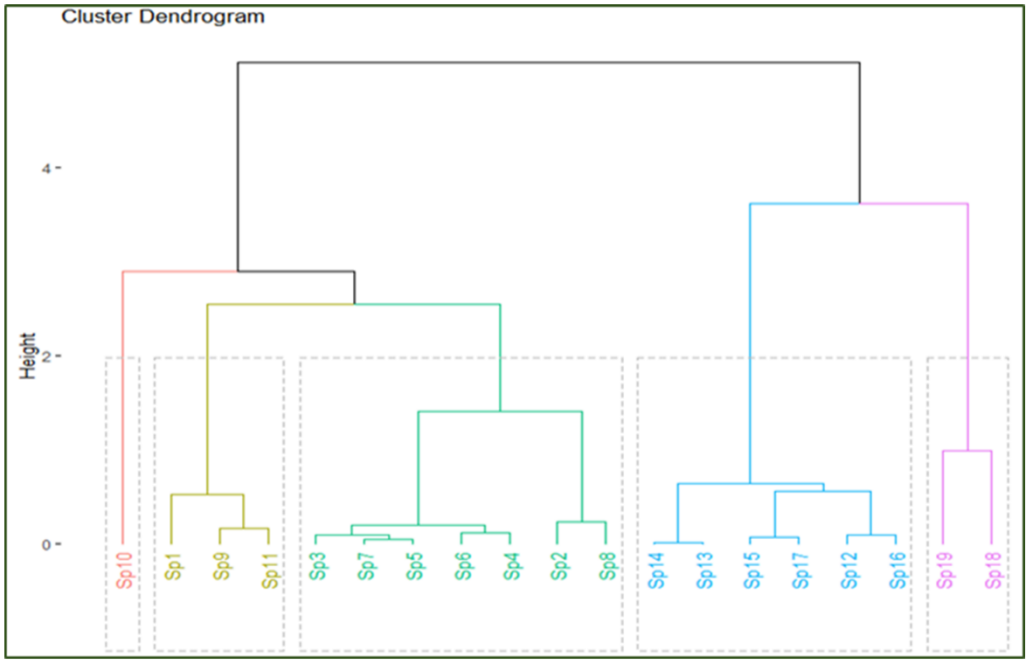

Figure 2.5. Dendrogram of the hierarchical cluster analysis of principal components (HCPC) using Ward's criterion on the first and the second principal components. The grey dashed rectangles point out the cut in the tree, resulting in five clusters: (1, Red), (2, Yellow), (3, Green), (4, Blue), and (5, Purple).

by the presence of hydroxy decarboxymethyl elenolic acid, dehydro 3,4-DHPEA-EA, gallic acid, and available potassium.

The third cluster consists of seven sampling sites (from Sp2 to Sp8) that are mainly distinguished by heavy rainfall and low altitudes. The cluster was further divided into two substantial sub-clusters. Where Sp2 and Sp8 included a high percentage of $CaCO_3$ and Decarboxymethyl elenolic acid dialdehyde showed no value. Besides, high similarity in sand percentage was shown in Sp3, Sp5, and Sp7. Cluster 4 comprised two important sub-clusters and six sampling sites (from Sp13 to Sp17), where Sp13 and Sp14 disclosed the highest content of hydroxy decarboxymethyl 3,4-DHPEA-EA among all examined locations. Further, Sp12 and Sp16 have reported the lowest percentage of $CaCO_3$ and β-tocopherol among all the studied locations. In general, this cluster is characterized by a high content of β-tocopherol, hydroxydecarboxymethyl-3,4-DHPEA-EA and α-tocotrienol. In contrast, $CaCO_3$, rainfall and relative humidity have shown a low value. Based on the comparison of averages of variables of the fifth cluster to the overall averages, a high rate of wind speed, apigenin, luteolin glucoside, methyl-3,4-DHPEA-EA, conductivity and a low amount of γ-tocopherol and rainfall were revealed.

Overall, most classified groups showed very close geographic proximity; With the exception of cluster one and two, fifteen sampling sites were well clustered geographically. Briefly, Moroccan EVOO quality is strongly influenced by the production zone as evidenced by the substantial differences observed in phytochemical composition between sampling areas. Remarkably, the achieved results could provide geographic traceability of the quality of EVOO in Morocco.

Crop season impact

As reported in various studies, the crop year could significantly influence the quality of the EVOO. Accordingly, the impact of the crop year on the quality of Moroccan "*Picholine marocaine*" EVOO was assessed through the analysis of bioactive compounds content in 2018 and 2019.

The histograms in **Figure 2.6** show a comparative analysis between the two crop seasons which demonstrate that the phenol groups and vitamin E levels were significantly different in the two crop seasons. With the exception of flavonoids, all other classes showed significant variability. Moreover, a two-way ANOVA analysis was performed with a post hoc test have confirmed these

observations; the effects of crop seasons, sampling sites and their interaction with vitamin E and phenolic compounds were significant ($p < 0.0001$).

Furthermore, remarkable differences can be seen clearly in the histogram where a two-way ANOVA statistical test was applied **Figure S2.1.** An important difference in the level of polyphenol content in EVOO from Ouazzane (Sp2) was noticed between the 2018 and 2019 crop years. Similarly, EVOOs from Azilal (Sp14) have shown significant differences regarding tocopherols. On the other hand, EVOOs from different geographic locations have shared quantitative similarity in the same crop year as regards phenolic compounds content, such as Fes and Azilal, Essaouira and Khenifra, and Chefchaouen, Marrakech, and Sefrou were similar in 2018 crop year, whereas values from Chefchaouen, Taza and Taounate were similar for 2019 season. Regarding tocopherols, Beni Mellal, Sefrou, Essaouira and Fes shared a similar quantity in 2018, whereas El Kelaa des Sraghna, Khenifra, and Sefrou were similar for the 2019 crop season.

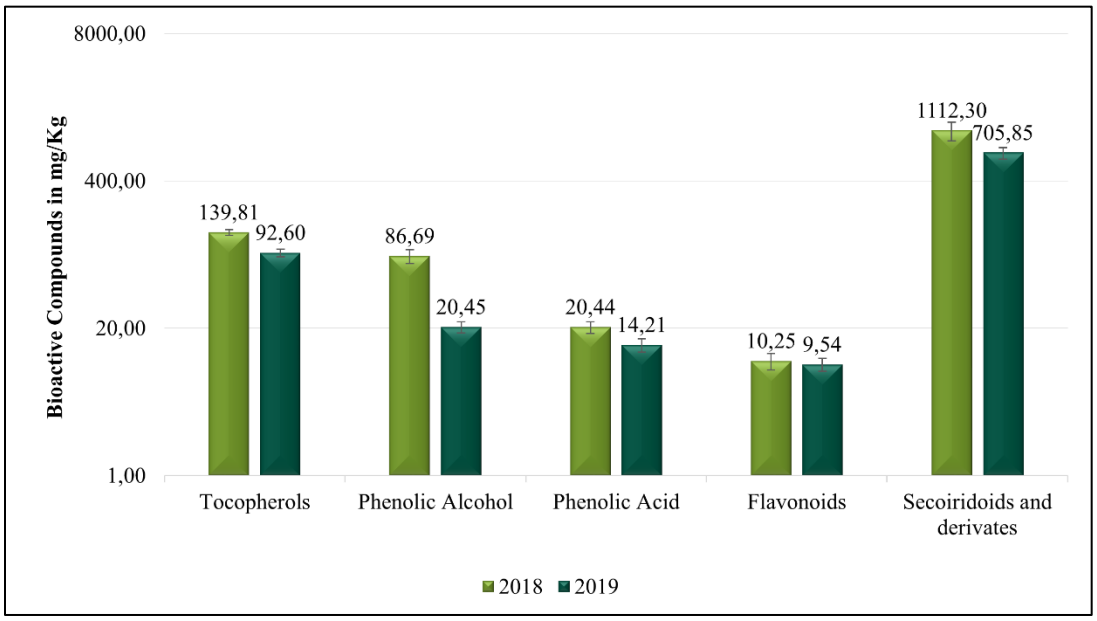

Figure 2.6. Classes of bioactive fractions (tocopherols, phenolic alcohol, phenolic acid, flavonoids and secoiridoids and derivates) amount expressed in (mg/kg) of the Moroccan EVOO during two successive crop seasons 2018 and 2019.

Although the harvest times for the two successive years were different, considering that the two consecutive years were conducted in November and December, respectively, it is possible to explain at least in part the dissimilarity observed by the different harvest times for the olive trees.

Previous studies have demonstrated a significant relationship between bioactive compounds and the season in which they are produced, with the evaluation of the quality differences between three Moroccan varieties of EVOO (Arbequina, Arbosana, and Koroneiki) grown over two crop seasons, Mansouri et al. [68] have concluded that phenols and oxidative stability were correlated to the production crop season, a considerable variability with a significant effect of the year ($p < 0.001$) was noticed by Romero et al. [62], as well as, Bajoub et al. [39]. On the other hand, some other authors have observed a minor influence on the crop season.

However, they have suggested that rather than seasonal weather variations, harvest times in each season may affect antioxidant conditions, which decrease as the olive fruit ripens [69]. Interestingly, tocopherol and phenolic compounds levels are reported to decrease in ripened fruits [70,71].

2.4 Conclusion

In the first part of this study, bioactive compounds including phenolic compounds, vitamin E and fatty acids of *Picholine marocaine* VOO obtained from 5 Moroccan provinces were assessed by HPLC-PDA/ESI-MS, NP-HPLC/FLD and GC–MS/FID, respectively. Among the *Picholine marocaine* VOOs tested, a variable amount of phenols was found, including tyrosol, hydroxytyrosol, oleuropein aglycone, and vitamin E. According to current international regulations, the phenolic content of three provinces, namely Taounate, Chefchaouen and Beni Mellal, coincide with the established limit values [30]. Whereas, in terms of vitamin E, only Taounate which was conformed with Regulation 432/2012 of the European Union [31]. As regards fatty acids content, all five studied provinces have satisfied the limits stated by COI 2001 [32].

The principal component analysis and heat-map permitted the clustering of the studied 5 provinces according to the VOO chemical composition, which facilitates the characterization of samples of different provinces based on their bioactive compounds. These results were considered preliminary ones for the second part of the study, which included EVOO from 19 different Moroccan provinces during two consecutive harvest years 2018 and 2019. Aiming to determine the effects of edaphic, climatic conditions and harvest year on the levels of bioactive EVOO compounds. The examined EVOO samples have disclosed 23 hydrophilic and 5 lipophilic phenolic compounds, where geographic origin has shown an important influence. Substantially, PCA has emphasized the established correlations between some bioactive compounds and different geographic factors, particularly pedo-climatic parameters. Moreover, crop year has also shown an important impact on phenolic compounds and vitamin E content. In particular, harvest time can influence significantly the phenolic fraction of EVOO. Eventually, the achieved findings support the impact of pedoclimatic conditions on EVOO quality.

2.5 References

1. Moroccan Ministry of Agriculture and Marine Fisheries. Statistiques du Secteur Oléicole Marocain. Available online: http://www.agriculture.gov.ma/pages/rapports-statistiques/campagne-agricole-2015-2016 (accessed on 5 October **2020**).
2. International Olive Council (IOC). The Olive Grove in Morocco. *O*ff. *J. Int. Olive Counc.* **2019**, *125*, 1–89. Available online: www.internationaloliveoil.org (accessed on 12 October 2020).
3. Azaizeh, Hassan, Hiba N. Abu Tayeh, and Yoram Gerchman. 2020. "Valorisation of Olive Oil Industry Solid Waste and Production of Ethanol and High Value-Added Biomolecules." In Biovalorisation of Wastes to Renewable Chemicals and Biofuels, 27–40. Elsevier.
4. Azbar, Nuri, Abdurrahman Bayram, Ayse Filibeli, Aysen Muezzinoglu, Fusun Sengul, and Adem Ozer. 2004. "A Review of Waste Management Options in Olive Oil Production." Critical Reviews in Environmental Science and Technology 34 (3): 209–47.
5. Campagne Agricole 2015–2016. Département de L'agriculture-Ministère de L'agriculture, de la pêche Maritime, du Développement Rural et des Eaux et Forêts. Available online: http://www.agriculture.gov.ma/ pages/rapports-statistiques/campagne-agricole-2015-2016 (accessed on 13 September **2020**).
6. Boskou, Dimitrios, ed. 2015. Olives and Olive Oil Bioactive Constituents. Urbana, Illinois: AOCS Press.
7. Bendini, Alessandra, Lorenzo Cerretani, Alegria Carrasco-Pancorbo, Ana Gómez-Caravaca, Antonio Segura-Carretero, Alberto Fernández-Gutiérrez, and Giovanni Lercker. 2007. "Phenolic Molecules in Virgin Olive Oils: A Survey of Their Sensory Properties, Health Effects, Antioxidant Activity and Analytical Methods. An Overview of the Last Decade Alessandra." Molecules 12 (8): 1679–1719.
8. Rodis, Panayotis S., Vaios T. Karathanos, and Antonia Mantzavinou. 2002. "Partitioning of Olive Oil Antioxidants between Oil and Water Phases." Journal of Agricultural and Food Chemistry 50 (3): 596–601.
9. Allaoui, Safae, Mohammed Naciri Bennani, Hamid Ziyat, Omar Qabaqous, Najib Tijani, Najim Ittobane, Mohammed Barbouchi, Aziz Bouymajane, and Fouzia Rhazi Filali. 2020. "Antioxidant and Antimicrobial Activity of Polyphenols Extracted after Adsorption onto Natural Clay 'Ghassoul.'" Journal of Chemistry 2020 (August): 1–6.

10. Dehmani, Younes, Abdelaziz Ed-Dra, Omar Zennouhi, Aziz Bouymajane, Fouzia Rhazi Filali, Laila Nassiri, and Sadik Abouarnadasse. 2020. “Chemical Characterization and Adsorption of Oil Mill Wastewater on Moroccan Clay in Order to Be Used in the Agricultural Field.” Heliyon 6 (1): e03164.
11. Klikarová, Jitka, Archimede Rotondo, Francesco Cacciola, Lenka Česlová, Paola Dugo, Luigi Mondello, and Francesca Rigano. 2019. “The Phenolic Fraction of Italian Extra Virgin Olive Oils: Elucidation Through Combined Liquid Chromatography and NMR Approaches.” Food Analytical Methods 12 (8): 1759–70.
12. Fanali, Chiara, Susanna Della Posta, Laura Dugo, Marina Russo, Alessandra Gentili, Luigi Mondello, and Laura De Gara. 2020. “Application of Deep Eutectic Solvents for the Extraction of Phenolic Compounds from Extra-virgin Olive Oil.” ELECTROPHORESIS 41 (20): 1752–59.
13. Russo, Marina, Ivana Lidia Bonaccorsi, Francesco Cacciola, Laura Dugo, Laura De Gara, Paola Dugo, and Luigi Mondello. 2021. “Distribution of Bioactives in Entire Mill Chain from the Drupe to the Oil and Wastes.” Natural Product Research 35 (21): 4182–87.
14. “Scientific Opinion on the Substantiation of Health Claims Related to Polyphenols in Olive and Protection of LDL Particles from Oxidative Damage (ID 1333, 1638, 1639, 1696, 2865), Maintenance of Normal Blood HDL-Cholesterol Concentrations (ID 1639), Maintenance of Normal Blood Pressure (ID 3781), ‘Anti-Inflammatory Properties’ (ID 1882), ‘Contributes to the Upper Respiratory Tract Health’ (ID 3468), ‘Can Help to Maintain a Normal Function of Gastrointestinal Tract’ (3779), and ‘Contributes to Body Defences against External Agents’ (ID 3467) Pursuant to Article 13(1) of Regulation (EC) No 1924/2006.” n.d. EFSA Journal, no. 2011;9(4):2033. Accessed December 8, 2022.
15. Gallina-Toschi, Tullia, Lorenzo Cerretani, Alessandra Bendini, Matteo Bonoli-Carbognin, and Giovanni Lercker. 2005. “Oxidative Stability and Phenolic Content of Virgin Olive Oil: An Analytical Approach by Traditional and High Resolution Techniques.” Journal of Separation Science 28 (9–10): 859–70.
16. Tura, Debora, Carmen Gigliotti, Stefano Pedò, Osvaldo Failla, Daniele Bassi, and Arnaldo Serraiocco. 2007. “Influence of Cultivar and Site of Cultivation on Levels of Lipophilic and Hydrophilic Antioxidants in Virgin Olive Oils (Olea Europea L.) and Correlations with Oxidative Stability.” Scientia Horticulturae 112 (1): 108–19.

17. Aparicio, Ramon, and Maria T. Morales. 1998. “Characterization of Olive Ripeness by Green Aroma Compounds of Virgin Olive Oil.” Journal of Agricultural and Food Chemistry 46 (3): 1116–22.
18. Bendini, Alessandra, Lorenzo Cerretani, Fabio Di Virgilio, Paolo Belloni, Matteo Bonoli-Carbognin, and Giovanni Lercker. 2007. “PRELIMINARY EVALUATION OF THE APPLICATION OF THE FTIR SPECTROSCOPY TO CONTROL THE GEOGRAPHIC ORIGIN AND QUALITY OF VIRGIN OLIVE OILS.” Journal of Food Quality 30 (4): 424–37.
19. EFSA Panel on Dietetic Products, Nutrition, and Allergies (NDA). 2015. “Scientific Opinion on Dietary Reference Values for Vitamin E as A-tocopherol.” EFSA Journal 13 (7).
20. Pérez-Rodrigo, C., and J. Aranceta. 2016. “Olive Oil: Its Role in the Diet.” In Encyclopedia of Food and Health, 158–66. Elsevier.
21. Ouni, Youssef, Ameni Taamalli, Ana Maria Gómez-Caravaca, Antonio Segura-Carretero, Alberto Fernández-Gutiérrez, and Mokhtar Zarrouk. 2011. “Characterisation and Quantification of Phenolic Compounds of Extra-Virgin Olive Oils According to Their Geographical Origin by a Rapid and Resolutive LC–ESI-TOF MS Method.” Food Chemistry 127 (3): 1263–67.
22. Ben Brahim, Samia, Hasim Kelebek, Sonda Ammar, Mounir Abichou, and Mohamed Bouaziz. 2017. “LC–MS Phenolic Profiling Combined with Multivariate Analysis as an Approach for the Characterization of Extra Virgin Olive Oils of Four Rare Tunisian Cultivars during Ripening.” Food Chemistry 229 (August): 9–19.
23. Ammar, Sonda, Hasim Kelebek, Akram Zribi, Mounir Abichou, Serkan Selli, and Mohamed Bouaziz. 2017. “LC-DAD/ESI-MS/MS Characterization of Phenolic Constituents in Tunisian Extra-Virgin Olive Oils: Effect of Olive Leaves Addition on Chemical Composition.” Food Research International 100 (October): 477–85.
24. Rotondi, Annalisa, Alessandra Bendini, Lorenzo Cerretani, Matteo Mari, Giovanni Lercker, and Tullia Gallina Toschi. 2004. “Effect of Olive Ripening Degree on the Oxidative Stability and Organoleptic Properties of Cv. Nostrana Di Brisighella Extra Virgin Olive Oil.” Journal of Agricultural and Food Chemistry 52 (11): 3649–54.
25. Klikarová, Jitka, Lenka Česlová, Petra Kalendová, Paola Dugo, Luigi Mondello, and Francesco Cacciola. 2020. “Evaluation of Italian Extra Virgin Olive Oils Based on the

Phenolic Compounds Composition Using Multivariate Statistical Methods." European Food Research and Technology 246 (6): 1241–49.

26. Dugo, Laura, Marina Russo, Francesco Cacciola, Filippo Mandolfino, Fabio Salafia, Alessandra Vilmercati, Chiara Fanali, et al. 2020. "Determination of the Phenol and Tocopherol Content in Italian High-Quality Extra-Virgin Olive Oils by Using LC-MS and Multivariate Data Analysis." Food Analytical Methods 13 (5): 1027–41.
27. Commission Regulation (EEC) No 2568/91 on the Characteristics of Olive Oil and Olive-Residue Oil and on the Relevant Methods of Analysis. Available online: https://eur-lex.europa.eu/legal-content/EN/TXT/?uri= CELEX%3A01991R2568-20151016 (accessed on 15 October 2020).
28. Różańska, Anna, Marina Russo, Francesco Cacciola, Fabio Salafia, Żaneta Polkowska, Paola Dugo, and Luigi Mondello. 2020. "Concentration of Potentially Bioactive Compounds in Italian Extra Virgin Olive Oils from Various Sources by Using LC-MS and Multivariate Data Analysis." Foods 9 (8): 1120.
29. Fanali, Chiara, Susanna Della Posta, Alessandra Vilmercati, Laura Dugo, Marina Russo, Tommasangelo Petitti, Luigi Mondello, and Laura de Gara. 2018. "Extraction, Analysis, and Antioxidant Activity Evaluation of Phenolic Compounds in Different Italian Extra-Virgin Olive Oils." Molecules 23 (12): 3249.
30. Commission Regulation (EU). No 432/2012. Establishing a list of permitted health claims made on foods, other than those referring to the reduction of disease risk and to children's development and health. *OJEU* 2012, *136*, 1–40.
31. Regulation (EC). No 1924/2006 of the European Parliament and of the Council of 20 December 2006 on nutrition and health claims made on foods. *OJEU* 2006, *404*, 9–25.
32. COI. Norme commerciale applicable à l'huile d'olive et à l'huile de grignions d'olive– COI/T.20/Doc. 2001.
33. Zarrouk, Amira, Lucy Martine, Stéphane Grégoire, Thomas Nury, Wiem Meddeb, Emmanuelle Camus, Asmaa Badreddine, et al. 2019. "Profile of Fatty Acids, Tocopherols, Phytosterols and Polyphenols in Mediterranean Oils (Argan Oils, Olive Oils, Milk Thistle Seed Oils and Nigella Seed Oil) and Evaluation of Their Antioxidant and Cytoprotective Activities." Current Pharmaceutical Design 25 (15): 1791–1805.
34. USD FoodData Central. Available online: https://fdc.nal.usda.gov/ (accessed on 4 September 2020).

35. Nevado, Juan José Berzas, Gregorio Castañeda Peñalvo, and Virginia Rodríguez Robledo. 2010. “Advantages of Using a Modified Orthogonal Sampling Configuration Originally Designed for LC–ESI-MS to Couple CE and MS for the Determination of Antioxidant Phenolic Compounds Found in Virgin Olive Oil.” Talanta 82 (2): 548–54.
36. Talhaoui, Nassima, Amani Taamalli, Ana María Gómez-Caravaca, Alberto Fernández-Gutiérrez, and Antonio Segura-Carretero. 2015. “Phenolic Compounds in Olive Leaves: Analytical Determination, Biotic and Abiotic Influence, and Health Benefits.” Food Research International 77 (November): 92–108.
37. Dierkes, Georg, Sonja Krieger, Roman Dück, Annette Bongartz, Oliver J. Schmitz, and Heiko Hayen. 2012. “High-Performance Liquid Chromatography–Mass Spectrometry Profiling of Phenolic Compounds for Evaluation of Olive Oil Bitterness and Pungency.” Journal of Agricultural and Food Chemistry 60 (31): 7597–7606.
38. Bajoub, Aadil, Alegría Carrasco-Pancorbo, El Amine Ajal, Noureddine Ouazzani, and Alberto Fernández-Gutiérrez. 2015. “Potential of LC–MS Phenolic Profiling Combined with Multivariate Analysis as an Approach for the Determination of the Geographical Origin of North Moroccan Virgin Olive Oils.” Food Chemistry 166 (January): 292–300.
39. Bajoub, Aadil, Elena Hurtado-Fernández, El Amine Ajal, Noureddine Ouazzani, Alberto Fernández-Gutiérrez, and Alegría Carrasco-Pancorbo. 2015. “Comprehensive 3-Year Study of the Phenolic Profile of Moroccan Monovarietal Virgin Olive Oils from the Meknès Region.” Journal of Agricultural and Food Chemistry 63 (17): 4376–85.
40. Olmo-García, Lucía, Aadil Bajoub, Sara Benlamaalam, Elena Hurtado-Fernández, María Bagur-González, Mohammed Chigr, Mohamed Mbarki, Alberto Fernández-Gutiérrez, and Alegría Carrasco-Pancorbo. 2018. “Establishing the Phenolic Composition of Olea Europaea L. Leaves from Cultivars Grown in Morocco as a Crucial Step Towards Their Subsequent Exploitation.” Molecules 23 (10): 2524.
41. Miho, H., J. Moral, M.A. López-González, C.M. Díez, and F. Priego-Capote. 2020. “The Phenolic Profile of Virgin Olive Oil Is Influenced by Malaxation Conditions and Determines the Oxidative Stability.” Food Chemistry 314 (June): 126183.
42. El Qarnifa, Samira, Abderraouf El Antari, and Abdellatif Hafidi. 2019. “Effect of Maturity and Environmental Conditions on Chemical Composition of Olive Oils of Introduced Cultivars in Morocco.” Journal of Food Quality 2019 (December): 1–14.

43. Commission Regulation (EU) No 432/2012. Establishing a list of permitted health claims made on foods, other than those referring to the reduction of disease risk and to children's development and health Text with EEA relevance. Off J Eur Union. 2012, 40:281–320.
44. Boskou, Dimitrios, Georgios Blekas, and Maria Tsimidou. 2006. "4 - Olive Oil Composition." In Olive Oil (Second Edition), edited by Dimitrios Boskou, 41–72. AOCS Press.
45. Diamantakos, Panagiotis, Kostas Ioannidis, Christos Papanikolaou, Annia Tsolakou, Aimilia Rigakou, Eleni Melliou, and Prokopios Magiatis. 2021. "A New Definition of the Term 'High-Phenolic Olive Oil' Based on Large Scale Statistical Data of Greek Olive Oils Analyzed by QNMR." Molecules 26 (4): 1115.
46. Miho, H., J. Moral, D. Barranco, C.A. Ledesma-Escobar, F. Priego-Capote, and C.M. Díez. 2021. "Influence of Genetic and Interannual Factors on the Phenolic Profiles of Virgin Olive Oils." Food Chemistry 342 (April): 128357.
47. Tuck, Kellie L, and Peter J Hayball. 2002. "Major Phenolic Compounds in Olive Oil: Metabolism and Health Effects." The Journal of Nutritional Biochemistry 13 (11): 636–44.
48. Bouymajane, Aziz, Yassine Oulad El Majdoub, Francesco Cacciola, Marina Russo, Fabio Salafia, Alessandra Trozzi, Fouzia Rhazi Filali, Paola Dugo, and Luigi Mondello. 2020. "Characterization of Phenolic Compounds, Vitamin E and Fatty Acids from Monovarietal Virgin Olive Oils of 'Picholine Marocaine' Cultivar." Molecules 25 (22): 5428.
49. Di Stefano, Vita, and Maria Grazia Melilli. 2020. "Effect of Storage on Quality Parameters and Phenolic Content of Italian Extra-Virgin Olive Oils." Natural Product Research 34 (1): 78–86.
50. FoodData Central. https://fdc.nal.usda.gov/. Accessed 16 Dec 2020.
51. Wiesman Z, 2009. Chapter 11—olive-oil quality biotechnologies. In: Wiesman Z (ed) Desert olive oil cultivation. Academic Press, San Diego, pp 257–302.
52. Bedbabis, Saida, Dhouha Trigui, Chedlia Ben Ahmed, Maria Lisa Clodoveo, Salvatore Camposeo, Gaetano Alessandro Vivaldi, and Béchir Ben Rouina. 2015. "Long-Terms Effects of Irrigation with Treated Municipal Wastewater on Soil, Yield and Olive Oil Quality." Agricultural Water Management 160 (October): 14–21.
53. Psomiadou, Eleni, Maria Tsimidou, and Dimitrios Boskou. 2000. "α-Tocopherol Content of Greek Virgin Olive Oils." Journal of Agricultural and Food Chemistry 48 (5): 1770–75.

54. IOC (2007) Production techniques in olive growing. International Olive Council, Madrid, Spain.
55. Bajoub A (2016) Virgin olive oil: Potential of different omics approaches to authenticate its geographical and botanical origin. Universidad de Granada.
56. Guerfel, Mokhtar, Youssef Ouni, Amani Taamalli, Dalenda Boujnah, Evagellia Stefanoudaki, and Mokhtar Zarrouk. 2009. “Effect of Location on Virgin Olive Oils of the Two Main Tunisian Olive Cultivars.” European Journal of Lipid Science and Technology 111 (9): 926–32.
57. Romero, Nalda, Jorge Saavedra, Francisco Tapia, Betsabet Sepúlveda, and Ramón Aparicio. 2016. “Influence of Agroclimatic Parameters on Phenolic and Volatile Compounds of Chilean Virgin Olive Oils and Characterization Based on Geographical Origin, Cultivar and Ripening Stage: Effect of Agroclimatic Parameters on Compounds Responsible for the Flavor of EVOO.” Journal of the Science of Food and Agriculture 96 (2): 583–92.
58. Neocleous, D., A. Koukounaras, A.S. Siomos, and M. Vasilakakis. 2014. “Assessing the Salinity Effects on Mineral Composition and Nutritional Quality of Green and Red ‘Baby’ Lettuce: Responses of Baby Lettuce to Salinity.” Journal of Food Quality 37 (1): 1–8.
59. Talhaoui, Nassima, Amani Taamalli, Ana María Gómez-Caravaca, Alberto Fernández-Gutiérrez, and Antonio Segura-Carretero. 2015. “Phenolic Compounds in Olive Leaves: Analytical Determination, Biotic and Abiotic Influence, and Health Benefits.” Food Research International 77 (November): 92–108.
60. Nisha, Chandak, Maiti Barnali, Pathan Shabana, Desai Meena, and Kamlesh Shah. n.d. “ISSN:2349-3372 NEWEST INTERNATIONAL REFERRED IOURNALS” 3: 7.
61. Friedman, Mendel, and Hella S. Jürgens. 2000. “Effect of PH on the Stability of Plant Phenolic Compounds.” Journal of Agricultural and Food Chemistry 48 (6): 2101–10.
62. Romero, M. Paz, M. Jesús Tovar, Tomas Ramo, and M. José Motilva. 2003. “Effect of Crop Season on the Composition of Virgin Olive Oil with Protected Designation of Origin ‘Les Garrigues.’” Journal of the American Oil Chemists’ Society 80 (5): 423–30.
63. Proietti P, Regni L (2016) Handbook for a sustainable management of the olive groves, vol 9. www.olive4climate.eu
64. Rouas S, Rahmani M, El Antari A, Baamal L, Idrissi Janati D, Souizi A, Maat N (2016) Effect of geographical conditions (altitude and pedology) and age of olive plantations on the typicality of olive oil in Moulay Driss Zarhoun. Mediterr J Biosci 1:128–137.

65. Rached, Mouna Ben, Gianni Galaverna, Martina Cirlini, Dalenda Boujneh, Mokhtar Zarrouk, and Mokhtar Guerfel. 2017. “Pedologic Factors Affecting Virgin Olive Oil Quality of ‘Chemlali’ Olive Trees (Olea Europaea L.).” Journal of Oleo Science 66 (8): 907–15.
66. Issaoui, Manel, Guido Flamini, Faten Brahmi, Samia Dabbou, Kaouther Ben Hassine, Amani Taamali, Hechmi Chehab, Myriem Ellouz, Mokhtar Zarrouk, and Mohamed Hammami. 2010. “Effect of the Growing Area Conditions on Differentiation between Chemlali and Chétoui Olive Oils.” Food Chemistry 119 (1): 220–25.
67. Mohamed Mousa, Yiasser, Dimitrios Gerasopoulos, Ioannis Metzidakis, and Apostolos Kiritsakis. 1996. “Effect of Altitude on Fruit and Oil Quality Characteristics of ‘Mastoides’ Olives.” Journal of the Science of Food and Agriculture 71 (3): 345–50.
68. Moumen, Kamal Belhaj, Farid Mansouri, Abdessamad Ben, Gaetan Richard Marie-Laure Fauconnier, Marianne Sindic, and Hana Serghini Caid Ahmed Elamrani. 2018. “Effect of Crop Season on the Quality and Composition of Extra Virgin Olive Oils from Greek and Spanish Varieties Grown in the Oriental Region of Morocco.” Emirates Journal of Food and Agriculture, August, 549.
69. Baccouri, Bechir, Wissem Zarrouk, Dhouha Krichene, Issam Nouairi, Nabil Ben Youssef, Douja Daoud, and Mokhtar Zarrouk. 2007. “Influence of Fruit Ripening and Crop Yield on Chemical Properties of Virgin Olive Oils from Seven Selected Oleasters (Olea Europea L.).” Journal of Agronomy 6 (3): 388–96.
70. Preedy VR, Watson RR (2010) Olives and olive oil in health and disease prevention. Academic Press, Cambridge.
71. Dag, Arnon, Zohar Kerem, Nir Yogev, Issac Zipori, Shimon Lavee, and Eric Ben-David. 2011. “Influence of Time of Harvest and Maturity Index on Olive Oil Yield and Quality.” Scientia Horticulturae 127 (3): 358–66.

Supplementary material

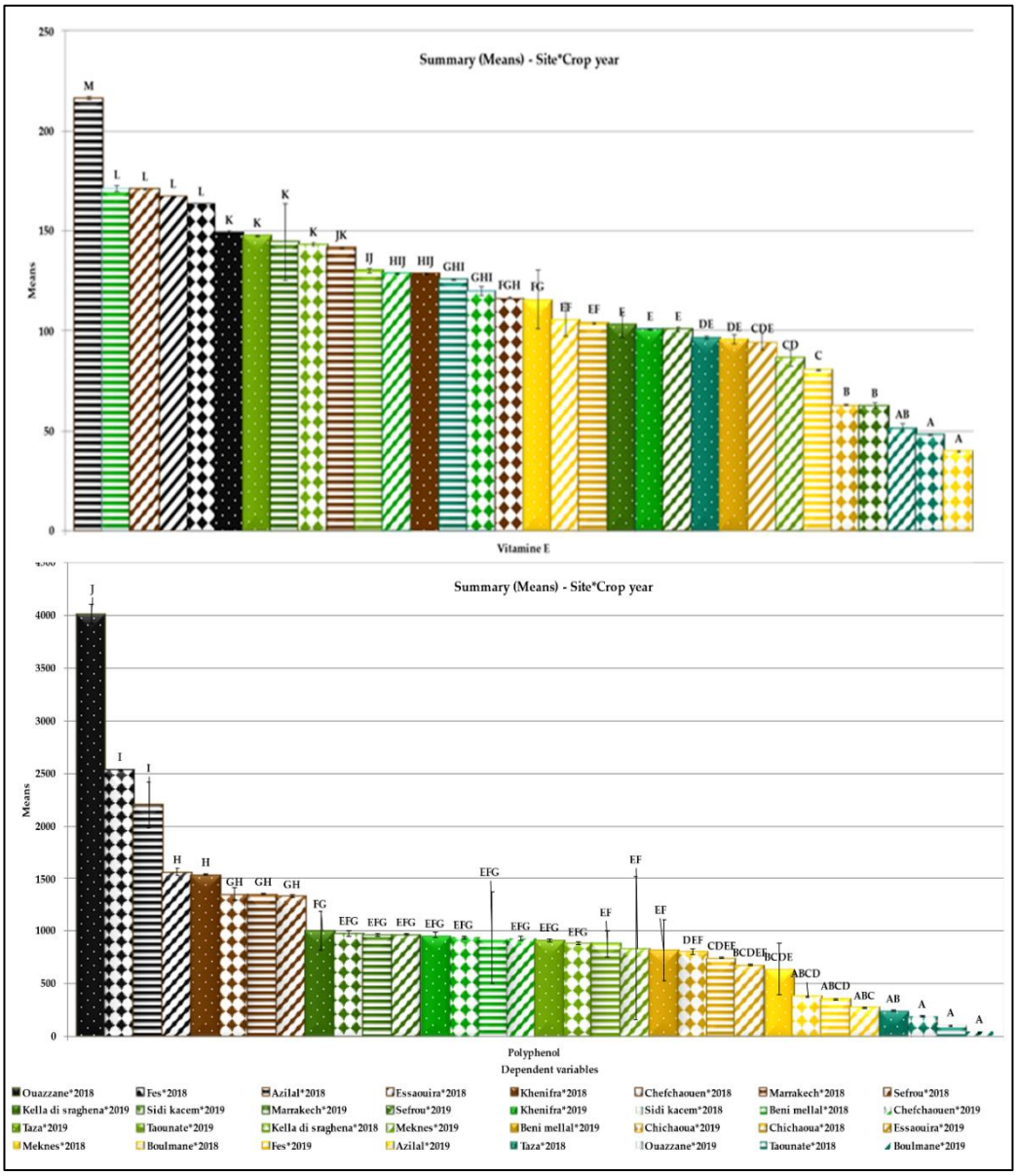

Figure S2.1. Graphical presentation of polyphenol and tocopherol content expressed in mg/kg during two successive crop years 2018 and 2019 from 19 Moroccan geographical sites. Values represent average ± standard deviation (n= 3). Similar letters indicate no significant ($p \geq 0.05$) difference between treatments, whereas all parameters have shown a significance with ($p \leq 0.0001$). Two-way ANOVA was performed to evaluate crop year, geographical site, and their interaction. sampling [Chefchaouen (Sp1), Ouazzane (Sp2), Sidi Kacem (Sp3), Meknes (Sp44, Sp5), Taounate (Sp6), Taza (Sp7), Fes (Sp8), Sefrou (Sp9), Boulmane (Sp10), Khenifra (Sp11), Beni Mellal (Sp12, Sp13), Azilal (Sp14), Kella di Sraghena (Sp15, Sp16), Marrakech (Sp17), Chichaoua (Sp18) and Essaouira (Sp19)].

Table S2.1. Quantification of polyphenols and tocopherols contents expressed as average (mg/kg) ± SD in Moroccan extra virgin olive oil of "*Picholine Marocaine"* collected from 19 Moroccan geographical sites.

Compounds	crop season	Sp1	Sp2	Sp3	Sp4	Sp5	Sp6	Sp7	Sp8	Sp9	Sp10	Sp11	Sp12	Sp13	Sp14	Sp15	Sp16	Sp17	Sp18	Sp19
Phenolic alcohols																				
Tyrosol	2018/2019	36.9±0.08	49.0±0.52	19.2±0.58	16.0±0.01	12.1±0.26	7.3±0.27	8.2±0.26	23.7±1.14	22.7±0.86	4.0±0.01	32.1±0.28	35.2±1.27	15.5±0.13	23.1±0.29	26.0±1.21	16.3±0.21	11.0±0.20	14.4±0.48	52.8±2.28
	2019/2020	12.5±0.36	3.5±0.28	5.9±0.51	10.6±0.68	14.1±0.60	10.6±0.94	12.2±0.26	10.8±0.63	15.5±0.68	2.5±0.14	16.4±1.71	11.2±0.65	13.4±0.98	1.3±0.10	15.2±0.93	8.8±0.94	12.6±0.49	8.5±0.15	11.4±0.14
Hydroxytyrosol	2018/2019	88.1±5.28	136.7±7.81	34.4±1.27	62.8±0.19	27.9±0.70	11.5±0.02	26.9±0.50	65.0±2.56	115.6±10.8	17.6±0.93	90.0±3.9	34.7±0.33	64.2±4.68	131.1±9.02	50.6±0.95	76.6±0.27	23.1±1.19	35.0±1.84	127.9±2.88
	2019/2020	10.3±0.46	<LOD	20.1±4.40	<LOQ	6.3±0.32	26.6±4.18	4.3±0.26	<LOD	17.0±0.55	5.7±0.08	2.2±0.13	22.9±1.85	9.7±0.25	4.5±0.15	19.3±0.21	9.3±0.50	12.4±2.42	11.9±0.93	7.5±0.26
Phenolic acids																				
Caffeic acid	2018/2019	<LOD	<LOD	2.2±0.12	5.8±0.35	1.8±0.03	1.7±0.14	4.9±0.29	<LOD	4.6±0.14	<LOQ	1.3±0.04	<LOD	1.4±0.10	2.1±0.13	7.7±0.03	1.1±0.02	<LOQ	<LOD	<LOD
	2019/2020	<LOD	<LOD	4.1±1.09	<LOQ	0.5±0.12	6.0±0.05	<LOD	<LOD	3.3±0.01	<LOQ	<LOQ	2.9±0.04	1.8±0.40	<LOD	4.2±0.26	<LOQ	<LOQ	1.5±0.10	1.0±0.13
Ferulic acid	2018/2019	<LOD	<LOD	3.70±0.37	7.53±0.07	16.87±0.65	7.66±0.11	1.82±0.11	<LOD	2.90±0.01	3.73±0.04	<LOD	<LOD	1.5±0.02	3.9±0.12	9.8±0.29	1.5±0.02	0.7±0.03	<LOD	3.1±0.16
	2019/2020	4.3±0.05	3.3±0.50	12.9±0.56	5.8±0.53	4.0±0.04	14.6±0.01	1.6±0.06	1.6±0.05	5.8±0.01	0.2±0.01	1.0±0.06	4.8±0.01	3.7±0.01	2.5±0.20	5.0±0.36	2.1±0.06	12.2±0.81	1.9±0.08	6.7±0.13
Gallic acid	2018/2019	48.1±11.26	34.4±4.56	<LOD	10.3±0.65	10.4±0.53	14.2±1.46	<LOD	19.9±2.03	13.2±2.23	7.5±0.25	8.5±2.04	18.7±1.73	9.3±0.22	6.0±0.39	15.3±5.35	15.2±0.28	20.3±2.81	22.2±3.33	13.3±0,02
	2019/2020	12.4±1.71	3.9±1.47	17.2±4.15	13.8±3.21	6.0±0.14	<LOD	16.8±5.28	11.4±0.69	13.3±3.35	7.9±2.21	21.0±1.06	16.6±3.38	<LOD	8.5±2.00	<LOD	<LOD	<LOD	<LOD	<LOD
Flavonoids																				
Luteolin	2018/2019	<LOQ	8.6±0.44	3.1±0.03	7.1±0.10	7.0±0.09	0.8±0.03	5.7±0.22	12.7±0.56	5.9±0.42	3.2±0.04	10.2±0.31	3.5±0.18	10.4±0.47	6.4±0.08	11.3±0.80	6.6±0.16	8.5±0.10	19.2±1.36	4.0±0.15
	2019/2020	6.4±0.15	2.4±0.22	5.4±0.02	6.6±0.79	16.1±0.03	9.2±0.43	2.1±0.06	1.2±0.03	12.3±0.09	8.2±0.09	9.0±0.05	13.1±0.09	5.9±0.25	9.0±0.25	12.6±0.04	20.4±0.01	16.9±0.61	15.1±0.64	5.1±0.26
Apigenin	2018/2019	<LOD	<LOQ	<LOQ	<LOQ	<LOQ	<LOQ	<LOQ	<LOD	<LOQ	<LOQ	<LOQ	<LOQ	<LOQ	<LOQ	<LOQ	<LOQ	<LOQ	2.9±0.51	<LOQ
	2019/2020	<LOQ	<LOQ	<LOQ	<LOQ	<LOQ	<LOQ	<LOQ	<LOQ	<LOQ	<LOQ	<LOQ	<LOQ	<LOQ	<LOQ	<LOQ	<LOQ	<LOQ	<LOQ	<LOQ
Luteolin gluc.	2018/2019	<LOD	6.0±0.63	4.2±0.14	2.8±0.01	1.6±0.03	2.3±0.31	4.8±0.19	<LOD	0.1±0.03	0.9±0.13	<LOQ	4.9±0.50	0.1±0.01	<LOQ	8.3±0.27	<LOQ	0.3±0.10	13.5±0.57	6.0±0.10
	2019/2020	<LOQ	<LOQ	<LOQ	<LOQ	<LOQ	1.7±0.18	<LOQ	<LOQ	<LOQ	1.6±0.08	<LOQ	0.02±0.00	<LOQ	<LOQ	<LOQ	<LOQ	<LOQ	<LOQ	<LOQ
Secoridoids and derivate																				
10-Hydroxy 3,4-DHPEA-EA	2018/2019	47.9±1.30	89.1±0.12	35.9±0.72	35.8±1.33	89.4±0.93	6.3±0.37	15.6±0.22	51.0±1.78	73.3±3.46	70.2±1.75	183.9±2.9	17.3±1.96	124.3±0.11	123.4±0.50	46.5±2.20	38.1±1.53	124.9±1.9	50.3±2.01	20.0±0.77
	2019/2020	10.4±0.07	1.8±0.05	12.1±0.46	1.9±0.19	54.9±3.26	48.0±3.27	17.6±0.52	9.1±0.28	31.4±0.61	<LOQ	16.1±0.08	24.1±0.05	24.8±0.11	6.2±0.64	13.8±0.02	5.8±0.10	34.9±1.03	10.6±0.23	9.7±0.23
3,4-DHPEA-EA	2018/2019	624.3±17.11	2459.0±54.56	486.5±5.74	425.1±4.2	140.5±1.68	22.5±1.26	78.0±0.85	1605.5±13	603.9±8.34	121.8±1.9	638.0±6.69	268.3±2.7	583.9±2.90	1041.4±0.22	324.2±7.47	496.9±4.2	513.2±4.9	325.7±20.53	942.1±9.38
	2019/2020	521.8±6.16	49.8±1.31	410.6± 1.97	94.8± 1.73	771.2± 26.71	397.5± 1.26	395.2± 0.47	80.9± 0.69	427.5± 4.01	3.4± 0.01	427.9± 14.29	258.7± 0.46	540.3± 17.38	90.1± 1.21	621.3± 5.82	462.7± 1.77	646.0± 12.58	390.6± 8.00	382.9± 10.88
P-HPEA-EDA	2018/2019	<LOD	<LOD	1.1±0.23	2.0±0.10	0.4±0.12	0.0±0.00	0.2±0.00	<LOD	0.6±0.52	<LOD	1.3±0.06	<LOD	0.8±0.04	<LOQ	3.5±2.28	0.8±0.06	0.1±0.05	<LOD	0.2±0.00
	2019/2020	<LOD	<LOD	<LOQ	0.1±0.14	0.1±0.01	<LOQ	<LOQ	<LOQ	0.7±0.02	<LOQ	<LOQ	<LOQ	0.1±0.03	<LOQ	1.6±0.00	0.3±0.09	0.5±0.03	0.8±0.10	0.1±0.02
3,4-DHPEA-EDA	2018/2019	48.7±0.44	185.6±4.27	111.9±2.87	29.0±0.18	14.7±0.64	0.3±0.07	0.9±0.10	163.4±0.0	31.9±0.65	6.6±0.11	22.9±0.61	25.1±0.46	182.2±1.2	182.9±0.07	95.7±1.78	96.1±0.82	137.8±0.3	87.0±2.83	55.9±0.34
	2019/2020	46.8±0.23	3.3±0.02	6.3±0.20	0.1±0.03	1.9±0.13	1.7±0.02	3.5±0.09	0.3±0.03	1.4±0.10	<LOQ	2.5±0.20	0.1±0.01	2.3±0.06	1.7±0.06	4.5±0.24	47.6±3.01	50.3±3.66	70.4±0.97	85.6±2.07
p-HPEA-EA	2018/2019	163.9±5.28	666.1±17.93	109.9±4.33	94.7±0.47	30.1±0.67	4.6±0.36	9.2±0.31	398.8±0.58	93.5±1.38	14.1±0.44	150.6±4.5	56.8±1.08	121.4±8.32	179.9±4.41	41.1±2.47	65.3±0.74	220.3±8.1	27.5±2.20	153.6±9.42
	2019/2020	170.7±14.82	49.7±1.76	53.7±2.17	10.8±0.10	162.1±6.30	37.8±2.18	299.6±2.3	123.3±2.15	93.1±0.06	4.4±0.04	232.2±8.75	10.0±0.03	106.3±1.75	19.1±1.57	99.7±0.82	119.0±10.7	51.7±0.08	25.7±0.49	39.3±1.74
Hydroxy decarboxymethyl 3,4-DHPEA-EA	2018/2019	<LOD	15.6±2.37	<LOD	<LOD	0.8±0.22	<LOD	<LOD	10.3±0.10	3.5±1.06	<LOD	7.1±0.52	<LOD	22.2±0.55	15.1±1.76	9.6±0.33	6.4±1.40	8.7±0.07	<LOD	<LOD
	2019/2020	0.5±0.26	<LOD	<LOD	<LOD	<LOD	<LOD	<LOD	<LOD	<LOD	<LOD	<LOD	<LOD	<LOD	<LOD	<LOD	1.9±0.12	0.6±0.11	<LOD	<LOD
Dehydro 3,4-DHPEA-EA	2018/2019	7.9±3.13	5.3±2.21	1.2±1.43	0.7±0.09	0.8±0.16	<LOD	<LOD	3.0±0.06	4.1±0.49	6.6±0.02	5.1±0.27	1.5±0.22	1.3±0.15	3.6±0.17	<LOD	0.4±0.41	2.1±0.25	<LOD	<LOD
	2019/2020	26.1±0.34	9.6±0.39	<LOD	<LOD	<LOD	29.3±1.15	<LOD	4.9±0.25	33.5±1.88	<LOD	<LOD	<LOD	<LOD	1.8±0.53	<LOD	<LOD	<LOD	<LOD	<LOD
Decarboxymethyl elenolic acid dialdehyde	2018/2019	9.4±0.25	<LOD	6.0±0.91	2.3±0.18	7.8±0.24	6.7±0.41	12.2±1.13	<LOD	8.5±1.03	2.3±0.35	9.4±0.37	8.9±0.33	1.6±0.43	1.1±0.31	<LOD	4.14±0.07	1.6±0.39	3.2±0.21	9.8±1.98
	2019/2020	0.6±0.32	0.5±0.11	0.9±0.15	1.2±0.18	<LOD	5.3±0.50	4.0±0.12	1.1±0.26	4.9±0.29	3.1±0.47	1.4±0.30	1.2±0.00	<LOD	<LOD	<LOD	<LOD	4.3±1.05	1.0±0.17	1.6±0.16
Hydroxy tyrosol acetate	2018/2019	<LOD	<LOD	<LOD	<LOD	<LOD	<LOD	<LOD	<LOD	<LOD	<LOD	<LOD	<LOD	<LOD	<LOD	<LOD	<LOD	<LOD	<LOD	<LOD
	2019/2020	<LOD	<LOD	6.3±0.83	<LOD	9.2±0.67	5.1±1.35	<LOD	<LOD	<LOD	<LOD	<LOD	<LOD	<LOD	<LOD	<LOD	<LOD	<LOD	<LOD	<LOD
Methyl decarboxymethyl 3,4-DHPEA-EA	2018/2019	<LOD	4.9±0.79	3.3±4.62	1.5±0.15	<LOD	<LOD	<LOD	1.5±0.18	1.1±0.09	<LOD	<LOQ	<LOD	<LOD	1.1±0.02	<LOD	<LOD	<LOD	<LOD	<LOD
	2019/2020	<LOD	<LOD	<LOD	<LOD	<LOD	<LOD	<LOD	<LOD	<LOD	<LOD	<LOD	<LOD	<LOD	<LOD	<LOD	<LOD	<LOD	<LOD	<LOD
Methyl 3,4-DHPEA-EA	2018/2019	2.0±0.40	<LOD	1.8±0.13	<LOD	<LOD	<LOD	<LOD	0.4±0.03	0.3±0.17	10.6±0.92	<LOD	<LOD	0.6±0.29	3.0±0.53	2.1±0.53	3.3±0.09	<LOD	5.0±0.75	10.9±0.70
	2019/2020	47.1±1.42	<LOD	4.2±1.64	<LOD	6.8±0.08	9.9±2.37	7.4±0.03	2.0±0.77	2.58±1.30	<LOD	<LOD	<LOD	5.7±0.12	<LOD	12.1±2.24	6.4±0.52	3.6±0.23	4.8±1.03	<LOD
Elenolic acid	2018/2019	212.2±1.71	451.6±24.13	103.2±5.41	126.6±6.8	32.8±0.74	13.2±0.25	61.2±0.29	169.3±9.8	306.5±7.0	78.8±0.74	321.3±4.1	71.1±1.23	154.0±5.8	300.8±0.38	89.1±7.23	151.3±0.5	241.8±4.9	117.7±8.51	145.1±5.30
	2019/2020	60.6±1.75	47.5±1.33	409.1±24.3	86.0±7.73	312.8±22.1	260.0±0.54	139.2±2.9	74.0±2.36	276.6±16.9	13.1±0.56	218.6±1.08	172.3±6.0	344.6±10.1	122.39± 0.56	329.06± 1.71	147.0±2.2	119.82± 6.75	247.55± 18.62	124.99± 5.89
Hydroxy decarboxymethyl elenolic acid	2018/2019	20.6±1.15	14.3±0.90	1.9±0.03	9.0±0.73	4.8±0.72	3.0±0.04	3.1±0.71	5.3±0.75	27.6±3.37	0.9±0.12	22.8±1.49	2.8±0.10	5.3±0.54	9.5±0.07	7.9±1.71	6.4±1.64	5.0±0.80	3.8±0.78	10.9±0.53
	2019/2020	1.3±0.22	0.8±0.49	1.2±0.45	2.2±0.33	4.5±0.30	3.1±0.61	0.5±0.04	2.5±0.06	7.2±0.58	<LOD	0.7±0.20	3.8±0.14	2.9±0.86	<LOD	3.8±0.38	1.1±0.01	0.8±0.25	0.4±0.46	<LOD
Hydroxy elenolic acid	2018/2019	39.9±24.59	27.7±0.49	9.7±0.71	17.3±1.21	30.7±0.20	6.7±0.00	16.8±0.31	6.4±0.20	10.3±5.90	29.2±0.40	32.7±0.41	7.3±1.09	13.3±0.42	14.4±1.78	15.9±0.50	4.6±0.22	30.0±0.49	17.2±3.06	5.9±0.32
	2019/2020	1.0±0.14	14.5±0.26	11.5±2.56	11.0±0.02	49.7±0.18	17.1±0.17	6.4±0.35	33.9±4.33	18.4±2.16	2.3±0.06	8.8±0.10	19.9±0.84	9.7±0.75	5.2±0.09	13.0±0.18	5.6±0.17	1.5±0.05	7.7±1.25	2.7±0.06
Desoxy elenolic acid	2018/2019	<LOD	<LOD	<LOD	<LOD	<LOD	0.86±0.41	<LOD	<LOD	<LOD	<LOD	<LOD	<LOD	0.14±0.05	<LOD	<LOD	<LOD	<LOD	<LOD	<LOD
	2019/2020	<LOD	0.44±0.09	<LOD	<LOD	<LOD	<LOD	<LOD	<LOD	<LOD	<LOD	<LOD	<LOD	<LOD	3.24±0.32	4.07±0.09	<LOD	<LOD	<LOD	<LOD
Vitamin E																				
α-tocopherol	2018/2019	104.2±1.36	133.6±0.39	106.0±0.60	116.3±0.5	89.36±10.1	113.4±0.63	80.50±4.5	153.15 ±1.	156.90 ±0.	32.93±0.4	116.13±0.2	156.26±0.4	158.5±1.0	201.1±0.08	114.3±0.50	119.1±0.9	130.3±1.9	94.9±0.70	154.3±0.50
	2019/2020	116.5± 0.6	39.8± 0.5	52.3± 0.3	70.2± 3.4	72.9± 5.3	118.9±1.7	129.2±0.4	72.0± 0.9	85.8±0.2	33.9± 0.4	86.9± 1.2	58.9± 2.4	74.0± 5.0	82.5± 2.3	85.1± 0.8	96.2± 6.0	125.1± 2.6	49.9±0.4	77.3± 0.6
α-tocotrienol	2018/2019	< LOQ	< LOQ	< LOQ	2.5±0.10	2.8±0.10	<LOQ	<LOQ	<LOQ	<LOQ	<LOQ	2.38±0.19	3.81±0.17	2.5±0.02	<LOQ	3.13±0.2	2.7±0.01	4.0±0.01	3.0±0.10	3.4±0.20
	2019/2020	2.9±0.20	2.2±0.10	2.6±0.10	3.1±0.01	8.4±0.20	13.3±0.01	5.0±0.30	<LOQ	7.0±0.50	4.1±0.10	<LOQ	<LOQ	<LOQ	<LOQ	<LOQ	<LOQ	<LOQ	5.4 ±0.20	5.1 ±0.10
β-tocopherol	2018/2019	2.4 ±0.12	2.8±0.15	2.4±0.08	2.2±0.1	2.61±0.26	2.56±0.09	2.84±0.18	2.26±0.10	2.78±0.50	1.43±0.10	2.40±0.09	2.24±0.13	3.0±0.02	3.2±0.01	3.60 ±0.10	2.6±0.1	3.2±0.2	2.5±0.1	2.7±0.1
	2019/2020	2.5±0.10	2.2±0.10	2.6±0.01	2.1±0.10	2.3±0.10	3.6±0.01	3.2±0.10	1.9±0.10	2.3±0.10	3.6±0.30	2.2±0.10	4.1±0.20	2.0±0.10	3.0±0.10	2.5±0.60	<LOQ	3.6±0.10	2.2±0.10	3.2±0.01
γ-tocopherol	2018/2019	7.5 ±0.13	9.0 ±0.07	6.0 ±0.13	6.6 ±0.20	8.13 ±0.53	7.04 ±0.11	7.36 ±0.38	6.48 ±0.3	7.50 ±0.20	3.55 ±0.10	7.13 ±0.15	6.99 ±0.22	6.8 ±0.02	7.9 ±0.02	7.2 ±0.30	6.5 ±0.10	4.4 ±0.10	3.4 ±0.10	5.8 ±0.01
	2019/2020	6.5±0.40	3.7±0.10	4.8±0.10	5.9±0.30	4.3±0.10	5.9±0.20	9.0±0.10	3.2±0.10	5.2±0.10	6.5±0.40	4.5±0.10	6.7±0.10	3.8±0.10	5.4 ±0.01	4.5±0.40	7.8±0.20	14.1±0.40	5.4±0.20	8.0±0.70
δ-tocopherol	2018/2019	0.6 ±0.05	0.6 ±0.04	1.1 ±0.05	0.6 ±0.0	0.54 ± 0.09	0.47 ±0.02	0.51 ±0.03	0.46 ±0.1	0.68 ±0.1	0.48 ±0.0	0.66 ±0.05	0.76 ±0.05	0.7 ±0.01	0.8 ±0.01	0.65 ±0.01	0.7 ±0.01	0.8 ±0.01	0.7 ±0.01	0.8 ±0.01
	2019/2020	0.7±0.01	0.6±0.01	0.8±0.01	<LOQ	0.7±0.01	0.9±0.01	0.9±0.01	0.6±0.01	0.7±0.01	0.8±0.01	0.9±0.10	<LOQ	<LOQ	0.3±0.01	0.3±0.01	0.2±0.01	<LOQ	0.3±0.01	0.3±0.01

***Σ*Phenolic alcohol**	2018/2019	125.1	185.8	53.7	78.8	40.0	18.9	35.2	88.7	138.4	21.6	122.1	70.0	79.8	154.2	76.7	92.9	34.1	49.5	180.7
	2019/2020	22.8	3.6	26.1	10.6	20.5	37.2	16.5	10.8	32.5	8.2	18.6	34.1	23.1	5.9	34.5	18.2	25.0	20.4	19.0
***Σ*Phenolic acids**	2018/2019	48.1	34.4	5.9	23.7	29.0	23.6	6.7	19.9	20.8	11.2	9.8	18.7	12.3	12.8	32.9	17.9	21.0	22.2	16.5
	2019/2020	16.8	7.2	34.3	19.6	10.6	20.6	18.4	13.0	22.5	8.1	22.1	24.4	5.6	11.1	9.2	2.1	12.2	3.5	7.7
***Σ*Flavonoids**	2018/2019	0.0	14.7	7.3	9.9	8.6	3.1	10.5	12.7	6.1	4.2	10.2	8.4	10.6	7.1	19.6	6.6	8.5	35.7	10.0
	2019/2020	6.4	2.4	5.4	6.6	16.1	10.9	2.1	1.2	12.3	9.8	9.0	13.1	5.9	9.0	12.6	20.4	16.9	15.1	5.1
***Σ*Secoridoids and derivate**	2018/2019	1177.1	3919.7	872.9	744.4	353.1	64.4	197.6	2415.2	1165.7	341.5	1395.6	459.6	1211.6	2025.6	636.2	874.3	1286.0	637.5	1354.8
	2019/2020	887.5	177.7	916.4	208.5	1373.5	815.3	873.8	332.4	897.7	26.6	908.6	490.5	1037.1	246.7	1099.1	797.8	914.3	760.0	647.1
***Σ*vitamin E**	2018/2019	114.8	146.0	115.4	128.2	130.45	123.3	171.7	162.3	167.8	38.3	128.6	170.0	171.6	213.0	128.9	131.7	142.7	104.5	166.8
	2019/2020	129.1	48.4	63.1	81.3	88.6	142.4	147.3	77.6	101	48.9	94.5	69.7	79.8	91.2	92.1	104.4	142.8	63.2	94
***Σ*phenolic compounds**	2018/2019	1350.4	4154.7	940.0	857.0	430.96	110.1	250.1	2536.6	1331.2	378.7	1537.9	556.9	1314.4	2199.9	765.5	991.9	1349.7	745.1	1562.2
	2019/2020	933.7	191.1	982.3	245.5	1420.8	884.2	911.0	357.6	965.1	52.8	958.4	562.2	1071.9	272.7	1155.6	838.7	968.5	799.2	679.1

Table S2.2. Geographic information about the 19 studied geographical sites of Morocco.

Code	Regions	Latitude	Longitude	Altitude: (m.)
Sp1	Tangier-Tetouan-Al Hoceïma	35.04756959	-5.18966503	795.05
Sp2	Tangier-Tetouan-Al Hoceïma	34.96390882	-5.55752702	215.6
Sp3	Rabat-Sale-Kenitra	34.32704667	-5.67162167	40.65
Sp4	Fes-Meknes	34.0959468	-5.69841077	178.62
Sp5	Fes-Meknes	34.06255139	-5.35884381	261.42
Sp6	Fes-Meknes	34.29534608	-4.68761767	225.23
Sp7	Fes-Meknes	34.14988513	-4.34951846	281.1
Sp8	Fes-Meknes	34.03218803	-4.8799319	256.18
Sp9	Fes-Meknes	33.86045216	-4.85226809	814.25
Sp10	Fes-Meknes	33.6024198	-4.5599905	947.11
Sp11	Beni Mellal-Khenifra	32.82915307	-5.61550233	831.16
Sp12	Beni Mellal-Khenifra	32.6203184	-5.97855724	752.17
Sp13	Beni Mellal-Khenifra	32.37114167	-6.32796833	521.9
Sp14	Beni Mellal-Khenifra	32.22453333	-6.53560333	456.8
Sp15	Marrakech-Safi	32.1467413	-7.2855471	411.59
Sp16	Marrakech-Safi	31.84095341	-7.33884281	628.87
Sp17	Marrakech-Safi	31.68413572	-8.13066243	388.78
Sp18	Marrakech-Safi	31.58301034	-9.03087293	382.92
Sp19	Marrakech-Safi	31.60415187	-9.52250093	203.41

CHAPTER 3

Assessment of bioaccessibility of *Hibiscus sabdariffa* L. polyphenols in simulated *in vitro* human digestion model by means of liquid chromatography coupled to mass spectrometry

3.1 Introduction

Hibiscus sabdariffa (*H.s.*) which is commonly known as roselle, bissap, or karkade belongs to the *Malvaceae* family. It is commonly grown in tropical and subtropical areas such as India, Mexico, Thailand, and Egypt. *H.s.* used to be consumed traditionally as a cold beverage or hot tisane. It is known by its red colour owing to the presence of anthocyanins, which are water-soluble flavonoids present in their glycosylated form. [1–5]. In addition to their antioxidant properties, anthocyanins increase a wide variety of biological functions after consumption.

Cyanidin-3-O-sambubioside (C3S) and delphinidin-3-O-sambubioside (D3S) are the main anthocyanins present in *H.s.* [6] alongside several bioactive compounds, which are responsible for numerous physiological and pharmacological effects. All bioactive compounds have a strong relationship to their availability at the site of action in terms of their *in vivo* biological activity. The bioaccessibility of polyphenols and their consequent absorption in the gastrointestinal tract (GIT) along with their biotransformation by enzymes from the gut microbiota represent one of the key limiting factors affecting their beneficial effects [7]. Bioaccessibility refers to the percentage of nutrients or phytochemicals that are released during digestion from complex food matrices and, therefore, likely available for absorption in the upper gastrointestinal tract. In earlier studies, the release of proteins, lipids and polyphenols from natural and blanched skins of almonds were examined during the simulated human digestion [8] and explained the influence of polyphenols bioaccessibility by the nature of food matrix during simulated human digestion [9]. Moreover, based on simulated human digestion of pistachio polyphenols, tocopherols, and xanthophylls, it was determined that a significant percentage of polyphenols were released during the gastric phase, whereas protocatechuic acid and luteolin were less bioaccessible in the presence of (muffin) as food matrix [10].

Based on a previous *in vivo* study conducted on the colonic fermentation of *H.s.* anthocyanins [6]. The present study is focused on the investigation of the bioaccessibility of *H.s.* polyphenols *in vitro* using a simulated human digestion model at the stomach and duodenum level [11]. *In vitro* bioaccessibility was performed on the dried extract of *H.s.* polyphenols,

and all the attained aliquots from gastric and duodenal digestion, besides the raw *H.s.* extract were analyzed using high-performance liquid chromatography coupled to photodiode array and mass spectrometry detection (HPLC-PDA-MS/MS).

3.2 Materials and methods

3.2.1 Chemicals and reagents

All employed acetonitrile (ACN), methanol (MeOH), water, ethyl acetate, trifluoroacetic acid (TFA), and formic acid were LC-MS grade and purchase from Merck KGaA, Darmstadt, Germany. Polyphenols standards used for the quantification comprise cyanidin-3-O-glucoside, quercetin, caffeic acid, coumarin, and kaempferol (purity ≥95.0%) were also obtained from Merck KGaA, Darmstadt, Germany. Each standard was prepared by dissolving 10 mg in 10 mL of methanol to prepare stock solution s of 1000 mg/L.

In the present study, all the employed enzymes and chemical reagents in the *in vitro* digestion are as follows: potassium chloride (KCl), sodium chloride (NaCl), calcium chloride ($CaCl_2$), urea, cholesterol, zinc sulphate heptahydrate ($ZnSO_4 \cdot 7H2O$), sodium phosphate monobasic (NaH2PO4), α-amylase from human saliva type XI (A1031-1KU), egg-phosphatidylcholine (PC, 840051P), pepsin from porcine gastric mucosa (P6887), trypsin type IX-S from porcine pancreas (T0303), lipase type VI-S from porcine pancreas (L0382), α-chymotrypsin type II from bovine pancreas (C4129), colipase from porcine pancreas (C3028), α-amylase type VI-B from porcine pancreas, sodium glycodeoxycholate (G9910), and taurocholic acid sodium salt hydrate (T4009) were purchased from Merck KGaA (Darmstadt, Germany). Whereas the gastric lipase employed in this work was fungal lipase analogue (F-AP15) purchased from Amano Enzyme Inc. (Nagoya, Japan).

3.2.2 Sample preparation

The dried samples of *H.s.* calyces were purchased from a market in Morocco, particularly in Meknes.

The plant material identification was accomplished by a botanist at the Department of Biology, Faculty of Sciences, University of Moulay Ismail, Meknes, Morocco.

The dried calyces of *H.s.* were reduced into powder before the preparation of the extract for the *in vitro* simulated human digestion (**Figure 3.1**). A decoction was prepared for *H.s.* by weighing 10 g *w/w* of dried *H.s.* calyces (dry matter of 93% (RSD = 0.11%)) into an Erlenmeyer flask with the addition of cold distilled water. Decoction lasted for 10 min and was filtered through a muslin cloth in 250 mL conical flasks, the extract was then centrifuged for 10 min at 2060× g and filtered through an Acrodisc nylon membrane of 0.45 µm (Merck Life Science, Merck KGaA, Darmstadt, Germany) [6]. The aqueous extract obtained was

dried and stored for 48 h at +4°C in darkness to be employed for simulated *in vitro* digestion and HPLC-PDA/MS analyses.

3.2.3 In vitro simulated human digestion

The present study aims to evaluate the bioaccessible polyphenols extracted from *H.s.* through an *in vitro* simulated human digestion in the duodenum and the stomach levels [12].

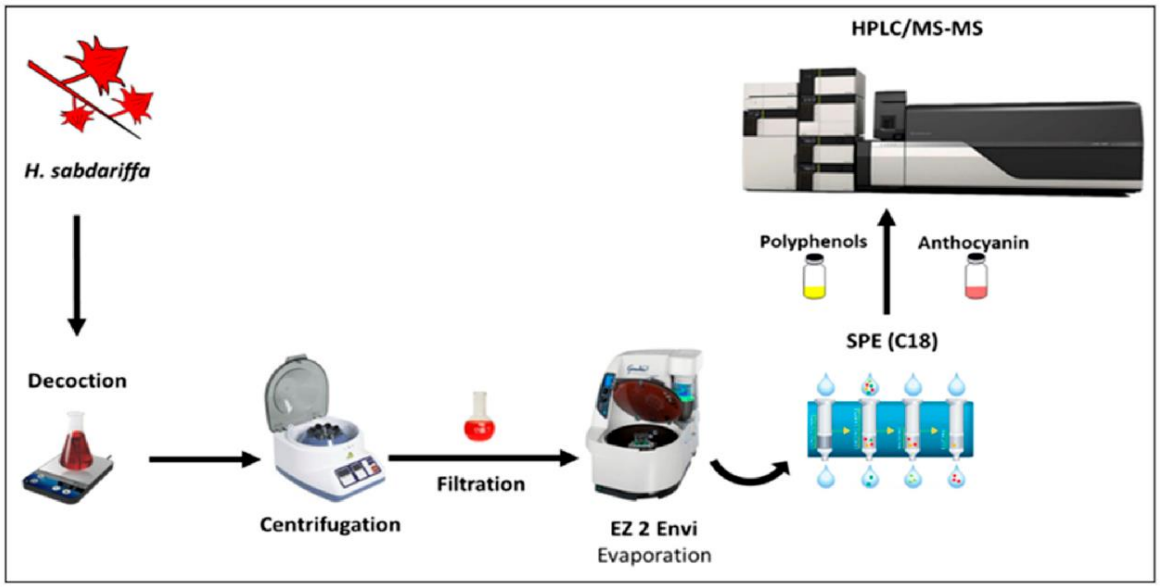

Figure 3.1. The extraction process of *H.s.* dried calyces, solid phase extraction of polyphenols and anthocyanins, and their analysis by liquid chromatography.

Gastric digestion

1 g of *H.s.* dried extract was put into a falcon plastic tube of 50 mL and mixed with 10 mL of a solution of simulated gastric acid containing NaCl (58 mM), KCl (30 mM), NaH_2PO_4 (0.864 mM), $CaCl_2$ (0.5 mM), and egg-phosphatidylcholine (0.127 mM). In order to adjust the pH of the gastric solution to 2.5, 1 M HCl was added, and porcine gastric mucosa pepsin and gastric lipase were dissolved at a final concentration of 9000 U/mL and 60 U/mL, respectively. An incubation of samples at +37 ˚C for 2 h with constant agitation (170 rpm) was achieved by using Innova 4000 Benchtop Incubator Shaker (New Brunswick Scientific, Edison, NJ, USA). During the digestion process, two aliquots were collected each 20 min. 1 M NaOH was added to the first aliquot in order to raise the stomach pH to 7.5 to terminate gastric reactions, consequently, was filtered through a 0.45 µm membrane filter and stored for chromatographic analyses. Whereas the second gastric digestion aliquot of 5 mL proceeded for the duodenal digestion.

Duodenal digestion

The 5 mL of the second aliquot that contains almost 0.5 g of extract was transferred to a different falcon plastic tube of 50 mL for 30 min under duodenal digestion conditions. This later is composed of a 4.33 mL simulated bile solution containing 12.5 mM sodium taurocholate, 12.5 mM sodium glycodeoxycholate, 6.5 mM dried lecithin, and 4 mM cholesterol, besides 12.17 mL of pancreatic enzyme solution consisting of NaCl (125.0 mM), $CaCl_2$ (0.6 mM), $MgCl_2$ (0.3 mM), $ZnSO_4 \cdot 7H_2O$ (4.1 µM), porcine pancreatic lipase (590 U/mL), porcine colipase (3.2 U/mL), porcine trypsin (11 U/mL), bovine α-chymotrypsin (24 U/mL), and porcine α-amylase (300 U/mL). The duodenal aliquot was incubated for 30 min at 37 ˚C under shaking conditions of 170 rpm. Every 10 minutes, an aliquot was harvested from the duodenum during digestion. All post-duodenal aliquots were filtered independently through a 0.45 µm membrane filter and kept at −80 ˚C for further analyses.

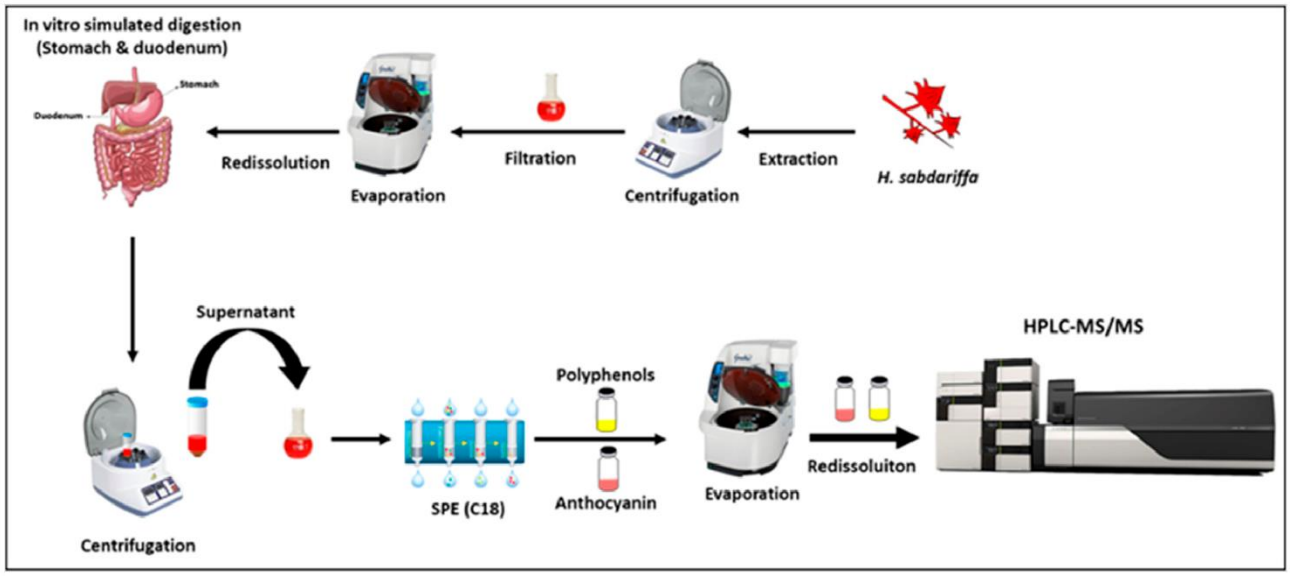

Figure 3.2. Procedure of extraction of *H.s.* polyphenols from *in vitro* human simulated digestion aliquots.

Polyphenols extraction after simulated digestion

As a result of gastric and duodenal simulated digestion, all the obtained aliquots of different samples were centrifuged and supernatant fractions that contain polyphenols were collected. All *H.s.* raw extract and aliquots supernatants were evaporated through Ez-2 and the obtained dried extracts were redissolved in 1 mL of acidified milli-Q water with 0.3% Formic acid. The aliquots were applied on solid phase extraction (SPE; Sep-Pak Vac C18 Octadecyl cartridge (3 mL, 200 mg), VWR International Srl, Milan, Italy) to dispose of undesirable

products (e.g., proteins, enzymes, and carbohydrates) according to the previously cited study [6] (**Figure 3.2**).

3.2.4 Instrumentation and method validation

Analysis of phenolic compounds by HPLC-PDA-MS

The phytochemical investigation of *H.s.* extracts and digestion aliquots was performed on HPLC-PDA-MS using a Shimadzu Prominence LC-20A (Shimadzu, Kyoto, Japan), composed of a CBM-20A controller, two LC-20AD dual-plunger parallel-flow pumps, a DGU-20 A5 degasser, an SPDM20A photodiode array detector, a CTO-20AC column oven at 25 ˚C, a SIL-20A auto-sampler and an Ascentis Express C18 column (150 × 4.6 mm, 2.7 µm) (Merck Life Science, Merck KGaA, Darmstadt, Germany). Triple quadrupole mass spectrometer LCMS-8050 supplied with an electrospray ionization source (ESI) was employed in both negative and positive ionization modes, employing the previously reported parameters [6]. Data acquisition was acquired using Shimadzu LabSolutions software (Ver. 5.65, Shimadzu, Kyoto, Japan).

Calibration curves and Limits of Detection (LoD) and Quantification (LoQ)

The following phenolic standards were employed in this study: cyanidin-3-O-glucoside, dissolved in acidified methanol with 0.1% HCl [13]; quercetin, caffeic acid, coumarin, and kaempferol, were all dissolved in methanol. 1000 mg/L of all stock standards solutions were prepared with six concentrations. A linear regression was generated by making three injections for each level. All cyanidin-3-O-sambubioside and delphinidin-3-O-sambubioside were acquired within the linear range of the standard curve of cyanidin-3-O-glucoside with R^2 = 0.998. The anthocyanin compounds were semi-quantified at a wavelength of 520 nm and expressed in µg/g of dried extract.

The HPLC analytical method for cyanidin-3-O-glucoside was validated using triplicate injections in the range of 1–100 mg/mL for cyanidin-3-O-glucoside as an external standard compound of anthocyanins. Accordingly, the LoD and LoQ values were determined using a standard deviation of blank response and slope of 3 and 10, respectively.

Analysis of *H.s.* anthocyanins

The mobile phase consisted of water/formic acid (90:10 *v/v*, solvent A) and water acetonitrile–formic acid (40:50:10 *v/v/v*) (solvent B) with the following gradient: 0 min, 12% B; 35 min, 30% B; 36 min, 100% B [14]. PDA acquisition was in the range of 200–550 nm; the *H.s.* anthocyanins in aqueous extracts were monitored at 520 nm (sampling frequency: 12.5 Hz; time constant: 0.08 s). The injection volume of the anthocyanins was 5 µL.

Analysis of *H.s.* polyphenols

The mobile phase containing water/formic acid (99.9/0.1 *v/v*, solvent A) and acetonitrile (solvent B) was used with the following gradient: 0 min, 0% B; 5 min, 5% B; 15 min, 10% B; 30 min, 20% B; 60 min, 50% B; and 70 min, 100% B. The flow rate of 1 mL/min was split by a T-piece to 0.2 mL/min after PDA and before MS detection. The injection volume was 5 µL. PDA acquisition was in the range of 200–400 nm (sampling frequency: 12.5 Hz; time constant: 0.08 s).

3.2.5 Statistical analysis

The Shapiro-Wilk test was used to determine the normality of the data and residuals; the white test was used to determine heteroscedasticity after the nonparametric regression was performed. Since the normal distribution was not verified, a comparison between the effect of the digestion phase and time on polyphenol release was performed employing Friedman's test (nonparametric repeated measures comparisons). Dunnett's and Nemenyi's tests were used when statistically significant differences were detected. Statistically significant effects were accepted at the 95% level. Data are presented as means ± SD. All statistical analyses were performed in Xlstat (version 2019.2.2).

3.3 Results and discussion

3.3.1 Identification of polyphenols in the extract of H.s.

The polyphenolic profile of *H.s.* has been investigated in previous studies [15–22]; It is, however, important to note that no characterization studies have been performed for this species in Morocco to date.

Figure 3.3 shows the polyphenolic profile of dried calyces of *H.s.*, achieved by HPLC-PDA-MS/MS. In total, up to twenty-three polyphenolic compounds were detected and among them, twenty-one were positively identified according to retention times, MS, and literature data (**Table 3.1**). Peak N°. 1 (t_R = 1.74 min, λmax = 260) was identified as hibiscus acid, based on the UV-vis spectrum, deprotonated molecule $[M-H]^-$ at *m/z* 189, and mass fragment at *m/z* 127 derived from the typical losses of water and carbon dioxide from the main ion. Such a compound was reported in all previous studies, and it represents a lactone of hydroxycitric acid.

Amongst phenolic acids, hydroxycinnamic acids are the most characterized with twelve compounds positively identified (peaks N°. 6–8,10,11,13–16, and 18–20). Peaks N°. 8, 11, 13, and 14 reported a characteristic λmax = 325, a deprotonated molecule $[M-H]^-$ at *m/z* 353, and mass fragments at *m/z* 191 and 179 and were consequently identified as caffeoylquinic

acids; on the other hand peaks 10,15, and 16 showed a λmax = 310 nm, a deprotonated molecule $[M-H]^-$ at *m/z* 337, and a mass fragment at *m/z* 191 and were identified as coumaroylquinic acids. Concerning flavonoids peaks Nº. 17,21,22, and 23 showed a λmax = 319, 345, 353, and 350 nm with deprotonated molecules $[M-H]^-$ at *m/z* 449, 595, 609, 593, 595, and 609, and mass fragments at *m/z* 317, 301, and 285 (corresponding to the loss of sugar moieties); such compounds were positively identified as myricetin-arabinoside, quercetin-sambubioside, quercetin-rutinoside, and kaempferol-rutinoside. Finally, peaks Nº. 3 and 4, λmax = 520 nm, deprotonated molecules $[M-H]^-$ at *m/z* 597 and 579, and mass fragments at *m/z* 303 and 287 were positively characterized as delphinidin-sambubioside and cyanidin-sambubioside.

3.3.2 Release of phenolic compounds and flavonoids from H.s. during in vitro

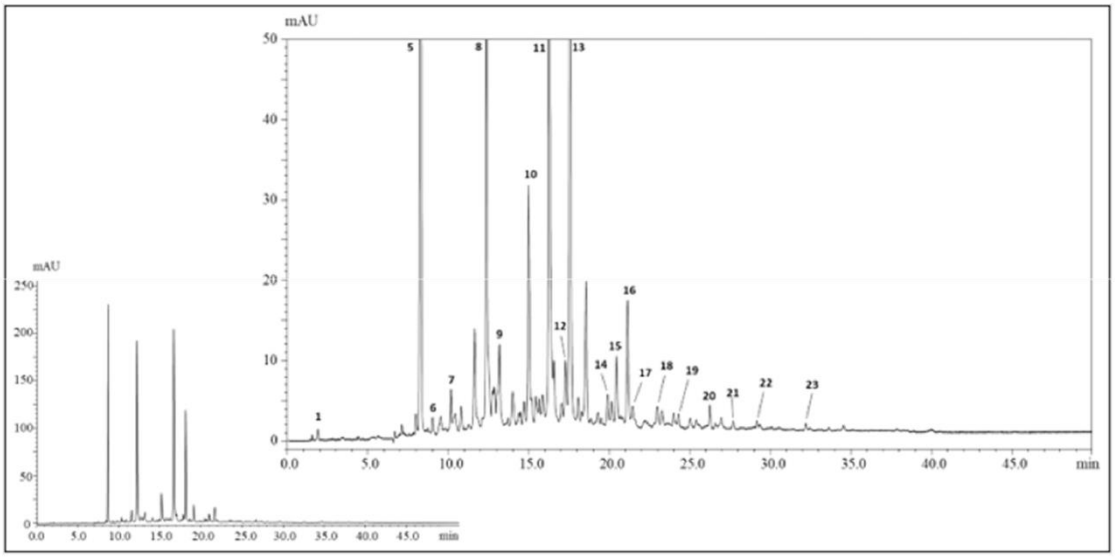

Figure 3.3 Profile of polyphenolic compounds in the aqueous extract of dried calyces of *H.s.* (λ = 280 nm). The inset illustrates the unzoomed chromatogram.

digestion

In vitro gastric digestion and gastric + duodenal digestion resulted in a decrease in certain compounds. Particularly peaks No. 8, 11, 13, and 14 assigned as caffeoylquinic acids began to decrease following stomach digestion of 20 minutes. Similarly, peaks No. 10, 15, and 16 identified as coumaroylquinic acids only persisted for a short time during the simulated human digestion due to the apparent degradation occurring in the gastric and duodenal compartments, as was reported previously [8]. As reported in **Table 3.1**, quinic acid was present only in samples obtained during duodenal digestion, suggesting that this compound was derived from the degradation of more complex caffeoylquinic and coumaroylquinic

acids. It was expected that hibiscus acid would be present in undigested extracts and persist throughout the simulation digestion, albeit at lower concentrations. Remarkably, all peaks eluted on or after 23 min were completely solubilized after 20 min of gastric incubation.

H.s polyphenols were primarily released through the stomach (23%), with a slight increase during gastric and duodenal digestion (31%, **Figure 3.4**). This can be explained by a rapid loss of polyphenols from the gastric compartment, which reduced the rate at which polyphenols were released (**Figure 3.5**).

It was previously stated that cell walls play a key role in regulating bioaccessibility of lipids, proteins, and vitamin E released from almond seeds during digestion [11]. According to a dynamic gastric model of digestion, over 90% of the polyphenols from pistachio seeds were released in the gastric compartment, with a virtual total release in the duodenal compartment [10].

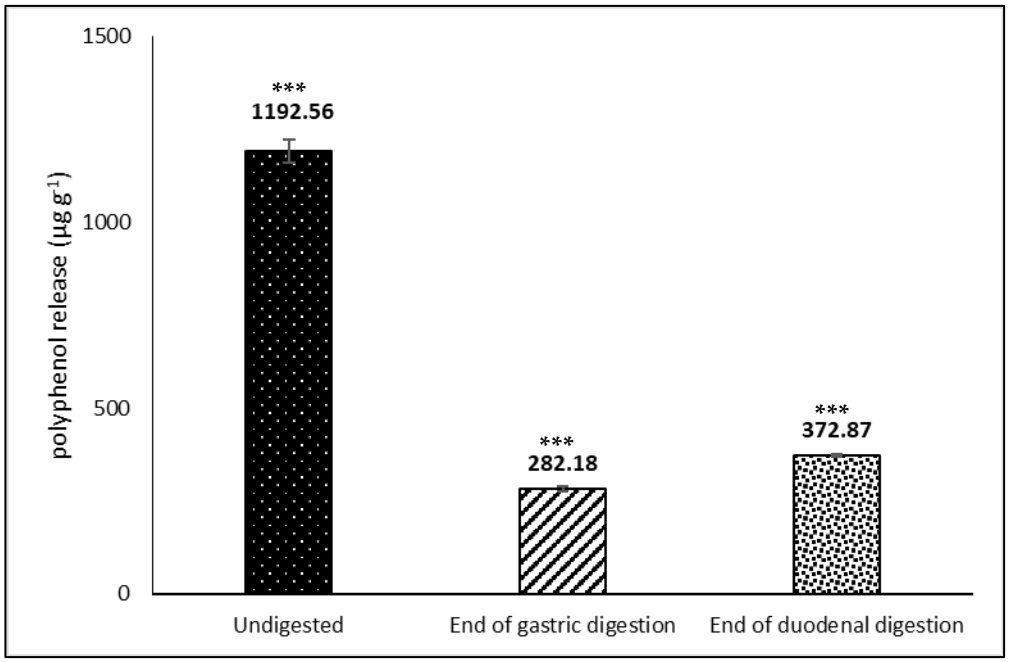

Figure 3.4. Evaluation of total polyphenols content in µg/g in the extract at the end of gastric and duodenal digestion. Values are given as the amount of polyphenols in the undigested extract (baseline) and in the soluble extract released during *in vitro* gastric and gastric + duodenal digestion. Values represent averages (±SD) of triplicate measurements. RSD was always <10%. Statistically significant differences were observed (Friedman's test followed by post hoc comparison with one-tailed Dunnett's test) and are characterized by the * symbol. Statistically significant differences were observed between the end of gastric and duodenal digestions and undigested extract ($p < 0.001$) (***).

Currently, there is no data available on the behaviour of individual health-promoting components in natural extracts, as well as their biotransformation by microbiota enzymes in the gut. This poses a significant challenge to understanding the role of individual health-promoting components in natural extracts. [7]. The impact of digestion conditions, such as pH, temperature, bile salts, gastric, and pancreatic enzymes on the bioaccessibility of specific polyphenols has also been reported [23,24]. Polyphenols are capable of binding proteins, resulting in possible protein denaturation (e.g., trypsin, amylase, lysozyme) that lowers digestibility in the upper GI tract and protects the large bowel against oxidative reactions [25,26]. Consequently, the health benefits associated with polyphenol intake depend on a variety of factors, including their release in the upper gastrointestinal tract, the food matrix, as well as the degree of bacterial fermentation in the large intestine [27].

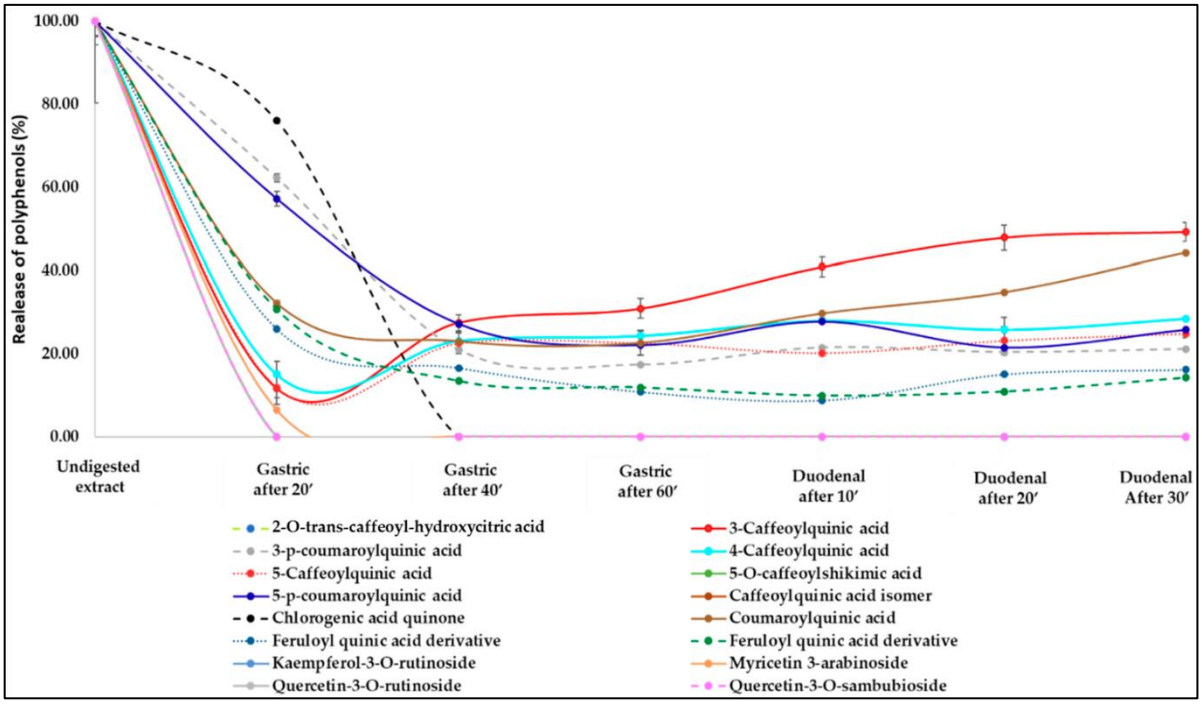

Figure 3.5. Dynamic evaluation of the release of polyphenolic compounds content during the *in vitro* simulated human digestion. Values represent averages (±SD) of triplicate measurements. RSD was always <10%.

Table 3.1. Characterization of the bioaccessible polyphenols in the extract of *H. sabdariffa* throughout the simulated human digestion. x indicates the presence of the compound in the extract. – indicates the absence of the compound in the extract.

Peak	t_R (min)	λ_{max} (nm)	$[M-H]^-$; MS/MS	Tentative identification	Undigested extract	Gastric digestion			Duodenal digestion			Ref.
						20 min	40 min	60 min	10 min	20 min	30 min	
1	1.74	260	189,127	Hibiscus acid	×	×	×	×	×	×	×	[15-22]
2	3.53	280	387	Quinic acid	-	-	-	-	×	×	×	
3	4.03	520	597,303*	Delphinidin-sambubioside	×	×	×	×	×	×	×	[15-20,22]
4	6.35	520	579,287*	Cyanidin-sambubioside	×	×	×	×	×	×	×	[15-20,22]
5	8.11	286	253	Unknown	×	×	-	-	-	-	-	-
6	8.89	314	315	Chlorogenic acid quinone	×	×	-	-	-	-	-	[16]
7	10.15	317	368,191	Caffeoyl-hydroxycitric acid	×	-	-	-	-	-	-	[16,18]
8	12.34	325	353,191,179	Caffeoylquinic acid	×	×	×	×	×	×	×	[20-22]
9	13.13	287	297	Unknown	×	-	-	-	-	-	-	-
10	15.06	310	337, 191	Coumaroylquinic acid	×	×	×	×	×	×	×	[16,18]
11	16.28	325	353,191,179	Caffeoylquinic acid isomer	×	×	×	×	×	×	×	[19-22]
12	17.23	326	367	Unknown	×	×	×	×	×	×	×	-
13	17.61	325	353,191,179	Caffeoylquinic acid isomer	×	×	×	×	×	×	×	[19-22]
14	19.74	325	353,191,179	Caffeoylquinic acid isomer	×	-	-	-	-	-	-	[21]
15	20.58	309	337,191	Coumaroylquinic acid isomer	×	×	×	×	×	×	×	[18,20]
16	21.16	308	337,191	Coumaroylquinic acid isomer	×	×	×	×	×	×	×	[10,20]
17	21.38	319	449,317	Myricetin-arabinoside	×	×	-	-	-	-	-	[15,17,18]
18	22.97	329	367,193	Feruloyl quinic acid derivative	×	×	×	×	×	×	×	[19]
19	24.33	326	335,179	Caffeoylshikimic acid	×	-	-	-	-	-	-	[15-18, 20]
20	26.29	329	367,193	Feruloyl quinic acid derivative	×	×	×	×	×	×	×	[19]
21	27.88	345	595,301	Quercetin-sambubioside	×	-	-	-	-	-	-	[15-18,20]
22	29.18	353	609,301	Quercetin-rutinoside	×	-	-	-	-	-	-	[15-18,20-22]
23	32.27	350	593,285	Kaempferol-rutinoside	×	-	-	-	-	-	-	[15-18,20,22]

*Acquired in $[M+H]^+$

3.3.3 Release of anthocyanins from H.s. during in vitro digestion

Besides organic acids, polysaccharides and flavonoids, anthocyanins, mainly delphinidin-sambubioside and cyanidin-sambubioside, represent the major constituents of *H.s.*, which are important for nutraceutical and pharmaceutical industries. **Figure 3.6** describes the content of delphinidin-3-sambubioside and cyanidin-3-sambubioside in the undigested extract of *H.s.* and throughout simulated human digestion. Regarding flavonoid release, most of the anthocyanins were bioaccessible in the gastric compartment, with a slight further increase in the duodenal phase. Overall, 49% (26% after 20 min gastric phase, 14% after 40 min gastric phase, and 9% after 60 min gastric phase) and 77% (31% after 20 min gastric phase, 25% after 40 min gastric phase, and 21% after 60 min gastric phase) of delphinidin-3-sambubioside and cyanidin-3-sambubioside were released in the gastric compartment, respectively. Additionally, 3% and 10% of delphinidin-3-sambubioside and cyanidin-3-sambubioside were solubilized in the small intestine, respectively. Recent research has demonstrated the feasibility of encapsulating anthocyanins in jelly candy using microparticles: up to 73% of the bioactive compounds of hibiscus extract were retained after encapsulation [28].

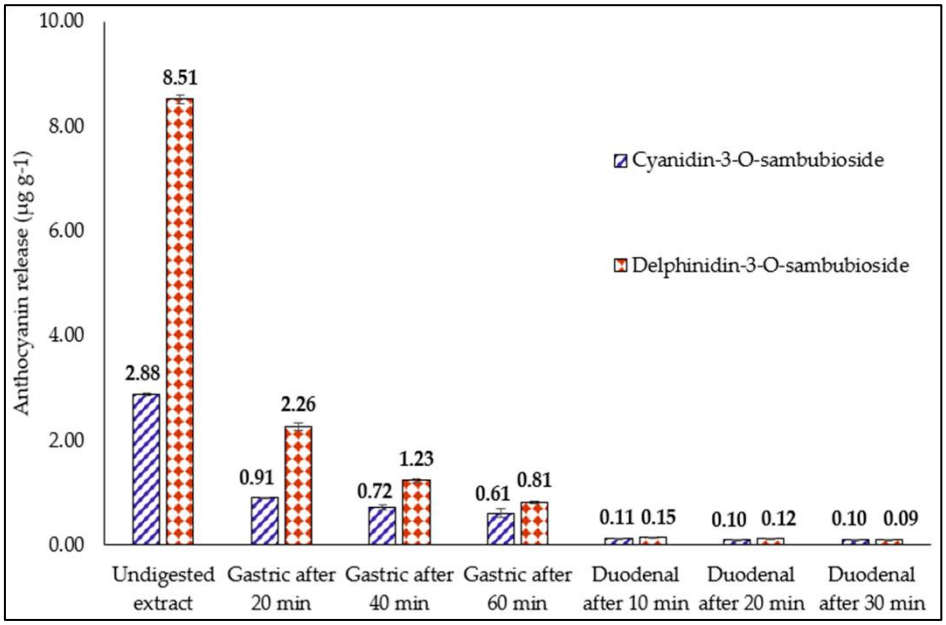

Figure 3.6. Quantification of anthocyanins in the raw extract and during *in vitro* gastric and duodenal digestion.

Anthocyanin release in the present study followed a similar trajectory to that of polyphenol release in terms of gastric and duodenal distribution, although at higher release levels.

On the other hand, de Moura et al. [28] have reported that in comparison with polyphenols, anthocyanins have exhibited lower release values, which may be due to their solubility and to

the employed enzymes. Anthocyanin bioavailability was examined by Elker et al, along with the possible implications for inter-individual variability [29]. As dietary bioactive compounds, anthocyanins have been demonstrated to provide beneficial effects against cardiovascular, neurological, and eye conditions. However, factors such as food matrix and food processing, enzymes involved in their metabolism and transport, as well as gut microbiota that metabolize anthocyanins may be responsible for the high inter- and intra-variability found in bioaccessibility studies.

3.4 Conclusion

The present study demonstrated that the polyphenolic compounds in *H. sabdariffa* are rapidly accessible in the stomach, thus maximizing absorption into the upper small intestine and contributing to the positive relationship between hibiscus consumption and health-related outcomes. In order to validate these *in vitro* findings regarding the release of bioactive compounds from the hibiscus and the metabolism of the undigested polyphenols by the gut microbiota, further clinical studies are needed in humans.

3.5 References

1. Kumar, Shashank, and Abhay K. Pandey. 2013. “Chemistry and Biological Activities of Flavonoids: An Overview.” The Scientific World Journal 2013: 1–16.
2. Tsao, Rong. 2010. “Chemistry and Biochemistry of Dietary Polyphenols.” Nutrients 2 (12): 1231–46.
3. Crozier, Alan, Indu B. Jaganath, and Michael N. Clifford. 2009. “Dietary Phenolics: Chemistry, Bioavailability and Effects on Health.” Natural Product Reports 26 (8): 1001.
4. Morohashi, Kengo, María Isabel Casas, Maria Lorena Falcone Ferreyra, María Katherine Mejía-Guerra, Lucille Pourcel, Alper Yilmaz, Antje Feller, et al. 2012. “A Genome-Wide Regulatory Framework Identifies Maize Pericarp Color1 Controlled Genes.” The Plant Cell 24 (7): 2745–64.
5. Fantini, Massimo, Monica Benvenuto, Laura Masuelli, Giovanni Frajese, Ilaria Tresoldi, Andrea Modesti, and Roberto Bei. 2015. “In Vitro and in Vivo Antitumoral Effects of Combinations of Polyphenols, or Polyphenols and Anticancer Drugs: Perspectives on Cancer Treatment.” International Journal of Molecular Sciences 16 (12): 9236–82.
6. Majdoub, Yassine Oulad El, Mohammed Diouri, Paola Arena, Adriana Arigò, Francesco Cacciola, Francesca Rigano, Paola Dugo, and Luigi Mondello. 2019. “Evaluation of the Availability of Delphinidin and Cyanidin-3-O-Sambubioside from Hibiscus Sabdariffa and 6-Gingerol from Zingiber Officinale in Colon Using Liquid Chromatography and Mass Spectrometry Detection.” European Food Research and Technology 245 (11): 2425–33.
7. Stevens, Jan F., and Claudia S. Maier. 2016. “The Chemistry of Gut Microbial Metabolism of Polyphenols.” Phytochemistry Reviews 15 (3): 425–44.
8. Mandalari, G., A. Tomaino, G.T. Rich, R. Lo Curto, T. Arcoraci, M. Martorana, C. Bisignano, et al. 2010. “Polyphenol and Nutrient Release from Skin of Almonds during Simulated Human Digestion.” Food Chemistry 122 (4): 1083–88.
9. Mandalari, Giuseppina, Maria Vardakou, Richard Faulks, Carlo Bisignano, Maria Martorana, Antonella Smeriglio, and Domenico Trombetta. 2016. “Food Matrix Effects of Polyphenol Bioaccessibility from Almond Skin during Simulated Human Digestion.” Nutrients 8 (9): 568.
10. Mandalari, Giuseppina, Carlo Bisignano, Angela Filocamo, Simona Chessa, Mariagiovanna Sarò, Germana Torre, Richard M. Faulks, and Paola Dugo. 2013. “Bioaccessibility of Pistachio Polyphenols, Xanthophylls, and Tocopherols during Simulated Human Digestion.” Nutrition 29 (1): 338–44.

11. Mandalari, Giuseppina, Richard M. Faulks, Gillian T. Rich, Vincenzo Lo Turco, David R. Picout, Rosario B. Lo Curto, Giuseppe Bisignano, et al. 2008. “Release of Protein, Lipid, and Vitamin E from Almond Seeds during Digestion.” Journal of Agricultural and Food Chemistry 56 (9): 3409–16.
12. Trombetta, Domenico, Antonella Smeriglio, Marcella Denaro, Roberto Zagami, Mara Tomassetti, Rosa Pilolli, Elisabetta De Angelis, Linda Monaci, and Giuseppina Mandalari. 2020. “Understanding the Fate of Almond (Prunus Dulcis (Mill.) D.A. Webb) Oleosomes during Simulated Digestion.” Nutrients 12 (11): 3397.
13. Kallam, Kalyani, Ingo Appelhagen, Jie Luo, Nick Albert, Huaibi Zhang, Simon Deroles, Lionel Hill, et al. 2017. “Aromatic Decoration Determines the Formation of Anthocyanic Vacuolar Inclusions.” Current Biology 27 (7): 945–57.
14. Russo, Marina, Chiara Fanali, Giusy Tripodo, Paola Dugo, Rosario Muleo, Laura Dugo, Laura De Gara, and Luigi Mondello. 2018. “Analysis of Phenolic Compounds in Different Parts of Pomegranate (Punica Granatum) Fruit by HPLC-PDA-ESI/MS and Evaluation of Their Antioxidant Activity: Application to Different Italian Varieties.” Analytical and Bioanalytical Chemistry 410 (15): 3507–20.
15. Beltrán-Debón, R., C. Alonso-Villaverde, G. Aragonès, I. Rodríguez-Medina, A. Rull, V. Micol, A. Segura-Carretero, A. Fernández-Gutiérrez, J. Camps, and J. Joven. 2010. “The Aqueous Extract of Hibiscus Sabdariffa Calices Modulates the Production of Monocyte Chemoattractant Protein-1 in Humans.” Phytomedicine 17 (3–4): 186–91.
16. Borrás-Linares, Isabel, María Herranz-López, Enrique Barrajón-Catalán, David Arráez-Román, Isabel Gonzálezlvarez, Marival Bermejo, Alberto Gutiérrez, Vicente Micol, and Antonio Segura-Carretero. 2015. “Permeability Study of Polyphenols Derived from a Phenolic-Enriched Hibiscus Sabdariffa Extract by UHPLC-ESI-UHR-Qq-TOF-MS.” International Journal of Molecular Sciences 16 (8): 18396–411.
17. Fernández-Arroyo, Salvador, Inmaculada C. Rodríguez-Medina, Raúl Beltrán-Debón, Federica Pasini, Jorge Joven, Vicente Micol, Antonio Segura-Carretero, and Alberto Fernández-Gutiérrez. 2011. “Quantification of the Polyphenolic Fraction and in Vitro Antioxidant and in Vivo Anti-Hyperlipemic Activities of Hibiscus Sabdariffa Aqueous Extract.” Food Research International 44 (5): 1490–95.
18. Herranz-López, María, Salvador Fernández-Arroyo, Almudena Pérez-Sanchez, Enrique Barrajón-Catalán, Raúl Beltrán-Debón, Javier Abel Menéndez, Carlos Alonso-Villaverde, Antonio Segura-Carretero, Jorge Joven, and Vicente Micol. 2012.

"Synergism of Plant-Derived Polyphenols in Adipogenesis: Perspectives and Implications." Phytomedicine 19 (3–4): 253–61.

19. Peng, Chiung-Huei, Charng-Cherng Chyau, Kuei-Chuan Chan, Tsung-Hsien Chan, Chau-Jong Wang, and Chien-Ning Huang. 2011. "Hibiscus Sabdariffa Polyphenolic Extract Inhibits Hyperglycemia, Hyperlipidemia, and Glycation-Oxidative Stress While Improving Insulin Resistance." Journal of Agricultural and Food Chemistry 59 (18): 9901–9.
20. Piovesana, Alessandra, Eliseu Rodrigues, and Caciano Pelayo Zapata Noreña. 2019. "Composition Analysis of Carotenoids and Phenolic Compounds and Antioxidant Activity from Hibiscus Calyces (Hibiscus Sabdariffa L.) by HPLC-DAD-MS/MS." Phytochemical Analysis 30 (2): 208–17.
21. Ramírez-Rodrigues, M.M., M.O. Balaban, M.R. Marshall, and R.L. Rouseff. 2011. "Hot and Cold Water Infusion Aroma Profiles of Hibiscus Sabdariffa: Fresh Compared with Dried." Journal of Food Science 76 (2): C212–17.
22. Jabeur, Inès, Eliana Pereira, Lillian Barros, Ricardo C. Calhelha, Marina Soković, M. Beatriz P.P. Oliveira, and Isabel C.F.R. Ferreira. 2017. "Hibiscus Sabdariffa L. as a Source of Nutrients, Bioactive Compounds and Colouring Agents." Food Research International 100 (October): 717–23.
23. D'Antuono, Isabella, Antonella Garbetta, Vito Linsalata, Fiorenza Minervini, and Angela Cardinali. 2015. "Polyphenols from Artichoke Heads (Cynara Cardunculus (L.) Subsp. Scolymus Hayek): In Vitro Bio-Accessibility, Intestinal Uptake and Bioavailability." Food & Function 6 (4): 1268–77.
24. Pérez-Vicente, Antonio, Angel Gil-Izquierdo, and Cristina García-Viguera. 2002. "In Vitro Gastrointestinal Digestion Study of Pomegranate Juice Phenolic Compounds, Anthocyanins, and Vitamin C." Journal of Agricultural and Food Chemistry 50 (8): 2308–12.
25. Jakobek, Lidija. 2015. "Interactions of Polyphenols with Carbohydrates, Lipids and Proteins." Food Chemistry 175 (May): 556–67.
26. Ozdal, Tugba, Esra Capanoglu, and Filiz Altay. 2013. "A Review on Protein–Phenolic Interactions and Associated Changes." Food Research International 51 (2): 954–70.
27. Saura-Calixto, Fulgencio, José Serrano, and Isabel Goñi. 2007. "Intake and Bioaccessibility of Total Polyphenols in a Whole Diet." Food Chemistry 101 (2): 492–501.

28. Moura, Sílvia C.S.R. de, Carolina L. Berling, Aline O. Garcia, Marise B. Queiroz, Izabela D. Alvim, and Miriam D. Hubinger. 2019. “Release of Anthocyanins from the Hibiscus Extract Encapsulated by Ionic Gelation and Application of Microparticles in Jelly Candy.” Food Research International 121 (July): 542–52.
29. Eker, Merve Eda, Kjersti Aaby, Irena Budic-Leto, Suzana Rimac Brnčić, Sedef Nehir El, Sibel Karakaya, Sebnem Simsek, Claudine Manach, Wieslaw Wiczkowski, and Sonia de Pascual-Teresa. 2019. “A Review of Factors Affecting Anthocyanin Bioavailability: Possible Implications for the Inter-Individual Variability.” Foods 9 (1): 2.

CHAPTER 4

Chemical characterization of three cultivars of *Brassica juncea* L. extracts from different plant tissues by Gas and Liquid chromatography coupled to mass spectrometry

4.1 Introduction

A large portion of the human diet consists of cruciferous vegetables, known as *Brassicaceae*, which contain an abundance of health-promoting substances that may help to reduce the risk of disease. This family is considered a potential source of glucosinolates, carotenoids, amino acids, vitamins (C and E), and phenolic compounds [1–13]. Among the vegetables consumed the most is *Brassica oleracea* L., a plant with many different forms, including kale, cabbage, broccoli, brussels sprouts, cauliflower, and many others. One of the most famous species, *Brassica juncea* (L.) Czern. (*B. juncea*), is well known for its green vegetable, also called Indian mustard or brown mustard. It is also consumed as a root and leaf vegetable in China and as a spice in Europe and America.

Generally, it has been stated that a high intake of *Brassicaceae* vegetables is correlated to the prevention of various types of cancer, such as colon and lung cancers [14]. Particularly, *B. juncea* leaf extract has demonstrated through *in vitro* studies anticancer activity against colon and lung cancer [15], antioxidant activities [16], a reduction in lipid peroxidation under diabetic oxidative stress [17] and inhibiting the accumulation of body fat [18]. Furthermore, polyphenols from *B. juncea* have also been shown to be beneficial in the treatment of cognitive disorders caused by diabetes [19].

Bioactive molecules present in *Brassica* species include flavonoids and phenolic acids. Where flavonoids consist of two aromatic benzene rings separated by an oxygenated heterocyclic ring, with differences in the number, distribution, and substitution of phenolic hydroxyl groups across the molecules [20]. Flavonoids protect plants from UV radiation, pathogenic microorganisms, insects and herbivorous. The most prevalent subclass of flavonoids in plant foods and *Brassica* plants in general are flavonols, with the most important aglycones, quercetin, kaempferol and isorhamnetin, present in the glycosidic form (O-glycosides), while myricetin is less common. Typically, flavonoids are present in plant tissues as complex conjugates containing one to five sugar moieties bound to the aglycones, and they are typically acylated with hydroxycinnamic acids.

There are several factors that affect polyphenol content in plants, including: cultivar, climate, post-harvest treatments, and agricultural practices and the environment [1].

The nutritional value of *Brassica* plants is relatively linked to their polyphenolic content, which can vary greatly between species and even between plants of the same species. The polyphenolic composition of different *Brassica* species has shown distinctive qualitative and quantitative profiles [21]. It has been reported that the total polyphenol content in edible parts of *B. oleracea* L. is twice that in brussels sprouts, cauliflower, and broccoli [22]. Where flavonol aglycones content was reported in detail [23–25].

In addition, it has been previously reported that volatile compounds present in plant foods, in addition to being responsible for organoleptic properties, have beneficial properties for human health [26]. A variety of volatile compounds have already been characterized in *B juncea*, including alkanes, ketones, and isothiocyanates [27–29].

The present study aims to evaluate the metabolite content of various portions (leaves, stems, roots, flowers and seeds) of three cultivars of *B. juncea*, ISCI 99 (sample A), ISCI Top (sample B), and ISCI "Broad-leaf" (sample C), through the use of HPLC-PDA/ESI-MS, in order to be furtherly employed as nutraceuticals in different food matrices. In addition, GC-FID/MS was also used to analyze the volatile content of the most complex sample, namely leaves, along with chemical analysis of defatted seed meals (DSM).

Sample A, one of the initial samples selected at CREA-CI (Bologna, Italy) [30,31] was selected based on the richness of tissues in glucosinolates, which are commonly induced by biofumigation in greenhouse environments. Moreover, the present plant is known by its short cycle and early summer flowering period, with good adaptation to different pedoclimatic conditions. Like the other small-seeded *Brassicaceae*, sample A can be seeded in both fall and spring season with refined soil as preference, although it can afford a turf seed. Sample B was newly listed in the Plant Variety Protection Office (PVPO) through a USDA PVP certificate (https://apps.ams.usda.gov/CMS/CropSearch.aspx). This cultivar was bred and selected at CREA-CI (Bologna, Italy) for biofumigation reasons, and was applied as green fertilizer by soil incorporation. The Sample C line shows some interesting characteristics in comparison with the other varieties, including high biomass production and a distinctive broadleaf, despite being more susceptible to low temperatures, pests, and diseases.

To date, only scarce information on both volatile and non-volatile compositions of the *B. juncea* species is available in the literature. The chemical composition of the three cultivars of the *B. juncea* was furtherly studied using comprehensive two-dimensional liquid chromatography coupled with a photodiode array and mass spectrometry detection [32].

4.2 Materials and methods

4.2.1 Chemical and reagents

All employed organic solvents; water, methanol, acetonitrile, and acetic acid were LC-MS grade and were acquired from Merck Life Science (Merck KGaA, Darmstadt, Germany). Kaempferol-3-*O*-glucoside (Km 3-*O*-glucoside), Isorhmanetin-3-O-glucoside (Is 3-*O*-glucoside), and Quercetin-3-*O*-glucoside (Qn 3-*O*-glucoside) were purchased from Merck Life Science (Merck KGaA, Darmstadt, Germany). Stock solutions of 1000 ppm were prepared for each standard by dissolving 10 mg of each standard in 10 mL of methanol.

4.2.2 Sample preparation

B. juncea samples were provided from the *Brassica* seed collection of CREA-CI [33]. Which were harvested in autumn on 15 October 2017, each in a 30 m^2 plot, at the CREA experimental farm located at Budrio (Bologna) in the Po Valley area (Emilia Romagna region, $44^{\circ}32^{0}00^{00}$ N; $11^{\circ}29^{0}33^{00}$ E, altitude 28 m a.s.l.). It consists primarily of flat land with alluvial deep loamy soil, with medium levels of total nitrogen and organic matter. The cultivation took place without fertilization, and no further agronomic inputs were required until harvest. Plant samples were collected at three different phenological phases: (i) the first phase, 12 ± 3 cm (Sample A) to 23 ± 3 cm (Sample B and Sample C) tall, the edible salad phase; (ii) the second phase, 18 ± 2 cm (Sample A) to 33 ± 4 cm (Sample B and Sample C) tall, the edible salad phase as the climax, when stems and leaves began to be of equal weight; and (iii) the third phase, when the inflorescence was fully developed. At each sampling time, six plants were manually harvested, and brushed (in order to remove soil debris physically), ensuring that different tissues were distinguished from one another (leaves, stems, roots, flowers. Samples were immediately frozen and lyophilized for storage in glass vacuum desiccators. Lyophilized tissues were finely pulverized to 0.5 µm size for analysis.

Seed cake preparation and characterization

B. juncea seed cake is the main by-product of this oilseed crop, and to date, oil yield is its primary economic value [34]. Seeds were subjected to extraction with n-hexane (1:10 *w/v*) in a rotary shaker overnight at room temperature. The aim was to obtain the largest possible number of bioactive molecules. Seed cake was crushed in a mortar and allowed to dry at 40°C to constant weight and finally ground to 0.5 mm size. The *B. juncea* defatted seed meals (DSMs) were analyzed for the determination of moisture, nitrogen, residual oil, and glucosinolate (GSL) content. Moisture content was controlled by determining the difference between its weight before and after oven drying at 105°C for 12 hours. Total nitrogen content was assessed in accordance with the American Society for Testing Materials (ASTM D5373

2016) [35], and the crude protein content has been expressed as a percentage of dry matter and calculated using the conventional soy protein factor of 6.25 as the basis for calculation [36]. The residual oil was extracted by n-hexane using a standard automated continuous extraction according to the Twisselmann principle using an E-816 Economic Continuous Extraction (ECE) unit (BÜCHI Labortechnik AG, Flawil, Switzerland). GSL content and profiles were evaluated by HPLC-UV analysis of desulfo-GSLs following the ISO 9167-1 method (ISO 9167-1:1992/Amd 1:2013) [37]. The desulfo GSLs were detected by monitoring their absorbance at 229 nm and identified based on their UV spectra and retention times [38,39]; Sinigrin was employed as external standard for the quantification of GSL amount. Each extraction and analysis were carried out in triplicate.

Sample preparation for HPLC-PDA-MS

The extraction of the metabolite content was performed based on the following slightly modified protocol [7]. All samples were spiked before the extraction with 50 µL of apigenin (1000 ppm), which was evaporated with the use of nitrogen. The powder of different plant parts (seed, root, stem, leaf and flower) of *B. juncea* was weighed in 100 mg in addition to the DSM of the three different cultivars. Samples extraction was performed in duplicates using 5 mL of a mixture of methanol:water (60:40, *v*/*v*) for 30 min in a sonicator followed by a centrifugation at 1000× *g* for 15 min. The obtained supernatant was then filtrated through 0.45 µm filter paper; Merck Life Science (Merck KGaA, Darmstadt, Germany). The obtained extracts were evaporated using EZ-2 evaporator and redissolved in 1 mL of the same solvent mixture of extraction. A volume of 10 µL was injected into HPLC. The extraction process is illustrated in **Figure 4.1**.

Sample preparation for GC-FID/MS

The extraction of the volatile compounds was accomplished with the use of a 50/30 µm DVB/CAR/PDMS (SPME fiber) (Merck Life Science, Merck KGaA, Darmstadt, Germany). SPME fiber was conditioned following the recommendation described by Merck Life Science, by the insertion of SPME into the GC injector at 270 ˚C for 30 min. In a 20 mL sealed vial with a magnetic cap and silicone/PTFE septum (Agilent Technologies, Santa Clara, CA, USA), 250 mg of each *B. juncea* sample was placed. The sample was stirred at 170 rpm for 45 min at a temperature of 70°C. The SPME fiber was exposed to the GC injector at a temperature of 260°C for 1 min, followed by 45 min exposure of the fibers to the headspace under the same conditions mentioned above. The extracted volatile compounds were injected into GC following a thermal desorption.

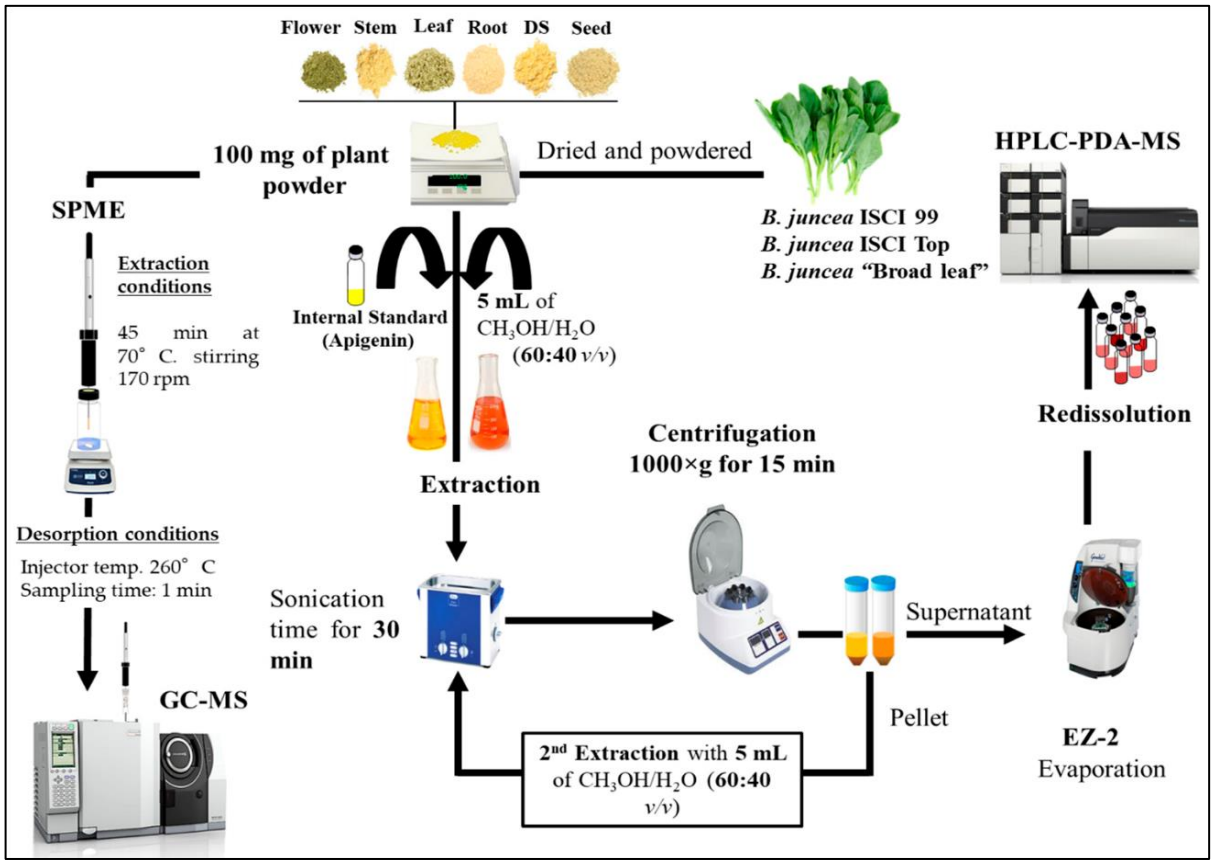

Figure 4.1. Extraction and analysis procedures of volatile and non-volatile compounds of *B. juncea* cultivars.

4.2.3 Instrumentation and method validation

GC-FID/MS

The chemical characterization of volatile compounds was performed on a GCMS-QP2010 system (Shimadzu, Kyoto, Japan) supplied with a split–splitless injector. Data files were furtherly elaborated by using Shimadzu "GCMS solution" software (version 4.45) (Kyoto, Japan).

The quantification of volatile compounds was carried out on a GC2010 system (Shimadzu, Kyoto, Japan). Where Data elaboration was conducted on a Shimadzu LabSolutions software (version 5.92) (Kyoto, Japan).

The analyses were performed on a GC-MS system equipped with an SLB-5ms fused-silica capillary column (30 m × 0.25 mm i.d. × 0.25 µm df film thickness) (Merck Life Science, Merck KGaA, Darmstadt, Germany). The injection was performed in splitless mode, at the temperature of 260 ˚C. Helium was kept at the linear velocity of 30.0 cm/sec corresponding to an inlet pressure of 24.2 KPa. The oven temperature program was set at 40 ˚C (held for 1 min); it was ramped up to 350 ˚C (held for 5 min) at a rate of 3 ˚C/min. The electron impact (EI) source temperature was maintained at 220 ˚C and the interface was set at the temperature

of 250 °C. Mass range acquisition was made in full scan mode in the mass range of 40–660 *m/z*, with an event time of 0.2 s. Compounds were identified with the support of "FFNSC 4.0" (Shimadzu Europa GmbH, Duisburg, Germany), which consisted of a library of volatile compounds obtained and stored by GC-MS separation and "W11N17" (Wiley11-Nist17, Wiley, Hoboken, NJ, USA; Mass Finder 3). Identification was performed applying a spectral similarity filter (match over 85%) using also linear retention indices (LRI) that were calculated using a C7–C30 saturated n-alkane homologue series (1000 g/mL, 49451-U) supplied by Merck Life Science, Merck KGaA, Darmstadt, Germany.

A GC-FID system was used to quantify the volatile compounds using the same capillary column and temperature program used in the qualitative analysis. The carrier gas (helium) was kept at the linear velocity of 30.0 cm/s corresponding to an inlet pressure of 97.4 KPa and the split mode of the injector was set to splitless. The flame temperature was set at 350 °C (sampling rate 200 ms). Makeup flow, hydrogen, and airflow were set as follows 40 mL/min, 30 mL/min, and 400 mL/min, respectively.

HPLC-PDA-MS

Analyses were performed on a Shimadzu system (Kyoto, Japan), consisting of a CBM-20A controller, two LC-30AD dual-plunger parallel-flow pumps, a DGU-20A$_5$R degasser, a CTO-20AC column oven, a SIL-30AC autosampler, and an SPD-M30A PDA detector (1.0 µL detector flow cell volume). The LC system was hyphenated to an LCMS-8050 triple quadrupole mass spectrometer through an ESI source (Shimadzu, Kyoto, Japan). For data handling, the Shimadzu LabSolutions software (version 5.93) (Kyoto, Japan) was employed. Analyses were performed on an Ascentis Express RP C18 column (150 × 4.6 mm, 2.7 µm I.D., Merck Life Science, Merck KGaA, Darmstadt, Germany).

The mobile phase consisted of water/acetic acid (99.85/0.15 *v/v*, solvent A) and acetonitrile (solvent B), with the following gradient elution: 0–5 min, 5% B, 5–15 min, 10% B, 15–30 min, 20% B, 30–60 min, 50% B, 60 min, 100% B.

Photodiode array detector was applied in the range of λ= 200–450 nm, where *B. juncea* polyphenols were detected at λ = 330 nm (sampling frequency: 12.5 Hz, time constant: 0.16 s). The flow rate was set at 1 mL/min and the injected volume was 10 µL.

MS analysis was performed in negative and positive mode and scan range was set at *m/z* 100–1400; scan speed of 2727 amu/s. The conditions of ESI were as follows: event time 0.5 s; nebulizing gas (N_2) flow rate 3 L/min; drying gas (N_2) flow rate, 10 L/min; interface temperature: 300 °C; heat block temperature: 400 °C; DL (desolvation line) temperature: 250 °C; DL voltage: 1 V; interface voltage: −3 kV; Qarray DL voltage 0 V, Q3 pre-rod bias 15 V.

Calibration curves

Owing to the unavailability of commercial standards for all identified polyphenols, a semi-quantification was carried out by employing three polyphenolic standards of the main representative phenolic compounds: Km 3-*O*-glucoside, Is 3-*O*-glucoside and Qn 3-*O*-glucoside. Calibration curves were prepared at five different concentration levels within the range of 0.1–100 mg/L. Triplicate injections were made for each level, and a linear regression was generated. The calibration curves with the external standards were obtained using concentration (mg/L) with respect to the area obtained from the integration of the PDA peaks acquired at a wavelength of 330 nm. The amount of the compound was finally expressed in µg/100 mg DW.

4.3 Results and discussion

4.3.1 Characterization of non-volatile compounds in B. juncea cultivars by HPLC-PDA/ESI-MS

The chemical composition of non-volatile compounds in *Brassica* vegetables were previously examined [2–8,25,32], where the glycosylated flavonols was reported as the main class present in *Brassicaceae*, including O-glycosides of quercetin, kaempferol, and isorhamnetin. The sugar moiety presents in *Brassicaceae* is glucose, occurring as mono-, di-, tri-, tetra-, and pentaglucosides, also frequently occurred acylated by different hydroxycinnamic acids. Furthermore, phenolic acids are also present in *Brassica* vegetables, where the most common compounds are p-coumaric, caffeic, sinapic, and ferulic acids. **Figure 4.2 and Table 4.1** report the phytochemical characterization of the flower extracts of the three *B. juncea* cultivars, where flowers parts turned out to be the most complex ones among the samples examined.

The polyphenolic identification was based on retention time, UV, ESI-MS spectra, besides literature data. For instance, Km 3-diglucoside-7-glucoside (peak 3) and Km glucoside (peak 30) had shown a typical UV λ_{max} around 265 and 345 nm, whereas Qn-3-diglucoside (Peak 14) or Is-3,7-diglucoside/Is-glucoside (peak 23/peak 29) exhibits a UV absorption around 256 (with a shoulder around 266 nm) and 354 nm. The binding of a hydroxycinnamoyl group with the glycosyl function leads to a shift of UV absorption maxima to 326–340 nm, while the molecular ion was increased by 162, 176, 192, and 206 Da (or the sum of two acyl groups when they occur in the glucoside) for caffeoyl, feruloyl, hydroferuloyl, and sinapoyl groups, respectively [6].

The first eluted compounds were represented by malic acid and citric acid. Whereas sinapic acid and ferulic acid derivatives were the principal phenolic acids occurred as aglycones in 13 phenolic compounds derivatives. As regards flavonoids, kaempferol derivatives were the most representative aglycones (occurred in 11 polyphenols), followed by quercetin (5) and isorhamnetin (2). Except for isorhamnetin glucosides and quercetin-3-diglucoside, all other flavonoids occurred acylated by different hydroxycinnamic acids. The sugar moiety was present in the form of by glucose or sophorose in the form of mono-, di-, tri-, and tetra-glucosides [2–8,25,32].

Regarding the quantification, generally, the evaluation of the phenolic compounds content in *Brassica* spp. is performed after acidic and/or alkaline hydrolysis, due to the unavailability of commercial standards [2,4,5]. Following the approach employed in our previous work, limited to only three samples of the different cultivars [31], semi-quantification of the native flavonoid composition of all thirty-six samples analyzed, the three cultivars of *B. juncea* was performed on the RP-HPLC system coupled to PDA detection. Particularly, due to the unavailability of corresponding reference materials, three selected standards, representatives of the distinct chemical classes, namely, Km 3-*O*-glucoside, Is 3-*O*-glucoside, and Qn 3-*O*-glucoside, were adopted, and corresponding calibration curves were prepared. **Table 4.2** describes information regarding calibration curves, correlation coefficients (R^2), limits of detection (LoDs), limits of quantification (LoQs), and relative standard deviations (RSDs) of the peak areas for each standard selected. R^2 values ranged from 0.9939 to 0.9963, LoQ and LoD values ranged from 13 to 48 ppb and from 43 to 159 ppb, respectively, whereas RSD values were lower than 0.41%.

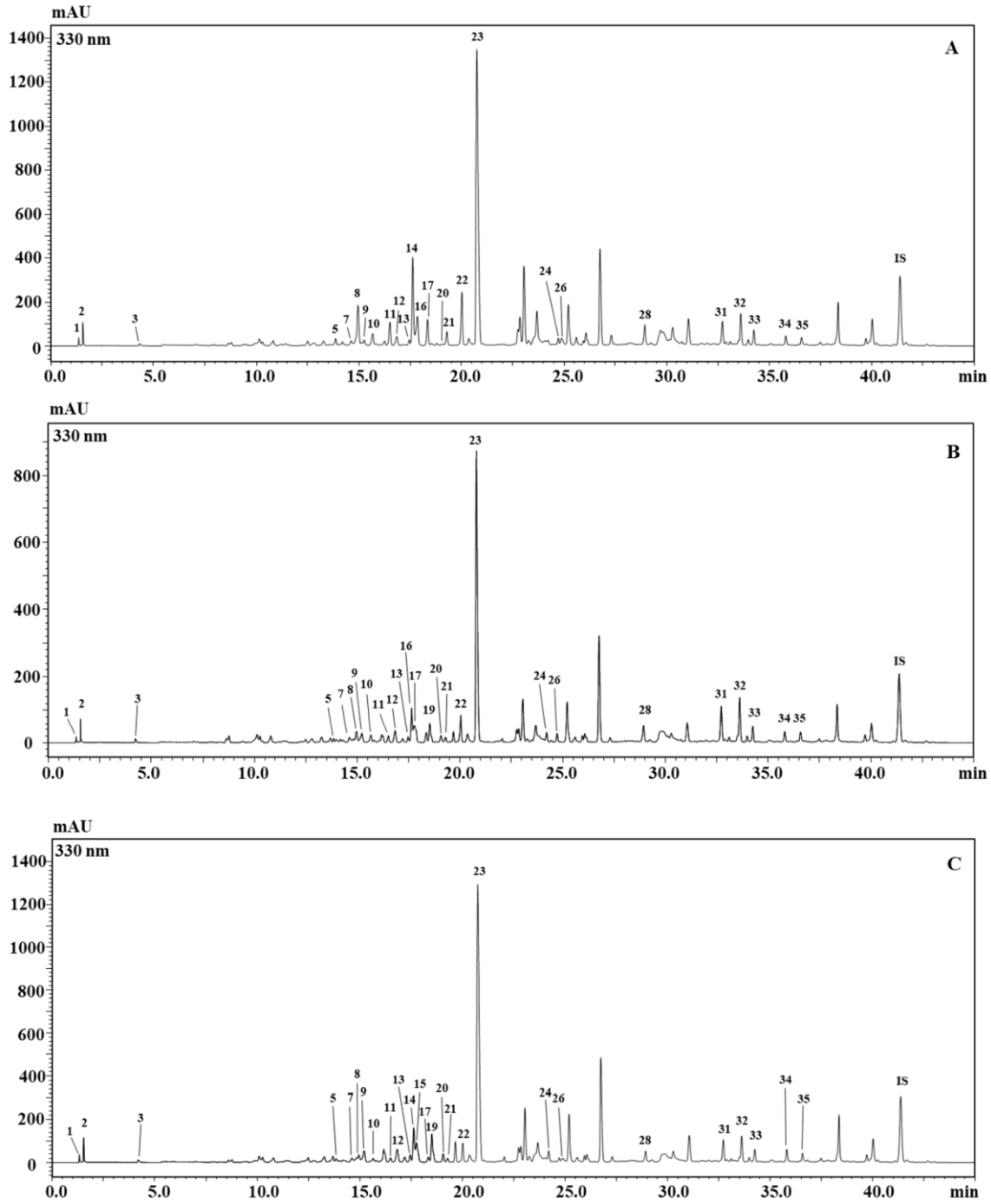

Figure 4.2. Chromatographic profiles of the polyphenolic fraction characterized in the flowers of the three B. juncea. (A) *B. juncea* ISCI 99; (B) *B. juncea* ISCI Top; (C) *B. juncea* ISCI "Broad-leaf".

Table 4.1. Characterization of polyphenols in the extracts of flowers of three *B. juncea* cultivars by HPLC-PDA-ESI-MS.

No	Tentative ID	λ max (nm)	t_R (min)	$[M-H]^-$	MS^2 ions	(µg/100 mg DW)		
						Sample A	Sample B	Sample C
1	Malic Acid	215; 260	1.34	133.0	-	*	*	*
2	Citric acid	215; 260	1.53	191.0	-	*	*	*
3	Km 3-diglucoside-7-glucoside	265; 345	4.20	771.2	609	*	*	*
4	Feruloylglucose	236; 285	13.40	355.2	193	Nd	Nd	Nd
5	Qn 3-sophoroside-7-glucoside	257; 352	13.90	787.2	625	9.73 ± 0.31	2.85 ± 0.64	3.63 ± 0.07
6	Rhamnosyl-ellagic acid	283; 313	14.28	447.0	-	Nd	Nd	Nd
7	Rhamnosyl-ellagic acid	283; 313	14.55	447.0	-	*	*	*
8	Qn 3-hydroxyferuloylsophoroside-7-glucoside	247; 335	15.07	979.2	625	65.60 ± 0.50	11.17 ± 2.12	6.60 ± 0.92
9	Km 3-sophoroside-7-glucoside	266; 343	15.33	771.2	609	5.25 ± 0.06	6.60 ± 0.86	19.05 ± 0.55
10	Qn 3-caffeoylsophoroside-7-glucoside	242; 330	15.77	949.2	625	22.04 ± 0.75	9.69 ± 2.32	5.53 ± 0.17
11	Km 3-hydroxyferuloylsophoroside-7-glucoside	232; 330	16.65	963.2	609	35.52 ± 0.07	8.16 ± 2.22	6.58 ± 0.00
12	Feruloylglucose	236; 326	16.88	355.2	193	*	*	*
13	Km 3-caffeoyldiglucoside-7-glucoside	233; 330	17.57	933.2	-	5.20 ± 0.10	4.91 ± 1.21	8.57 ± 0.04
14	Qn 3-diglucoside	256; 360	17.76	625.1	463; 301	71.75 ± 3.11	31.12 ± 8.80	40.05 ± 0.60
15	Qn 3-sinapoyltriglucoside-7-glucoside	238; 330	17.90	1155.3	993	Nd	Nd	21.86 ± 0.34
16	Qn 3-sinapoyltriglucoside-7-glucoside	245; 340	18.03	1155.3	993	49.06 ± 0.89	18.83 ± 3.89	Nd
17	Km 3-hydroxyferuloylsophoroside-7-glucoside	254; 338	18.51	963.2	625	35.62 ± 0.08	9.87 ± 2.66	5.93 ± 0.06
18	Km 3-hydroxyferuloylsophorotrioside-7-glucoside	268; 330	18.53	1125.3	963	Nd	Nd	Nd

19	Km 3-sinapoylsophorotrioside-7-glucoside	268; 330	18.78	1139.3	771	Nd	14.12 ± 3.33	23.17 ± 0.55
20	Km 3-sinapoylsophorotrioside-7-glucoside	268; 330	19.29	1139.3	771	1.80 ± 0.06	7.85 ± 2.02	10.72 ± 0.11
21	Km 3-sinapoylsophoroside-7-glucoside	268; 333	19.50	977.2	609; 815	18.69 ± 0.10	5.36 ± 1.30	5.29 ± 0.00
22	Km 3-feruloylsophoroside-7-glucoside	266; 341	20.26	947.2	609	72.18 ± 0.08	29.23 ± 8.00	25.17 ± 0.50
23	Is 3,7-diglucoside	252; 352	21.20	639.1	477; 315	683.62 ± 1.14	433.65 ± 2.94	644.43 ± 0.63
24	Feruloyl malate	242; 323	24.23	309.1	-	*	*	*
25	Sinapic acid	270; 326	24.27	223.1	179	Nd	Nd	Nd
26	Sinapoyl malic acid	240; 326	25.05	339.1	223	*	*	*
27	Sinapoyl-feruloyl-triglucoside	280; 325	25.21	885.3	499	Nd	Nd	Nd
28	Sinapoyl-hydroxyferuloyl-diglucoside	244; 330	29.46	739.2	515	*	*	*
29	Isorhamnetin glucoside	256; 351	31.94	477.1	-	48.63 ± 0.10	30.37 ± 8.49	49.87 ± 0.07
30	Km glucoside	269; 330	31.49	447.0	-	Nd	Nd	Nd
31	Disapoyl-gentiobiose	240; 330	33.32	753.2	529; 499	*	*	*
32	Sinapoyl-feruloyl-gentiobiose	240; 330	34.20	723.2	529; 499	*	*	*
33	Diferuloyldiglucoside	240; 326	34.82	693.1	499	*	*	*
34	Trisinapoylgentiobiose	240; 326	36.53	959.3	735; 529	*	*	*
35	Feruoyl-disapoyl-gentiobiose	240; 326	37.28	929.3	705; 511	*	*	*

Nd: not detected. * Not quantified in absence of standard. DW: Dry weight.

Table 4.2. External standards employed for the semi-quantification of flavonoids in *B. junceae*.

Phenolic Standards	Standard Curve	R^2	LoD (μg/mL)	LoQ (μg/mL)	Precision (RSD %)
Qn 3-*O*-glucoside	y = 13,424x + 898.59	0.9939	0.013	0.043	0.41
Is 3-*O*-glucoside	y = 14,948x ⁻ 2966.9	0.9963	0.048	0.159	0.34
Km 3-*O*-glucoside	y = 17,660x – 10,681	0.9963	0.021	0.072	0.36

The characterized flavonoids in the three *B. juncea* cultivars are reported in **Figure 4.3**, and **Table 4.1**. Among all samples of three *B. juncea* cultivars analyzed, the flowers were the richest part in flavonoids (sample A, 1124.69 μg/100 mg dry weight (DW); sample B, 623.78 μg/100 mg DW; sample C, 876.45 μg/100 mg DW). Isorhamnetin derivatives accounted for the highest content in the three cultivars: sample A (732.24 μg/100 mg), sample C (694.30 μg/100 mg), and sample B (464.02 μg/100 mg). Remarkably, the most abundant flavonoid in all cultivars examined was Is 3,7-diglucoside (683.62 μg/100 mg DW in sample A, 433.65 μg/100 mg DW in sample B, and 644.43 μg/100 mg DW in sample C), followed by Km 3-feruloylsophoroside-7-glucoside (72.18 μg/100 mg DW) in sample A, Qn 3-diglucoside (31.112 μg/100 mg DW) in sample B, and Is glycoside (49.87 μg/100 mg DW) in sample C.

4.3.2 Determination of volatile compounds in B. juncea cultivars using GC-FID/MS

In recent years, there has been a greater interest in the identification of organic compounds from plants and plant material so as to determine their potential biological activity [29]. Bioactive compounds that are volatile and semi-volatile are most effectively analyzed by GC–MS [40]. In general, it is not recommended to use % abundance (% area) when using an MS detector in scan mode, due to the narrow linear dynamic range of this detector. However, there is also the option to quantify in the Selected Ion Monitoring (SIM) mode, where selected ions are calibrated with external standards. In the present study all samples were analyzed using GC-MS for compounds identification as well as FID for peak quantification [41,42]. **Figure 4.4** describes the GC-MS profiles of the volatile content in the leaves of three *B. juncea* cultivars harvested at the edible salad phase where plants were about 15–20 cm tall. It can be seen how all extracts from the three *B. juncea* cultivars are distinguished by mixtures of various types of organic compounds.

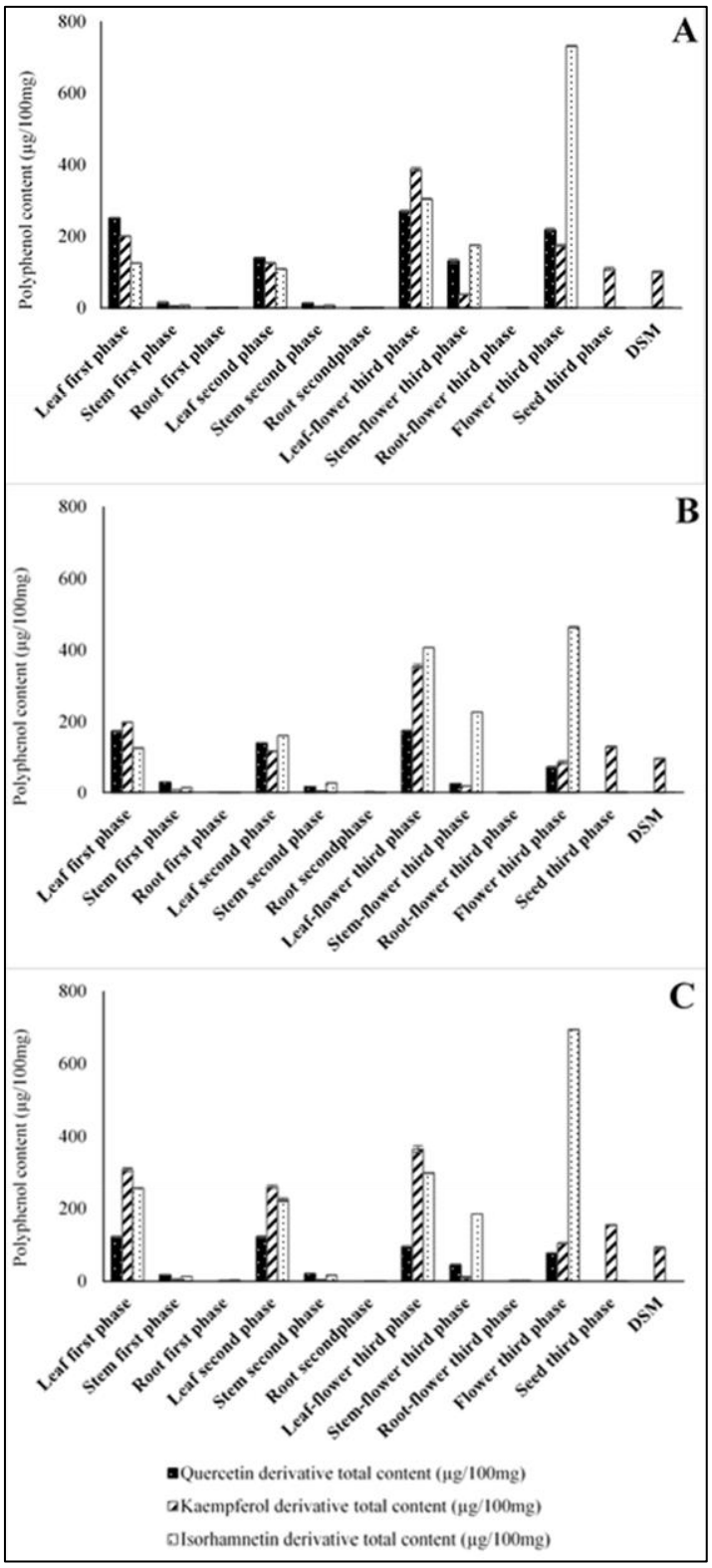

Figure 4.3. Total phenolic compounds content reported in (µg/100 mg DW) of different portions of three cultivars of *B. juncea.* (A) *B. juncea* ISCI 99; (B) *B. juncea* ISCI Top; (C) *B. juncea* ISCI "Broad-leaf".

A wide variety of compounds have been identified, including alcohols, aldehydes, esters, fatty acids, ketones, sulfur compounds, and others. *B. juncea* L. leaf extracts from three cultivars contained benzenepropanenitrile as the major volatile constituent (34.94% in sample B, 8.16 % in sample A, 6.24% in sample C) followed by benzofuranone (8.54% in sample A, 6.32% in sample C, 3.64% in sample B), and phytone (3.77% in sample B, 2.85% in sample A, 1.01% in sample C) [29,43]. The concentration and profile of different compounds in Brassica genus vary according to cultivar and stage of development [44]. The most abundant alcohol in all cultivars was phenethyl alcohol (4.16% in sample A, 2.68% in sample C, 2.39% in sample B). Among the esters examined, methyl benzoate (0.42% in Sample B, 0.27 in Sample C, and 0.22% in Sample A) was the most abundant. Whereas n-Nonanal in sample B (1.24%) and sample B (1.13%) were the most abundant aldehydes [45], while safranal (1.80%) was the most abundant in sample C. Among the fatty acids (Z,Z,Z)-9,12,15-Octadecatrienoic acid was the most abundant and was detected only in sample C (0.51%) and sample A (0.11%). As a matter of interest, selected sulfur compounds (isothiocyanates, ITC) were also found to be major secondary metabolites in Brassicaceae species. Among the ITCs detected, 2-propenyl-isothiocyanate was the most prevalent derived from aliphatic glucosinolates (2.07% in sample B, 0.74% in sample A, and 0.61% in sample C). A variety of factors may influence the ITC content, including the plant species studied, side-chain substitutions, cellular pH, and iron concentration [46,47].

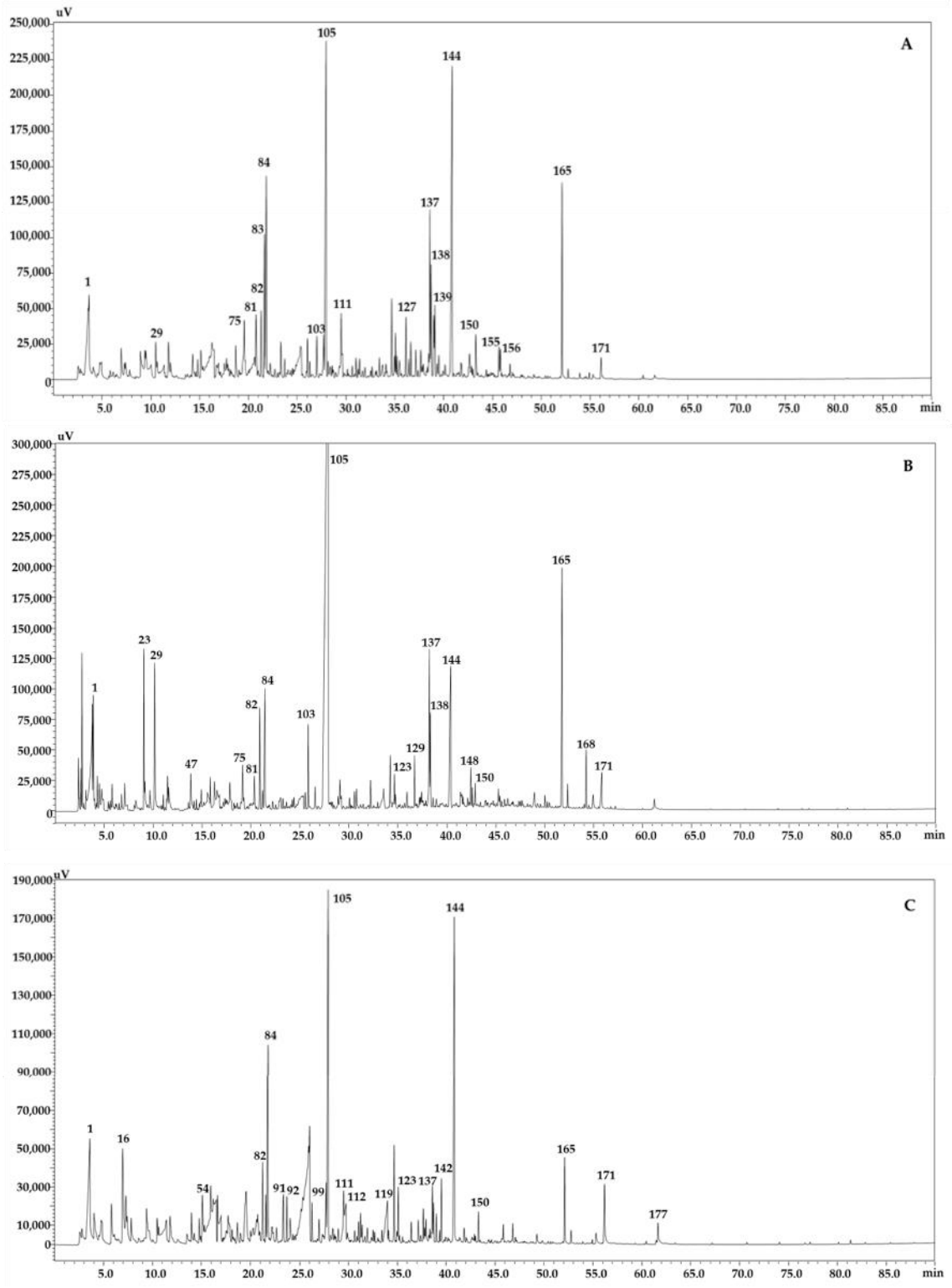

Figure 4.4. Characterization of the volatile compounds by GC-MS in the leaves extracts of three *B. juncea* cultivars harvested at the edible salad phase. (A) *B. juncea* ISCI 99; (B) *B. juncea* ISCI Top; (C) *B. juncea* ISCI "Broad-leaf".

4.4 Conclusion

An extensive characterization of the chemical profile of various tissues of *B. juncea* cultivars has been reported. Particularly, flowers, leaves, stems, and roots of *B. juncea* were subjected to analysis by HPLC-PDA/ESI-MS. In addition, the leaf extracts with the largest number of volatile compounds were analyzed by GC-FID/MS, as well as a chemical characterization of defatted seed meals (DSM). Approximately 179 chemical constituents were identified in terms of the volatile content; however, 35 metabolites were identified in terms of the non-volatile content, revealing a large number of highly glycosylated and acylated isorhamnetin, quercetin, and kaempferol derivatives. Interestingly, proteins represented 44.0% DW, 37.4% DW, and 36.8% DW among DSMs for Sample A, Sample B, and Sample C, respectively. According to the phytocomponents identified, this crop may have significant pharmaceutical and nutraceutical applications. Additionally, cultivar selection and validation are important due to the differences between varieties and plant tissues. The bioactivity and toxicity profile of materials derived from the most promising varieties need to be evaluated using both in vitro and in vivo models.

4.5 References

1. Podsędek, Anna. 2007. “Natural Antioxidants and Antioxidant Capacity of Brassica Vegetables: A Review.” LWT - Food Science and Technology 40 (1): 1–11.
2. Harbaum, Britta, Eva Maria Hubbermann, Christian Wolff, Rainer Herges, Zhujun Zhu, and Karin Schwarz. 2007. “Identification of Flavonoids and Hydroxycinnamic Acids in Pak Choi Varieties (Brassica Campestris L. Ssp. Chinensis Var. Communis) by HPLC–ESI-MSn and NMR and Their Quantification by HPLC–DAD.” Journal of Agricultural and Food Chemistry 55 (20): 8251–60.
3. Harbaum, Britta, Eva Maria Hubbermann, Zhujun Zhu, and Karin Schwarz. 2008. “Impact of Fermentation on Phenolic Compounds in Leaves of Pak Choi (Brassica Campestris L. Ssp. Chinensis Var. Communis) and Chinese Leaf Mustard (Brassica Juncea Coss).” Journal of Agricultural and Food Chemistry 56 (1): 148–57.
4. Olsen, Helle, Kjersti Aaby, and Grethe Iren A. Borge. 2009. “Characterization and Quantification of Flavonoids and Hydroxycinnamic Acids in Curly Kale (Brassica Oleracea L. Convar. Acephala Var. Sabellica) by HPLC-DAD-ESI-MS n .” Journal of Agricultural and Food Chemistry 57 (7): 2816–25.
5. Olsen, Helle, Kjersti Aaby, and Grethe Iren A. Borge. 2010. “Characterization, Quantification, and Yearly Variation of the Naturally Occurring Polyphenols in a Common Red Variety of Curly Kale (Brassica Oleracea L. Convar. Acephala Var. Sabellica Cv. ‘Redbor’).” Journal of Agricultural and Food Chemistry 58 (21): 11346–54.
6. Lin, Long-Ze, Jianghao Sun, Pei Chen, and James Harnly. 2011. “UHPLC-PDA-ESI/HRMS/MSn Analysis of Anthocyanins, Flavonol Glycosides, and Hydroxycinnamic Acid Derivatives in Red Mustard Greens (Brassica Juncea Coss Variety).” Journal of Agricultural and Food Chemistry 59 (22): 12059–72.
7. Sun, Jianghao, Zhenlei Xiao, Long-ze Lin, Gene E. Lester, Qin Wang, James M. Harnly, and Pei Chen. 2013. “Profiling Polyphenols in Five Brassica Species Microgreens by UHPLC-PDA-ESI/HRMSn” Journal of Agricultural and Food Chemistry 61 (46): 10960–70.
8. Cartea, María Elena, Marta Francisco, Pilar Soengas, and Pablo Velasco. 2010. “Phenolic Compounds in Brassica Vegetables.” Molecules 16 (1): 251–80.

9. Mageney, Vera, Susanne Baldermann, and Dirk C. Albach. 2016. “Intraspecific Variation in Carotenoids of Brassica Oleracea Var. Sabellica.” Journal of Agricultural and Food Chemistry 64 (16): 3251–57.
10. De Nicola, Gina Rosalinda, Manuela Bagatta, Eleonora Pagnotta, Donato Angelino, Lorenzo Gennari, Paolino Ninfali, Patrick Rollin, and Renato Iori. 2013. “Comparison of Bioactive Phytochemical Content and Release of Isothiocyanates in Selected Brassica Sprouts.” Food Chemistry 141 (1): 297–303.
11. Park, Suhyoung, Mariadhas Valan Arasu, Min-Ki Lee, Jin-Hyuk Chun, Jeong Min Seo, Sang-Won Lee, Naif Abdullah Al-Dhabi, and Sun-Ju Kim. 2014. “Quantification of Glucosinolates, Anthocyanins, Free Amino Acids, and Vitamin C in Inbred Lines of Cabbage (Brassica Oleracea L.).” Food Chemistry 145 (February): 77–85.
12. Piccinini, E., V. Ferrari, G. Campanelli, F. Fusari, L. Righetti, E. Pagnotta, and L. Lazzeri. 2015. “Effect of Two Liquid Formulations Based on Brassica Carinata Co-Products in Containing Powdery Mildew on Melon.” Industrial Crops and Products 75 (November): 48–53.
13. Franco, P., S. Spinozzi, E. Pagnotta, L. Lazzeri, L. Ugolini, C. Camborata, and A. Roda. 2016. “Development of a Liquid Chromatography–Electrospray Ionization–Tandem Mass Spectrometry Method for the Simultaneous Analysis of Intact Glucosinolates and Isothiocyanates in Brassicaceae Seeds and Functional Foods.” Journal of Chromatography A 1428 (January): 154–61.
14. Higdon, J, B Delage, D Williams, and R Dashwood. 2007. “Cruciferous Vegetables and Human Cancer Risk: Epidemiologic Evidence and Mechanistic Basis.” Pharmacological Research 55 (3): 224–36.
15. Kwak, Youngeun, Jungjae Lee, and Jihyeung Ju. 2016. “Anti-Cancer Activities of Brassica Juncea Leaves in Vitro.” EXCLI Journal; 15:Doc699; ISSN 1611-2156.
16. Young Kim, Hyun, Takako Yokozawa, Eun Ju Cho, Hong Sik Cheigh, Jae Sue Choi, and Hae Young Chung. 2003. “In Vitroand in Vivo Antioxidant Effects of Mustard Leaf (Brassica Juncea).” Phytotherapy Research 17 (5): 465–71.
17. Yokozawa, Takako, Hyun Young Kim, Eun Ju Cho, Noriko Yamabe, and Jae Sue Choi. 2003. “Protective Effects of Mustard Leaf (Brassica Juncea) against Diabetic Oxidative Stress.” Journal of Nutritional Science and Vitaminology 49 (2): 87–93.

18. Lee, Jae-Joon, Hyun A Kim, and Joomin Lee. 2018. “The Effects of Brassica Juncea L. Leaf Extract on Obesity and Lipid Profiles of Rats Fed a High-Fat/High-Cholesterol Diet.” Nutrition Research and Practice 12 (4): 298.
19. Thakur, Ajit Kumar, Shyam Sunder Chatterjee, and Vikas Kumar. 2013. “Beneficial Effects of Brassica Juncea on Cognitive Functions in Rats.” Pharmaceutical Biology 51 (10): 1304–10.
20. Harborne, J. B. 1998. Phytochemical Methods: A Guide to Modern Techniques of Plant Analysis. 3rd ed. London ; New York: Chapman and Hall.
21. Nicácio, Antonio Eduardo, Carina Alexandra Rodrigues, Jesuí Vergilio Visentainer, and Liane Maldaner. 2021. “Evaluation of the QuEChERS Method for the Determination of Phenolic Compounds in Yellow (Brassica Alba), Brown (Brassica Juncea), and Black (Brassica Nigra) Mustard Seeds.” Food Chemistry 340 (March): 128162.
22. Sikora, Elżbieta, Ewa Cieślik, Teresa Leszczyńska, Agnieszka Filipiak-Florkiewicz, and Paweł M. Pisulewski. 2008. “The Antioxidant Activity of Selected Cruciferous Vegetables Subjected to Aquathermal Processing.” Food Chemistry 107 (1): 55–59.
23. Justesen, Ulla, Pia Knuthsen, and Torben Leth. 1998. “Quantitative Analysis of Flavonols, Flavones, and Flavanones in Fruits, Vegetables and Beverages by High-Performance Liquid Chromatography with Photo-Diode Array and Mass Spectrometric Detection.” Journal of Chromatography A 799 (1–2): 101–10.
24. Huang, Zhiliang, Baowu Wang, Doris H. Eaves, James M. Shikany, and Ralphenia D. Pace. 2007. “Phenolic Compound Profile of Selected Vegetables Frequently Consumed by African Americans in the Southeast United States.” Food Chemistry 103 (4): 1395–1402.
25. Zhang, Junmei, Mary B. Satterfield, Jennifer S. Brodbelt, Steven J. Britz, Beverly Clevidence, and Janet A. Novotny. 2003. “Structural Characterization and Detection of Kale Flavonoids by Electrospray Ionization Mass Spectrometry.” Analytical Chemistry 75 (23): 6401–7.
26. Maarse, Henk. 2017. Volatile Compounds in Foods and Beverages. Edited by Henk Maarse. 1st ed. Routledge.
27. Kumar, Sandeep, Dhiraj Singh, and M Dutta. n.d. “Quality Characteristics in Rapeseed-Mustard and Role of Some Anti-Nutritional Factors in Plant Defense: Future Strategies,” 9.

28. Rangkadilok, Nuchanart, Marc E Nicolas, Richard N Bennett, Robert R Premier, David R Eagling, and Paul W.J Taylor. 2002. “Developmental Changes of Sinigrin and Glucoraphanin in Three Brassica Species (Brassica Nigra, Brassica Juncea and Brassica Oleracea Var. Italica).” Scientia Horticulturae 96 (1–4): 11–26.
29. Sharma, Anubhuti, P.K. Rai, and Surendra Prasad. 2018. “GC–MS Detection and Determination of Major Volatile Compounds in Brassica Juncea L. Leaves and Seeds.” Microchemical Journal 138 (May): 488–93.
30. Official Journal of the European Union C 13, Volume 62, 11 January 2019 (European Commission 2019/C 13/01), Common Catalogue of Varieties of Agricultural Plant Species-37th Complete Edition. Available online: https://eur-lex.europa.eu/legal-content/EN/TXT/PDF/?uri=OJ:C:2019:013:FULL&from=EN (accessed on 21 October 2020).
31. Available online: http://ec.europa.eu/food/plant/plant_propagation_material/plant_variety_catalogues_databases/search/public/index.cfm?event=SearchVariety&ctl_type=A&species_id=237&variety_name= &listed_in=8&show_current=on&show_deleted (accessed on 21 October 2020).
32. Arena, Katia, Francesco Cacciola, Laura Dugo, Paola Dugo, and Luigi Mondello. 2020. “Determination of the Metabolite Content of Brassica Juncea Cultivars Using Comprehensive Two-Dimensional Liquid Chromatography Coupled with a Photodiode Array and Mass Spectrometry Detection.” Molecules 25 (5): 1235.
33. Lazzeri, L., L. Malaguti, M. Bagatta, L. D’Avino, L. Ugolini, G.R. De Nicola, N. Casadei, S. Cinti, R. Matteo, and R. Iori. 2013. “CHARACTERIZATION OF THE MAIN GLUCOSINOLATE CONTENT AND FATTY ACID COMPOSITION IN NON-FOOD BRASSICACEAE SEEDS.” Acta Horticulturae, no. 1005 (September): 331–38.
34. Sandhu, Surinder K., Pritpal Singh, Jasneet Kaur, Manpreet Singh, and Karanveer Kaur. 2020. “Selection Indices for Enhanced Selection Efficiency in Indian Mustard under Terminal Heat Stress Conditions.” Indian Journal of Genetics and Plant Breeding (The) 80 (01).
35. ASTM D5373. Standard Test Methods for Determination of Carbon, Hydrogen and Nitrogen in Analysis Samples of Coal and Carbon in Analysis Samples of Coal and Coke; ASTM International: West Conshohocken, PA, USA, 2016.

36. Smith, A.K.; Circle, S.J. 1972. Soybeans: Chemistry and Technology; Avi Publishing Co.: Westport, CT, USA; Volume 1, pp. 62–63.
37. ISO 9167-1:1992/Amd 1:2013. Graines de Colza—Dosage des Glucosinolates—Partie 1:Methode par Chromatographie Liquide à Haute Performance, 1992. Available online: https://www.iso.org/fr/standard/ 72207.html (accessed on 21 October 2020).
38. Wathelet, Jean-Paul; Iori, Renato; Leoni, Onofrio; Quinsac, Alain; Palmieri, Sandro. 2004. Guidelines for glucosinolates analysis in green tissues used for biofumigation. Agroindustria 2004, 3, 257–266.
39. Pagnotta, Eleonora, Niels Agerbirk, Carl E. Olsen, Luisa Ugolini, Susanna Cinti, and Luca Lazzeri. 2017. "Hydroxyl and Methoxyl Derivatives of Benzylglucosinolate in Lepidium Densiflorum with Hydrolysis to Isothiocyanates and Non-Isothiocyanate Products: Substitution Governs Product Type and Mass Spectral Fragmentation." Journal of Agricultural and Food Chemistry 65 (15): 3167–78.
40. Grover, N., and V. Patni. 2013. "Phytochemical Characterization Using Various Solvent Extracts and GC-MS Analysis of Methanolic Extract of Woodfordia Fruticosa (L.) Kurz. Leaves." International Journal of Pharmacy and Pharmaceutical Sciences 5 (4): 291–95.
41. Sciarrone, Danilo, Daniele Giuffrida, Archimede Rotondo, Giuseppe Micalizzi, Mariosimone Zoccali, Sebastiano Pantò, Paola Donato, Rosana Goncalves Rodrigues-das-Dores, and Luigi Mondello. 2017. "Quali-Quantitative Characterization of the Volatile Constituents in Cordia Verbenacea D.C. Essential Oil Exploiting Advanced Chromatographic Approaches and Nuclear Magnetic Resonance Analysis." Journal of Chromatography A 1524 (November): 246–53.
42. Das, Sourav, Barbara Vörös-Horváth, Tímea Bencsik, Giuseppe Micalizzi, Luigi Mondello, Györgyi Horváth, Tamás Kőszegi, and Aleksandar Széchenyi. 2020. "Antimicrobial Activity of Different Artemisia Essential Oil Formulations." Molecules 25 (10): 2390.
43. Valette, L, X Fernandez, S Poulain, A.-M Loiseau, L Lizzani-Cuvelier, R Levieil, and L Restier. 2003. "Volatile Constituents from Romanesco Cauliflower." Food Chemistry 80 (3): 353–58.
44. Kessler, André, and Ian T. Baldwin. 2002. "P LANT R ESPONSES TO I NSECT H ERBIVORY : The Emerging Molecular Analysis." Annual Review of Plant Biology 53 (1): 299–328.

45. Kesen, Songul, Hasim Kelebek, Kemal Sen, Mehmet Ulas, and Serkan Selli. 2013. “GC–MS–Olfactometric Characterization of the Key Aroma Compounds in Turkish Olive Oils by Application of the Aroma Extract Dilution Analysis.” Food Research International 54 (2): 1987–94.
46. Fenwick, G. Roger, Robert K. Heaney, W. John Mullin, and Cecil H. VanEtten. 1983. “Glucosinolates and Their Breakdown Products in Food and Food Plants.” C R C Critical Reviews in Food Science and Nutrition 18 (2): 123–201.
47. Gil, Victor, and Alexander J. MacLeod. 1980. “Benzylglucosinolate Degradation in Lepidium Sativum: Effects of Plant Age and Time of Autolysis.” Phytochemistry 19 (7): 1365–68.

CHAPTER 5

Discrimination of Moroccan *Lamiaceae* species by analysis of polyphenol compounds using Liquid Chromatography (HPLC-PDA-MS), and Rapid Evaporative Ionization Mass Spectrometry (REIMS) approaches

5.1 Introduction

Medicinal and aromatic plant has raised significant interest in recent decades due to the growing demand for health and well-being products [1]. The family of *Lamiaceae* is considered one of the most employed plants in traditional medicine due to their therapeutic and various health-beneficial effects [2]. *Lamiaceae* includes over 245 genera with 7886 species, commonly distributed in temperate and tropical regions, including Mediterranean regions, Asia, Europe, the United States, and Australia [3]. Species of this family contain considerable phytochemical compounds, including volatile ad non-volatile components, such as phenolic acids, flavonoids, terpenoids, and terpenes. These compounds are responsible for many biological activities such as antioxidant, antitumor, anti-inflammatory, and antimicrobial [4,5]. Moreover, certain *Lamiaceae* species are considered endemic due to their tight relationship with specific pedoclimatic factors [6]. Recently, different *Lamiaceae* derivative products such as essential oils, herbal spices, perfumes, cosmetics, and beverages are highly commercialized at the industrial level [7,8]. Consequently, a matter of economic interest may give rise to eventual unlawful practices expected through the use of worthless plants, and misleading or incorrect labelling products.

As a result of the interest that these plants have received for both their economic and scientific value, recent research has focused on the development of innovative analytical techniques in order to investigate the phytochemical profile and to determine discriminative compounds of different botanical species. Moreover, chemometrics was also involved in the creation of classification models.

Chromatographic methods and mass spectrometry (MS) are typically employed to investigate phytochemical composition, whereas a majority of applications involving the detection of fraud rely on fast fingerprinting techniques, such as infrared spectroscopy [9-16]. A wide variety of chromatographic techniques such as liquid chromatography (LC), or gas chromatography (GC) had been commonly used for the analysis of phytochemical compounds, aiming to identify and quantify volatile and non-volatile bioactive components

[17-23]. While LC and GC techniques offer the advantage of allowing a thorough metabolomic profile of the investigated plants to be elucidated in detail, pre-analysis sample preparation needs to be performed in an orderly manner prior to the injection of the targeted analytes. Moreover, for a comprehensive profile of all metabolites, volatile and non-volatile, both LC and GC methods are required, which render the total analytical workflow laborious and time consuming.

In addition, a powerful combination between ambient mass spectrometry data and chemometrics has been usefully employed, allowing for the simultaneous identification of molecular markers, as well as their differentiation, through statistical analysis [24,25]. Generally, fingerprinting achieved with spectrometric instruments is limited to major compounds [26,27].

Besides spectroscopic technologies which are also employed for the investigation of authentic species, such as infrared spectroscopy (IR), Nuclear Magnetic Resonance (NMR) [26, 28,29], direct mass spectrometry approaches coupled with chemometrics are of great importance and reliable for the identification of authentic species [30,31]. Rapid evaporative ionization mass spectrometry (REIMS) represents an innovative ambient mass spectrometry technique employed for fingerprinting. REIMS has already been applied to a variety of vegetable materials, such as determining the geographical origin of pistachios [32], identifying the botanical origins of honey [33], as well as distinguishing extra virgin olive oils, according to a trademark or cultivar of olives that is protected under the PDO (protected designation of origin) denomination, considering both technological processes as well as pedoclimatic conditions as well as genetic factors [34].

The present research aims to evaluate the metabolome of *Lamiaceae* species by employing the innovative approach of REIMS which takes place directly on raw samples under natural atmospheric conditions, in combination with integrative chemometrics, and conventional chromatographic technique HPLC-MS to confirm the identification of polyphenol markers of each plant species.

5.2 Materials and methods

5.2.1 Chemicals and reagents

Methanol, water, acetonitrile, 2-propanol, and formic acid were all LC-MS grade, and were purchased from Merck life Science (Merck KGaA, Darmstadt, Germany). Reagent grade sodium chloride (NaCl) was also obtained from Merck life Science (Merck KGaA, Darmstadt, Germany).

5.2.2 Plants material

All six *Lamiaceae* species employed in the present study were harvested from two different Moroccan geographical sites, and assigned as follows: *Thymus zygis, Mentha suaveolens* and *Sideritis incana* were obtained from Ifran (Middle Atlas Mountain). Whereas *Melissa officinalis, Mentha pulegium, Calamintha officinalis* were collected from Ouazzane (North of Morocco).

5.2.3 Sample preparation

All plant materials were left to dry in the air under darkness and reduced into powder. For polyphenols analysis with the conventional HPLC technique, a suitable extraction is required. One gram of each plant was dissolved in 20 mL of MeOH:H_2O (80:20 *v:v*). The mixture was sonicated in an ultrasonic bath at 37°C for 30 min, centrifuged at 3000 RCF for 20 min and the obtained supernatant was evaporated using EZ-2. The dried extract was redissolved in the same organic solvent mixture of extraction, filtered through a 0.2 µm Acrodisc nylon membrane (Merck Life Science, Merck KGaA, Darmstadt, Germany) and injected into HPLC-PDA-MS.

For the untargeted analysis by REIMS, 0.5 g of each dried plant sample was mixed with sodium chloride at 0.9% for electrical conduction improvement in order to facilitate REIMS burns.

5.2.4 LC-MS instrumentation and analytical conditions

Phenolic compounds were analyzed using high-performance liquid chromatography coupled to a photodiode array detector and electrospray ionization-mass spectrometry (HPLC-PDA/ESI-MS) (Shimadzu, Kyoto, Japan), which comprises two LC-20 AD binary pumps, a DGU-20A3 degasser, an SPD-M20A photodiode array detector (PDA), a CBM-20A controller unit and an LCMS-2020 mass spectrometer, supplied with an electrospray (ESI) interface.

Chromatographic separation was performed on C18 reversed-phase column Ascentis Express with the following dimensions and operated as follows: 150 × 4.6 mm, 2.7 µm, obtained from Merck Life Science (Merck KGaA, Darmstadt, Germany), and kept at 30 °C; the employed mobile phase comprises water (mobile phase A) and acetonitrile (mobile phase B) both acidified with 0.1 % formic acid, with a flow rate of 0.8 mL/min, and gradient elution using the following program: 0–5 min (5 % B), 5–15 min (10 % B), 15–30 min (20 % B), 30–60 min (50% B), 60 min (100 % B). The sample injection volume was 5 µL and the PDA wavelength acquisition ranged between 100 and 400 nm. The eluted compounds were

subsequently analyzed by mass spectrometer in both negative and positive ionization modes, using the following conditions:

m/z scan range 100–800, nebulizing gas (N_2) flow rate: 1.5 L/min, drying gas (N_2) flow rate: 15 L/min, interface temperature: 350 °C. The acquisition was performed by the LabSolutions software ver. 5.92 (Shimadzu, Kyoto, Japan).

5.2.5 REIMS instrumentation and analytical conditions

REIMS instrument was equipped with an electrosurgical diathermy apparatus for sampling. It consists of a monopolar electrosurgical handpiece (iknife) connected to a high-frequency electrical current generator (Erbe VIO 50 C, Tübingen, Germany). Two different cut modalities are possible; forced coagulation cut (FC) and dry cut (DC), with an examined power range of 10-40 W. The DC mode and power of 20W were adopted for the present study. The generated aerosols by the surgical iknife from the samples due to the joule effect are then aspirated by a Venturi device through a PTFE tube (4 m × 4.11 mm o.d., 2.53 mm i.d) to reach the mass spectrometer system Xevo G2 XS qTOF (Waters Corporation, Wilmslow, UK) supplied with REIMS source. This later is supported by a spiral ribbon collision surface heated by a constant current power supply 4.5 A and a voltage of 4.2 V (Kanthal D 1.0 × 0.1 mm) to reach a temperature of almost 800 °C. The instrument was also coupled to a syringe pump (fixed Luer lock LC pump priming syringe by Trajan Scientific, Crownhill, UK) for the infusion of 2-propanol inside the REIMS source at a constant flow rate of 50 µL/min to ensure that the source remains clean and to aid in the transfer of molecular species to the heated surface as well as their ionization.

Instrument calibration was executed ahead of the analysis, by introducing 0.5 mM of sodium formate ($CHNaO_2$) in 2-propanol. The mass range of acquisition was set between 100 and 1000 *m/z* at a scan rate of 0.5 sec and was performed in both negative and positive modes.

5.2.6 Chemometrics processing

Raw data profiles of untargeted analyses obtained by REIMS-TOF through the platform MassLynx v. 4.1 (Waters Corporation, Wilmslow, UK), were furtherly processed applying the following steps: Lock mass correction of the acquired mass spectra by REIMS-TOF using as endogenous matrix 135.0440 *m/z* which belongs to 4-ethenylbenzene-1,2-diol in deprotonated form, besides rosmarinic acid (360.31 g/mol) as a referential compound of the *Lamiaceae* matrix. All obtained spectra in the region of interest (ROI) were combined to produce a single spectrum, further background chemical reduction was applied by the means of an adaptive background subtraction algorithm (ABS). Moreover, all spectra were normalized by the acquisition in total ion current (TIC). All obtained data were furtherly

processed automatically through the integrative multivariate statistical software LiveID (Waters Corporation, Wilmslow, UK). Both principal component analysis (PCA) and linear discriminant analysis (LDA) were applied to generate statistical models, which allows us to discern the similarities and differences between the *Lamiaceae* samples. Consequently, a database was created based on the acquired characteristic spectra of each sample.

To evaluate the predictive capacity and robustness of the statistical model, the PCA/LDA classifiers were tested using 5-fold cross-validation according to 20%-out strategy.

Finally, real-time and playback recognition were tested to distinguish each class of the generated models.

Furthermore, the created model by LiveID of *Lamiaceae* species was subjected to the verification of its robustness by testing a *Lamiaceae* plant of Italian origin (*Thymus vulgaris*), which is not included in the built model.

5.3 Results and discussion

5.3.1 LC-MS targeted analysis of polyphenols in Lamiaceae plants

The obtained phenolic profiles of the six different extracts from the aerial parts of *Lamiaceae* species performed on the high-performance liquid chromatography coupled to mass spectrometry are shown in **Figures 5.1** and **5.2**, and their corresponding phenolic compounds are listed in **Tables S5.1 - S5.6**.

A qualitative difference has been observed in the chromatographic profiles of all six *Lamiaceae* species studied. Over 48 different phenolic compounds were detected, where *T. zygis* was the richest sample with 36 compounds positively detected, followed by *C. officinalis* (33 compounds), *M. officinalis* (28 compounds), *M. pulegium* (23 compounds), *M. suaveolens* (16 compounds), and *S. incana* as the poorest sample with only 13 positively detected.

Polyphenol identification was accomplished based on retention times, maximum wavelength absorbance, MS spectra, and literature data.

In the six species studied, polyphenolic compounds were distributed as follows:

T. zygis (**Figure 5.1. A**) was characterized by the presence of flavonoids (apigenin and its derivatives, luteolin and its derivatives, quercetin derivatives, eriodictyol, chrysoeriol, naringenin derivatives, danshensu, hispidulin, and cirsimaritin) and phenolic acids (quinic acid, caffeic acid, salvianolic acid isomers, rosmarinic acid, hydroxyjasmonic acid-hexoside isomers, and feruloylquinic acid). Only four major peaks were present at high concentrations, notably apigenin-(6,8)-C-diglucoside. rosmarinic acid, salvianolic acid K and luteolin-7-O-glucuronide isomer. Whereas *C. officinalis* (**Figure 5.1. B**) has shown a common profile rich

in usual flavonoids (apigenin and quercetin derivatives e.g., quercetin-*O*-acetylhexoside and 6,8-C-dihexosylapigenin, and hydroxydaidzein-8-C-glucoside) and phenolic acids (caffeic acids and its derivative e.g., caffeoylquinic acid, rosmarinic acid, and coumaroylquinic acid) with caffeoylquinic acid as the main compound. On the other hand, *M. officinalis* (**Figure 5.1. C**) contained only one flavonoid (luteolin-3'-O-glucuronide) and specific phenolic acids besides the usual ones, salvianolic acid L and H, lithospermic acid A. In particular, rosmarinic acid-O-hexoside, rosmarinic acid, lithospermic acid A, salvianolic acid H/I (isomer), and salvianolic acid C derivative occurred as the main concentrated compounds. Likewise, *M. pulegium* (**Figure 5.2. A**) has shown a different polyphenolic profile, with the presence of some similar flavonoids and phenolic acids with different intensities with respect to the five other studied species. Furthermore, some characteristic compounds such as salvianolic acid W and medioresinol-*O*-hexoside, and diosmin also occurred. Where 3- and 5-O-caffeoylquinic acid, luteolin-7-O-rutinoside, quercetin-O-rhamno-hexoside, and rosmarinic acid were the most important 5 peaks in this specie. *M. suaveolens* (**Figure 5.2. B**) was characterized by flavonoids (apigenin and luteolin derivatives, jaceosidin, and dihydroxy-tetramethoxyflavone) and phenolic acids (quinic acid, salvianolic acid isomers, and caffeic acid derivatives such as rosmarinic acid, salvianolic acid and caffeoylquinic acid). *M. suaveolens* polyphenolic profile was characterized by three main concentrated polyphenols, rosmarinic acid, luteolin-7-O-glucuronide, and salvianolic acid A. The poorest qualitative profile among the six studied species belongs to *S. incana* (**Figure 5.2. C**), which was considerably characterized by the presence of phenylethanoid glucosides (verbascoside and leucoseptoside A), and some particular flavonoids such as hypolaetin and isoscutellarein derivatives, besides two common phenolic acids (two caffeoylquinic acids). Where only four main polyphenols were presented with high intensity, 5-O-caffeoylquinic acid, hypolaetin 7-O-allosyl-(1→2)-[6″-O-acetyl]-glucoside, isoscutellarein 7-O-allosyl-(1→2)-[6″-O-acetyl]-glucoside, and 4'-O-methylhypolaetin 7-O-[6"'-O-acetyl]-allosyl (1→2) glucoside.

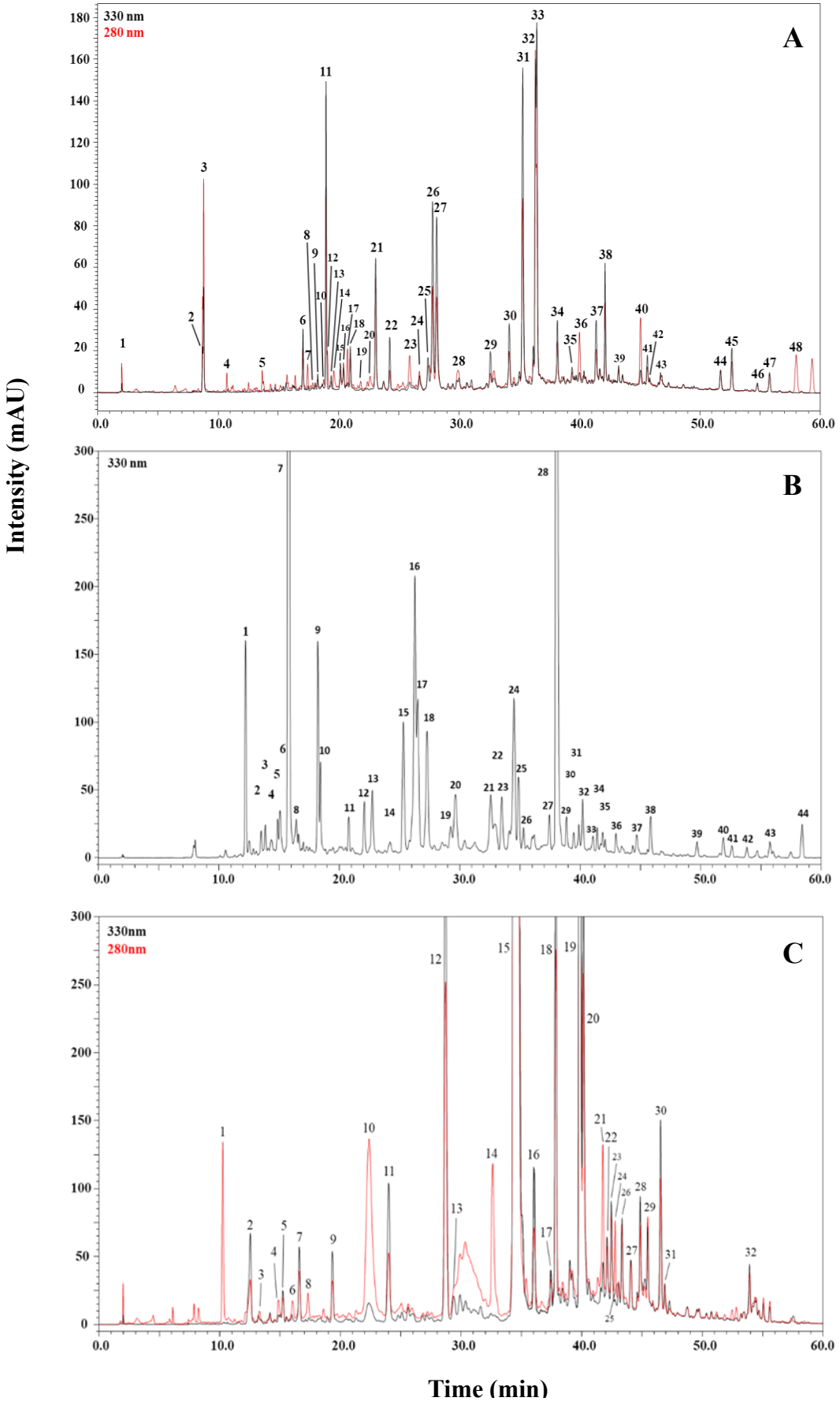

Figure 5.1. Profile of phenolic compounds in hydromethanolic extracts of *Lamiaceae species* extracted at 280 and 330 nm; **A**. *Thymus zygis*, **B**. *Calamintha officinalis*, **C**. *Melissa offcinalis*.

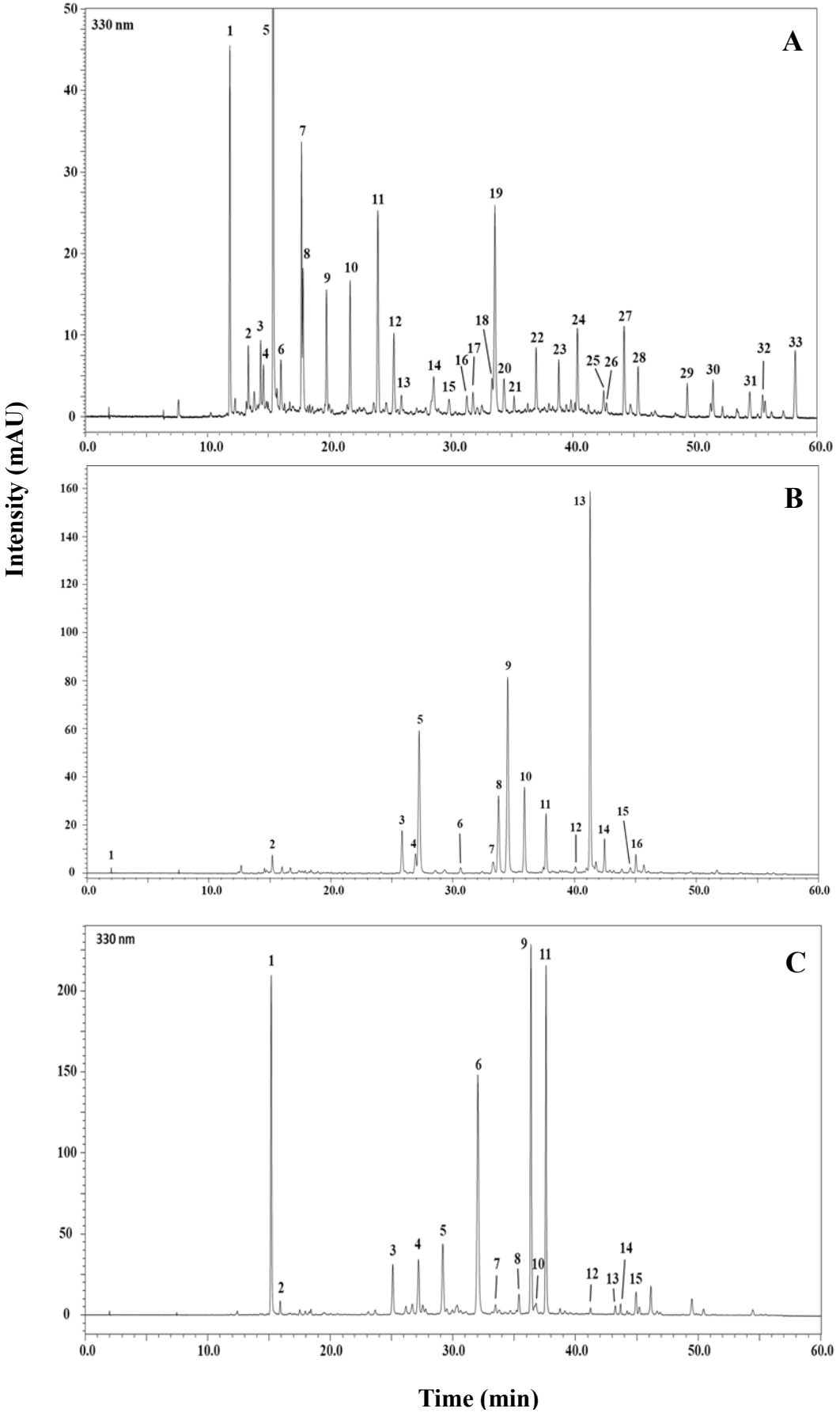

Figure 5.2. Profile of phenolic compounds in hydromethanolic extracts of *Lamiaceae* species extracted at 280 and 330 nm; **A**. *Mentha pulegium*, **B**. *Mentha suaveolens*, **C**. *Sideretis incana*.

5.3.2 REIMS untargeted analysis and model validation

Mass spectra

The REIMS technique applied to the exploration of botanical species allows the identification of both non-volatile compounds, particularly phenolic compounds and fatty acids, and volatile components. On the contrary, the targeted conventional approach by using the liquid chromatographic technique showed a determined profile of phenolic compounds. The comparison with a conventional technique was useful during the REIMS optimization phase to evaluate which experimental conditions provide a more likely qualitative-quantitative profile. It is well-known that the chemical composition of *Lamiaceae* botanical species is constituted by polyphenols (flavonoids and phenolic acids derivatives), chlorophyll (a and b), proteins, fatty acids (SFA, MUFA, PUFA) (e.g., linoleic acid, palmitic acid, and linolenic acid), and mono, di, and sesquiterpenes [35-37].

Since the REIMS technique provides an untargeted approach, a complex profile containing all the chemical compounds in the studied samples is expected. **Figure 5.3** reports the acquired total ion current spectra in negative ionization mode by iknife-REIMS of two *Lamiaceae* botanical species, **A.** *T. zygis* and **B.** *M. pulegium*. Only the main compounds are reported.

The obtained spectra were generated by 20 consecutive cuts of *Lamiaceae* samples, which are considered sufficient replications to be implemented in a statistical model.

The investigated mass range (100–750 m/z) allowed the detection of polyphenols, fatty acids, and terpenes and terpenoids. For the purposes of building the statistical model, the mass range was reduced, in order to attain the greatest degree of correctness during the execution of the validation test with the LiveID software. Furthermore, a 6-million peak detection threshold was set in order to improve the quality of the spectra.

In this regard, the total metabolome can be more significant than a single class of analytes since it takes into account all factors, both genetic and pedoclimatic. The proportions between the various chemical classes can in fact be fundamental for differentiating species belonging to the same genus.

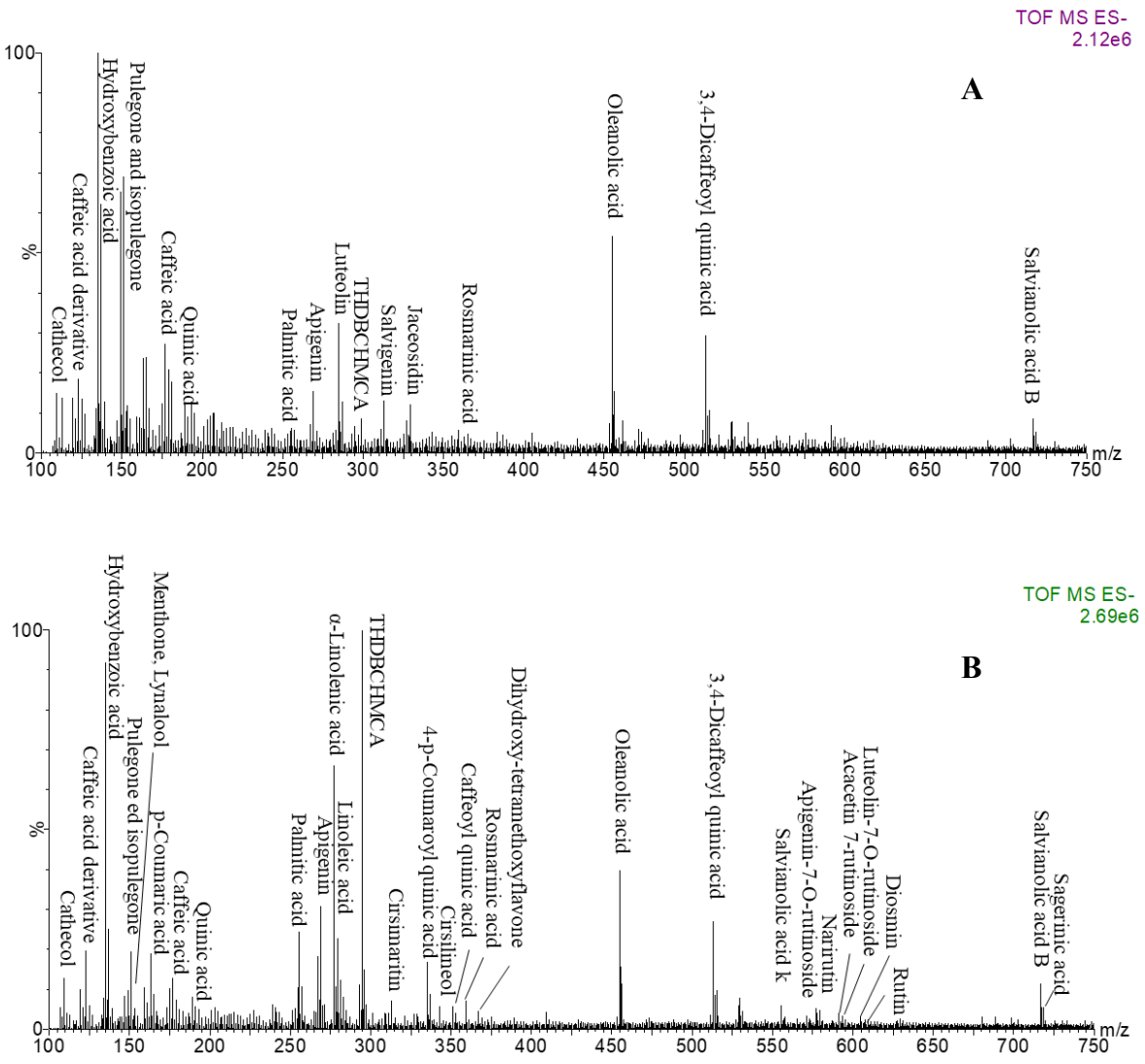

Figure 5.3. Comprehensive total ion current (TIC) profiles acquired by REIMS-TOF in negative ionization, with application of dry-cut mode and 20 W, for two *Lamiaceae* species, **A.** *T. zygis* and **B.** *M. pulegium*.

Model building validation

The purpose of this study was to evaluate the results obtained through the analysis of six botanical species using a REIMS source coupled with a high-resolution mass spectrometer. In order to create two distinct PCA/LDA models, multivariate statistics were applied to the MS data ("training set"). To establish the training models, spectral libraries were compiled from 290 REIMS-TOF files acquired in negative ionization mode in a mass range (100 - 750 *m/z*). Furthermore, initial REIMS models were established by MS spectra acquired in a complete mass range (100-950 m/z), which was reduced to 100-500 m/z including the most intense signals present in this mass range, such as rosmarinic acid, caffeic acid and its

derivatives. To improve the discrimination of species in the statistical analyses, some discriminative compounds such as salvianolic acids were also included by extending the mass range to 750 m/z. The generated spectra were employed in principal component analysis (PCA) for a reduction of model dimension to 50. Using this approach, significant variances could be visualized, and correlation between the studied spectral data. Three-dimensional PCA plots have shown a clear clusterization which can be explained by the separative potential of iKnife technique, describing the distribution of the studied species alongside the second principal component PC2 (data not shown). After PCA, data were supervised with the application of linear discriminant analysis (LDA), which was conducted without further reduction of dimensions with the aim of obtaining a valid method for identifying unknown samples within well-defined classes. In **Figure 5.4**, three-dimensional representations of the resulting PCA/LDA statistical models have reported similar discrimination of the species with a clear spatial distribution, in such cases, it is possible to clearly distinguish the separated botanical species *T. zygis* and *S. incana* alongside LD2 (highlighted in red and brown). Whereas the four remained botanical species were clusterized well along LD1. In the real-time recognition step, which aims to classify the MS spectra of unknown samples ("testing set") into one of the defined classes. The established discrimination was perfectly assigned to each specific specie within the same botanical family (**Figure 5.5**), based on their characteristic phytochemical profile. iknife technique has provided its potential to generate distinctive models as a result of its sensitivity and ability to reveal not only the major components characterized by polyphenolic compounds, such as caffeoylquinic acid, rosmarinic acid, and salvianolic acid and derivatives. But also, the minor components which are likely responsible for the resulting discrimination, in particular organic acids, glycosylated flavones, and some other volatile components.

The validation results shown in **Table 5.1**, confirmed that the iKnife model revealed higher correctness score values and offered a method of evaluating its predictive potential.

Furthermore, the created model by REIMS-TOF has classified properly the tested *Lamiaceae* plant of Italian origin (*Thymus vulgaris*) as an outlier (**Figure 5.6**). It can be concluded from the present results the robustness of the created model and the discriminative efficiency of iKnife technique.

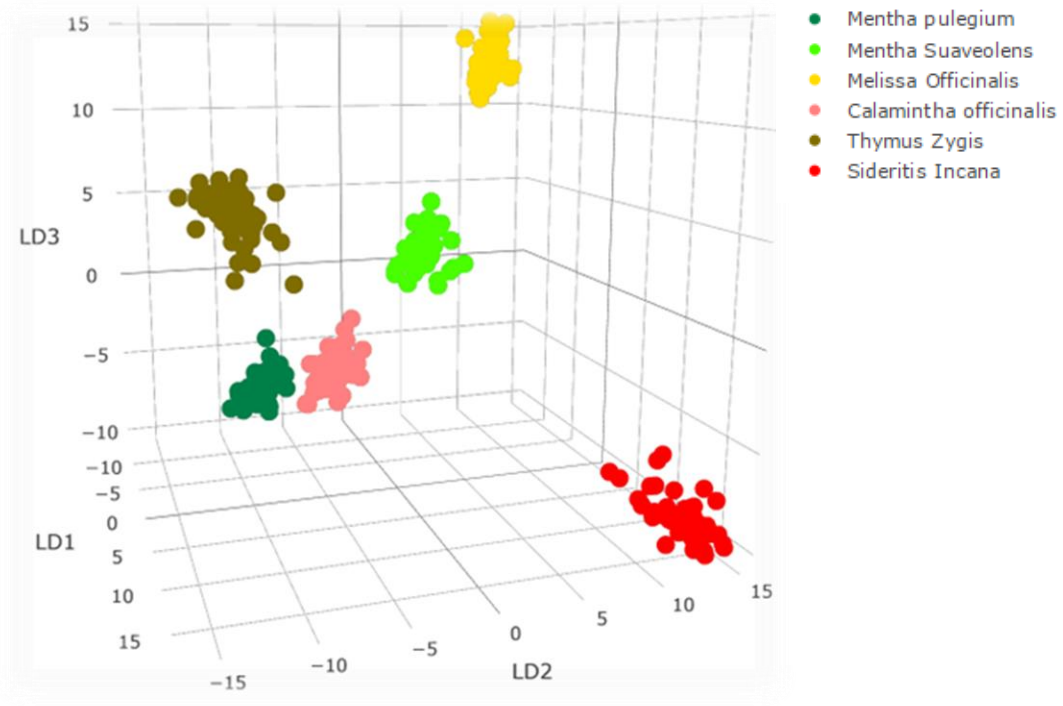

Figure 5.4. 3D supervised spatial clusterization of six Moroccan *Lamiaceae* species involving Linear Discriminant Analysis (PCA/LDA) generated by LiveID including 290 REIMS spectra acquired in negative ionization mode.

Table 5.1. validation model of six *Lamiaceae* botanical species using matrix confusion.

	Spectra	Passes	Failures	Outliers	Correctness score
Total	340	292	18	30	85.88%

Confusion matrix

	Mentha pulegium	Mentha Suaveolens	Melissa Officinalis	Calamintha officinalis	Thymus Zygis	Sideritis Incana	Outlier	Total
Mentha pulegium	50	0	0	10	0	0	0	60
Mentha Suaveolens	0	50	0	0	0	0	4	54
Melissa Officinalis	2	0	53	0	0	0	0	55
Calamintha officinalis	6	0	0	54	0	0	0	60
Thymus Zygis	0	0	0	0	44	0	13	57
Sideritis Incana	0	0	0	0	0	41	13	54

Figure 5.5. Identification of *M. pulegium* and *S. incana* by LiveID based on the built model.

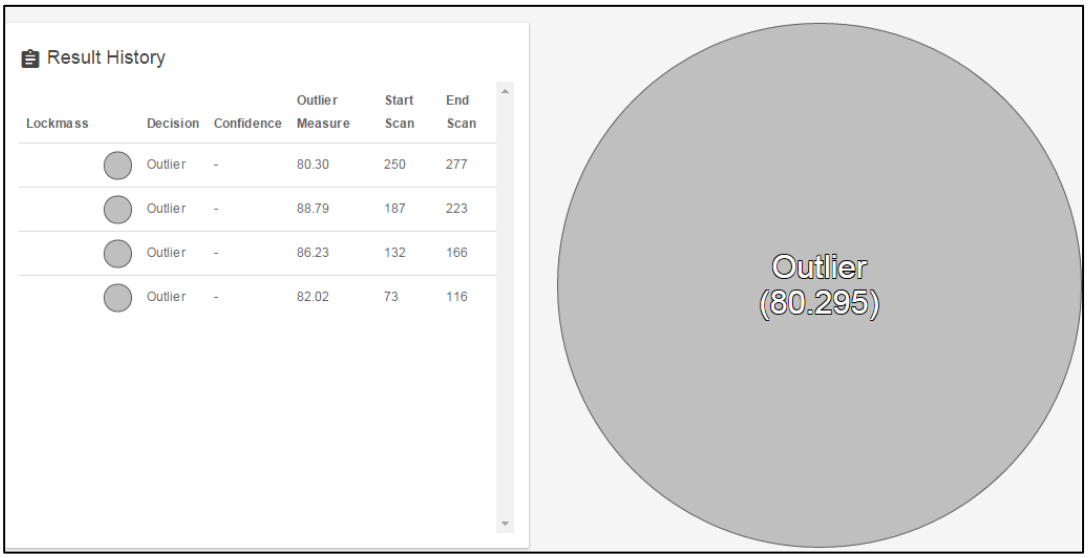

Figure 5.6. Robustness validation of the built REIMS model for commercial *Thymus vulgaris* of Italian origin.

5.4 Conclusion

The results obtained from the innovative iknife technique described in the present study, have proven its potentiality in the successful discrimination of *Lamiaceae* botanical species. Discrimination can be assigned to both major and minor biomarkers of authenticity, which are highlighted as discriminant features for chemometric analysis. The comparison with conventional chromatographic techniques enabled the identification of biomarker candidates with a high degree of reliability. This technique can be considered a promising shotgun approach to the exploration of traditional medicine, and to the analysis of plants with more significant economic influence.

5.5 References

1. Arantes, Sílvia Macedo, Andreia Piçarra, Marisa Guerreiro, Cátia Salvador, Fátima Candeias, A. Teresa Caldeira, and M. Rosário Martins. 2019. "Toxicological and Pharmacological Properties of Essential Oils of Calamintha Nepeta, Origanum Virens and Thymus Mastichina of Alentejo (Portugal)." Food and Chemical Toxicology 133 (November): 110747.
2. WHO. WHO Guidelines on Good Agricultural and Collection Practices (GACP) for Medicinal Plants; World Health Organization: Geneva, Switzerland, 2002.
3. Galanakis, Charis M., ed. 2018. Polyphenols: Properties, Recovery, and Applications. Duxford, United Kingdom: Woodhead Publishing, an imprint of Elsevier.
4. Çelik, Gonca, Gözde Kılıç, Şeyda Kanbolat, Sıla Özlem Şener, Mustafa Karaköse, Nurettin Yaylı, and Şengül Alpay Karaoğlu. 2021. "Biological Activity, and Volatile and Phenolic Compounds from Five Lamiaceae Species." Flavour and Fragrance Journal 36 (2): 223–32.
5. Ouakouak, Hamza, Naima Benchikha, Aicha Hassani, and Mohamed L. Ashour. 2019. "Chemical Composition and Biological Activity of Mentha Citrata Ehrh., Essential Oils Growing in Southern Algeria." Journal of Food Science and Technology 56 (12): 5346–53.
6. Stefanaki, Anastasia, and Tinde van Andel. 2021. "Mediterranean Aromatic Herbs and Their Culinary Use." In Aromatic Herbs in Food, 93–121. Elsevier.
7. Aguilar-Veloz, L.M., Calderón-Santoyo, M., González, Y.V., Ragazzo-Sánchez, J.A., 2020. Application of essential oils and polyphenols as natural antimicrobial agents in postharvest treatments: Advances and challenges. Food Sci. Nutr. 8, 2555-2568.
8. Fatih, Brahmi, Khodir Madani, Mohamed Chibane, and Pierre Duez. 2017. "Chemical Composition and Biological Activities of Mentha Species." In Aromatic and Medicinal Plants - Back to Nature, edited by Hany A. El-Shemy. InTech.
9. Galvin-King, Pamela, Simon A. Haughey, and Christopher T. Elliott. 2021. "Garlic Adulteration Detection Using NIR and FTIR Spectroscopy and Chemometrics." Journal of Food Composition and Analysis 96 (March): 103757.
10. Kaavya, R., R. Pandiselvam, Mahadhir Mohammed, R. Dakshayani, Anjineyulu Kothakota, S. V. Ramesh, Daniel Cozzolino, and C. Ashokkumar. 2020. "Application of Infrared Spectroscopy Techniques for the Assessment of Quality and Safety in Spices: A Review." Applied Spectroscopy Reviews 55 (7): 593–611.

11. Cantarelli, Miguel Á., Carlos A. Moldes, Eduardo J. Marchevsky, Silvana M. Azcarate, and José M. Camiña. 2020. “Low-Cost Analytic Method for the Identification of Cinnamon Adulteration.” Microchemical Journal 159 (December): 105513.
12. Li, Shuailing, Bingcong Xing, Ding Lin, Haojun Yi, and Qingsong Shao. 2020. “Rapid Detection of Saffron (Crocus Sativus L.) Adulterated with Lotus Stamens and Corn Stigmas by near-Infrared Spectroscopy and Chemometrics.” Industrial Crops and Products 152 (September): 112539.
13. Hu, Leqian, Chunling Yin, Shuai Ma, and Zhimin Liu. 2018. “Assessing the Authenticity of Black Pepper Using Diffuse Reflectance Mid-Infrared Fourier Transform Spectroscopy Coupled with Chemometrics.” Computers and Electronics in Agriculture 154 (November): 491–500.
14. Petrakis, Eleftherios A., and Moschos G. Polissiou. 2017. “Assessing Saffron (Crocus Sativus L.) Adulteration with Plant-Derived Adulterants by Diffuse Reflectance Infrared Fourier Transform Spectroscopy Coupled with Chemometrics.” Talanta 162 (January): 558–66.
15. Lohumi, Santosh, Sangdae Lee, Wang-Hee Lee, Moon S. Kim, Changyeun Mo, Hanhong Bae, and Byoung-Kwan Cho. 2014. “Detection of Starch Adulteration in Onion Powder by FT-NIR and FT-IR Spectroscopy.” Journal of Agricultural and Food Chemistry 62 (38): 9246–51.
16. Yang, I-Chang, Chao-Yin Tsai, Kuang-Wen Hsieh, Ci-Wen Yang, Fu Ouyang, Yangming Martin Lo, and Suming Chen. 2013. “Integration of SIMCA and Near-Infrared Spectroscopy for Rapid and Precise Identification of Herbal Medicines.” Journal of Food and Drug Analysis 21 (3): 268–78.
17. Ayşar Güzelsoy, Nurcan, Filiz Çavuş, and Oya Kaçar. 2020. “Discrimination of Thymus, Origanum, Satureja and Thymbra Species from the Family Labiatae by Untargeted Metabolomic Analysis.” Czech Journal of Food Sciences 38 (No. 3): 151–57.
18. Ziaková, Alica, and Eva Brandšteterová. 2003. “Validation of HPLC Determination of Phenolic Acids Present in Some Lamiaceae Family Plants.” Journal of Liquid Chromatography & Related Technologies 26 (3): 443–53.
19. Hossain, Mohammad B., Dilip K. Rai, Nigel P. Brunton, Ana B. Martin-Diana, and Catherine Barry-Ryan. 2010. “Characterization of Phenolic Composition in

Lamiaceae Spices by LC-ESI-MS/MS." Journal of Agricultural and Food Chemistry 58 (19): 10576–81.

20. Taamalli, Amani, David Arráez-Román, Leila Abaza, Ihsan Iswaldi, Alberto Fernández-Gutiérrez, Mokhtar Zarrouk, and Antonio Segura-Carretero. 2015. "LC-MS-Based Metabolite Profiling of Methanolic Extracts from the Medicinal and Aromatic Species Mentha Pulegium and Origanum Majorana: Phenolic Compounds in Mentha Pulegium and Origanum Majorana." Phytochemical Analysis 26 (5): 320–30.
21. Ahn, Jiyoun, Andie R. Alford, and Emily D. Niemeyer. 2020. "Variation in Phenolic Profiles and Antioxidant Properties among Medicinal and Culinary Herbs of the Lamiaceae Family." Journal of Food Measurement and Characterization 14 (3): 1720–32.
22. Park, Yun, Seung-A Baek, Yongsoo Choi, Jae Kim, and Sang Park. 2019. "Metabolic Profiling of Nine Mentha Species and Prediction of Their Antioxidant Properties Using Chemometrics." Molecules 24 (2): 258.
23. Hajdari, Avni, Behxhet Mustafa, Lirie Hyseni, Ani Bajrami, Genista Mustafa, Cassandra L. Quave, and Dashnor Nebija. 2020. "Phytochemical Study of Eight Medicinal Plants of the Lamiaceae Family Traditionally Used as Tea in the Sharri Mountains Region of the Balkans." The Scientific World Journal 2020 (February): 1–9.
24. Chandra, Preeti, Vikas Bajpai, Mukesh Srivastva, K. B. Ramesh Kumar, and Brijesh Kumar. 2014. "Metabolic Profiling of Piper Species by Direct Analysis Using Real Time Mass Spectrometry Combined with Principal Component Analysis." Analytical Methods 6 (12): 4234.
25. Ayşar Güzelsoy, Nurcan, Filiz Çavuş, and Oya Kaçar. 2020. "Discrimination of Thymus, Origanum, Satureja and Thymbra Species from the Family Labiatae by Untargeted Metabolomic Analysis." Czech Journal of Food Sciences 38 (No. 3): 151–57.
26. Kuballa, Thomas, Tobias Stephan Brunner, Tienthong Thongpanchang, Stephan Gerhard Walch, and Dirk Walter Lachenmeier. 2018. "Application of NMR for Authentication of Honey, Beer and Spices." Current Opinion in Food Science 19 (February): 57–62.
27. Senizza, Biancamaria, Gabriele Rocchetti, Silvia Ghisoni, Matteo Busconi, Marcelino De Los Mozos Pascual, José Antonio Fernandez, Luigi Lucini, and Marco Trevisan.

2019. “Identification of Phenolic Markers for Saffron Authenticity and Origin: An Untargeted Metabolomics Approach.” Food Research International 126 (December): 108584.

28. Pacholczyk-Sienicka, Barbara, Grzegorz Ciepielowski, and Łukasz Albrecht. 2021. “The Application of NMR Spectroscopy and Chemometrics in Authentication of Spices.” Molecules 26 (2): 382.
29. Windarsih, Anjar, Abdul Rohman, and Respati Tri Swasono. 2019. “Application of 1H-NMR Based Metabolite Fingerprinting and Chemometrics for Authentication of Curcuma Longa Adulterated with C. Heyneana.” Journal of Applied Research on Medicinal and Aromatic Plants 13 (May): 100203.
30. Giffen, Justine E., Ashton D. Lesiak, A. John Dane, Robert B. Cody, and Rabi A. Musah. 2017. “Rapid Species-Level Identification of Salvias by Chemometric Processing of Ambient Ionisation Mass Spectrometry-Derived Chemical Profiles: Rapid Species-Level Identification of Salvias by DART-HRMS.” Phytochemical Analysis 28 (1): 16–26.
31. Prchalová, J., F. Kovařík, and A. Rajchl. 2017. “Evaluation of the Quality of Herbal Teas by DART/TOF-MS: Evaluation Herbal Teas by DART-TOF.” Journal of Mass Spectrometry 52 (2): 116–26.
32. Rigano, Francesca, Sara Stead, Domenica Mangraviti, Renata Jandova, Davy Petit, Nino Marino, and Luigi Mondello. 2019. “Use of an ‘Intelligent Knife’ (Iknife), Based on the Rapid Evaporative Ionization Mass Spectrometry Technology, for Authenticity Assessment of Pistachio Samples.” Food Analytical Methods 12 (2): 558–68.
33. Wang, Zi-Chao, Yuzhen Yan, Tanzeela Nisar, Lijun Sun, Yang Zeng, Yurong Guo, Huichun Wang, and Zhongxiang Fang. 2019. “Multivariate Statistical Analysis Combined with E-Nose and e-Tongue Assays Simplifies the Tracing of Geographical Origins of Lycium Ruthenicum Murray Grown in China.” Food Control 98 (April): 457–64.
34. Mangraviti, Domenica, Francesca Rigano, Adriana Arigò, Paola Dugo, and Luigi Mondello. 2021. “Differentiation of Italian Extra Virgin Olive Oils by Rapid Evaporative Ionization Mass Spectrometry.” LWT 138 (March): 110715.
35. Demirtas, Ibrahim, Bulent Ayhan, Ayse Sahin, Hüseyin Aksit, Mahfuz Elmastas, and Isa Telci. 2011. “Antioxidant Activity and Chemical Composition of Sideritis Libanotica Labill. Ssp. Linearis (Bentham) Borm. (Lamiaceae).” Natural Product Research 25 (16): 1512–23.

36. Marchioni, Ilaria, Basma Najar, Barbara Ruffoni, Andrea Copetta, Luisa Pistelli, and Laura Pistelli. 2020. “Bioactive Compounds and Aroma Profile of Some Lamiaceae Edible Flowers.” Plants 9 (6): 691.
37. Sivanesan, Iyyakkannu, Ramesh Kumar Saini, Rafi Noorzai, Ahmad Jawid Zamany, and Doo Hwan Kim. 2016. “In Vitro Propagation, Carotenoid, Fatty Acid and Tocopherol Content of Ajuga Multiflora Bunge.” 3 Biotech 6 (1): 91.

General conclusion

In conclusion, several factors may affect the chemical composition of food products and accordingly have a considerable impact on the nutritional, and bioactive properties of food. Some of these factors include geographical origin, climate, and manufacturing practices. To ensure the authenticity and traceability of food products, reliable, and powerful analytical methods are required.

In this regard, chromatographic analytical techniques employed in the investigation of monocultivar Moroccan olive oils "*Picholine marocaine"*, including HPLC-MS and GC–MS have proven their effectiveness and specificity for the characterization of both volatile and non-volatile chemical compounds in olive oils during two consecutive harvest years 2018 and 2019 in 19 Moroccan provinces. Additionally, the combination of chemometrics with the applied methodology could be considered a useful tool for the authentication of the Moroccan olive oil origins and/or detection of possible fraudulent mixtures.

Furthermore, hyphenated liquid chromatography coupled with mass spectrometry has also shown its usefulness in the assessment of the nutraceutical effect of polyphenols from *H. sabdariffa* through the characterization of the bioaccessible compounds in the stomach.

Moreover, the comprehensive chemical characterization of volatile and non-volatile functional compounds in different cultivars of *Brassica juncea* L. was evaluated by means of liquid and gas chromatography techniques coupled with mass spectrometry which enabled interestingly the identification of approximately 215 metabolites.

On the other hand, ambient mass spectrometry, through the iKnife technique has demonstrated a simplified approach which allows a thorough characterization of the chemical composition of *Lamiaceae* plants from Morocco. Consequently, through the constructed profiles and the integrative chemometric tools, iKnife approach resulted to be a high potency approach to verify the authenticity of *Lamiaceae* botanical species based on polyphenols as biomarkers.

Finally, the appropriate choice of the advanced analytical techniques result indispensable for a comprehensive characterization of biological compounds in food products. Alongside the implementation of suitable chemometric demonstrated their effectiveness in the authentication, discrimination, and traceability of food products.

Supplementary material

Table S5.1. Characterization of phenolic compounds in *C. officinalis* extract by HPLC-PDA-MS.

Peak	Compound (Tentative identification)	t_R (min)	UV_{max} (nm)	$[M-H]^-$ *m/z*	$[M+H]^+$ *m/z*
1	3-*O*-caffeoylquinic acid	12.20	324	353	181
2	Caffeic acid glucuronide (isomer)	13.50	313	355	
3	Dicaffeic acid	13.85	325	341 (281)	
4	4-*O*-caffeoylquinic acid	14.34	319	353	
5	Dicaffeic acid (isomer)	14.86	325	341	
6	5-*O*-caffeoylquinic acid	15.06	324	353 (191)	
7	Caffeoylquinic acid (isomer)	15.76	323	353	181
8	Caffeic acid	16.40	292 ; 325	179	
9	Caffeoylquinic acid (isomer)	18.19	326	353	181
10	6,8-*C*-dihexosylapigenin	18.40	271 ; 334	593	595
11	Quercetin 3-*O*-rhamnosyl-rhamnosyl-glucoside	20.76	254 ; 348	755	303
12	4-p-Coumaroylquinic acid	22.05	335	337 (173)	
13	Rutin	22.72	254 ; 353	609	303
14	Feruloylquinic acid	24.19	325	367	
15	Quercetin-O-rhamno-hexoside	25.29	354	609	303
16	Unknown	26.25	330	755	
17	Quercetin-3-*O*-[6”-*O*-(3-hydroxy-3-methyl-glutaroyl)] hexoside	26.50	347	607 (463 ; 301)	
18	Verbascoside	27.27	329	623	
19	Salvianolic acid C derivative	29.23	289 ; 324	715 (671 ; 339, 191)	
20	Isoscutellarein 7-*O*-allosyl-(1→2)-[6″-*O*-acetyl]-glucoside	29.64	338	651 (505 ; 477)	
21	Quercetin-*O*-acetylhexoside	32.56	348	505	303
22	Unknown	32.91	287 ; 329	1073 (649 ; 339 , 191)	
23	Quercetin-3-*O*-[6”-*O*-(3-hydroxy-3-methyl-glutaroyl)] hexoside (isomer)	33.48	344	607	
24	Rosmarinic acid	34.49	329	359	
25	Caffeic acid pentamer	34.87	287 ; 325	895 (681 ; 447 ; 191)	
26	Ferulic acid derivative	35.28	267_{sh} ; 335	489	
27	Salvianolic acid B	37.44	287 ; 329	717 (519 ; 359 ; 191)	
28	Unknown	38.02	268 ; 347	649 (285)	651
29	Caffeic acid hexamer	38.84	286 ; 330	1075 (537 ; 359 ; 191)	
30	Unknown	39.42	285 ; 329_{sh}	665 (411)	
31	Unknown	39.86	286 ; 325_{sh}	553	
32	Caffeic acid hexamer (isomer)	40.17	286 ; 330	1075 (879 ; 537 ; 359)	
33	Unknown	41.04	268 ; 335	633 (285)	

34	Unknown	41.39	285 ; 328_{sh}	896	
35	Unknown	41.85	341	663	
36	Caffeic acid hexamer (isomer)	42.94	284 ; 331_{sh}	1075 (691)	
37	Jaceosidin	44.67	290 ; 334	329	
38	Unknown	45.83	287 ; 344	327	
39	Jaceidin (isomer)	49.69	281 ; 346	359	
40	Unknown	51.87	289 ; 341	737 (309)	
41	Cirsilineol	52.59	278 ; 341	343	
42	Unknown	53.83	317	307	
43	Methyl rosmarinate	55.76	279 ; 344	373	
44	Hydroxydaidzein-8-*C*-glucoside (isomer)	58.42	276 ; 341	431 (311)	

Table S5.2. Characterization of phenolic compounds in *M. officinalis* extract by HPLC-PDA-MS.

Peak	Compound (Tentative identification)	t_R (min)	UV max (nm)	$[M-H]^-$ *m/z*	$[M+H]^+$ *m/z*
1	dimer R(+)-β-(3,4-dihydroxyphenyl) lactic acid	10.25	280	395 ; 197	
2	Caftaric acid	12.54	327	311 ; 179	
3	p-Hydroxybenzoic acid	13.3	279 ; 312	137	
4	Caffeic acid-*O*-hexoside	14.88	280 ; 318	341 ; 179	181
5	3-*O*-caffeoylquinic acid	15.22	323	353	355
6	Unknown	16.05	270	538	540
7	Caffeic acid	16.59	323	179	
8	Unknown	17.32	272	433	
9	Unknown	19.33	327	377 (295 ; 179)	
10	Salvianolic acid H/I	22.38	276 ; 322_{sh}	537	
11	Caftaric acid hexoside	24.00	328	473 (311 ; 179 ; 149)	475
12	Rosmarinic acid-*O*-hexoside	28.72	319	521 (359)	
13	Salvianolic acid B	29.38	280 ; 316	717	754
14	Sagerinic acid	32.63	282	719	
15	Rosmarinic acid	34.45	322	359	
16	Luteolin-3'-*O*-glucuronide	36.05	337	461 (285)	
17	Unknown	37.44	287; 323	683	
18	Lithospermic acid A	37.85	289_{sh} ; 323	537 (493 ; 295)	
19	Salvianolic acid H/I (isomer)	39.83	285_{sh} ; 323	537 (493 ; 359 ; 295)	
20	Salvianolic acid C derivative	40.14	323	829 (414 ; 311 ; 667)	
21	Salvianolic acid B	41.75	277	717 (295 ; 359 ; 519)	
22	Lithospermic acid A (isomer)	42.11	282; 326	537 (493)	
23	Salvianolic acid C derivative	42.45	269; 318	813 ; 535	
24	Salvianolic acid L/I	42.78	278 ; 323_{sh}	717 (359 ; 293 ; 537)	
25	Sagecoumarin	43.07	284 ; 330	535	
26	Salvianolic acid B (isomer)	43.35	287 ; 330	717 (519 ; 293)	
27	Methyl isolithospermate	44.08	285 ; 326	551	
28	Salvianolic acid C derivative	44.86	321	715 (535)	
29	Salvianolic acid	45.49	287 ; 322_{sh}	717 (519 ; 359)	
30	Methyl isolithospermate	46.54	330	551	
31	Salvianolic acid L	46.89	289 ; 317	895	
32	Salvianolic acid C	53.93	317	849 ; 307	

Table S5.3. Characterization of phenolic compounds in *M. pulegium* extract by HPLC-PDA-MS.

Peak	Compound (Tentative identification)	t_R (min)	UV max (nm)	$[M-H]^-$ *m/z*	$[M+H]^+$ *m/z*
1	3-O-Caffeoyl quinic acid	11.83	325	353	355 ; 181
2	Dicaffeic acid	13.35	325	341	181
3	Dicaffeic acid isomer	14.36	325	341	181
4	4-O-Caffeoyl quinic acid	14.58	325	353	355
5	5-O-caffeoylquinic acid	15.35	325	353	355 ; 181
6	Caffeic acid	16.05	324	179	
7	Luteolin-7-O-rutinoside	17.74	271 ; 334	593	595
8	Unknown	17.86	329	377	
9	Quercetin 3-O-rhamnosyl-rhamnosyl-glucoside	19.78	355	755	611 ; 303
10	Rutin	21.72	354	609	611 ; 303
11	Quercetin-O-rhamno-hexoside	24.00	353	609	611 ; 303
12	Quercetin 3-O-glucoside	25.31	349	463	465 ; 303
13	Unknown	25.92	322	511 ; 419	535
14	Quercetin 3-O-(6"-malonyl-glucoside)	28.56	348	549 ; 505	303
15	Luteolin-7-O-glucoside	29.83	331	447 ; 285	449
16	Unknown	31.29	349	561 ; 505	507
17	Diosmin	31.79	339	607	609
18	3,4-Dicaffeoyl quinic acid	33.35	325	515	517
19	Rosmarinic acid	33.59	329	359	
20	Unknown	34.34	287 ; 313	896.0	535 ; 359
21	Medioresinol-O-hexoside	35.16	323	549	
22	Salvianolic acid B	36.96	288 ; 331	717	359
23	Isosalvianolic acid B	38.82	286 ; 330	537	359
24	Salvianolic acid W	40.34	286 ; 330	537	359
25	Unknown	42.50	284 ; 329	895	359
26	Unknown	42.79	285 ; 330	716	359
27	5,7,4’-trihydroxy-6,3’-dimethoxyflavone (Jaceosidin)	44.19	293 ; 334	329	331
28	Unknown	45.23	288 ; 347	327	361
29	Jaceidin	49.36	279 , 349	359	361
30	Unknown	51.48	289 ; 343	728 ; 555	375
31	Unknown	54.49	288 ; 334	343	345
32	Dihydroxy-tetramethoxyflavone	55.54	280 ; 348	373	375
33	Unknown	58.22	276 ; 340	311	359

Table S5.4. Characterization of phenolic compounds in *M. suaveolens* extract by HPLC-PDA-MS.

Peak	Compound (Tentative identification)	t_R (min)	UV max (nm)	$[M-H]^-$ *m/z*	$[M+H]^+$ *m/z*
1	Quinic acid	1.95		191	
2	THDBCHMCA: 1,2,6,7-tetrahydroxy-5H-dibenzo[a,d]cycloheptene-5-methyl-11-carboxylic acid	15.18	313	295	
3	Luteolin-7-O-rutinoside	25.66	348	593	595
4	Luteolin-7-O-glucoside	26.79	346	447	449
5	Luteolin-7-O-glucuronide	27.07	347	461	463
6	Apigenin 7-O-rutinoside	30.47	324	577	579
7	Apigenin 7-O-glucoronide	33.20	267 ; 334	445 ; 269	
8	Salvianolic acid B	33.63	284 ; 336	717	323
9	Rosmarinic acid	34.42	328	359	
10	Luteolin-O-glucuronide	35.80	268 ; 336	461 ; 285	463
11	Salvianolic acid J	37.60	323	537	341
12	Dihydroxy-tetramethoxyflavone	40.02	284 ; 323	373	
13	Salvianolic acid A	41.22	288 ; 322	493	359
14	Salvianolic acid A isomer	42.42	288 ; 320	493	359
15	5,7,4’-trihydroxy-6,3’-dimethoxyflavone (Jaceosidin)	44.52	284 ; 323	329	331
16	Salvianolic acid B/E	45.00	285 ; 319	717 ; 519	

Table S5.5. Characterization of phenolic compounds in *S. incana* extract by HPLC-PDA-MS.

Peak	Compound (Tentative identification)	t_R (min)	UV max (nm)	$[M-H]^-$ *m/z*	$[M+H]^+$ *m/z*
1	5-O-caffeoylquinic acid	15.18	325	353 ; 191	
2	4-O-caffeoylquinic acid	15.91	325	353 ; 191	
3	Hyplaetin 7-O-allosy (1→2) glucoside	25.09	276 ; 341	625 ; 463	
4	Verbascoside	27.19	330	623 ; 461	
5	Isoscutellarein 7-O-allosyl(1→2) glucoside	29.17	277 ; 305 ; 325	609 ; 285	611
6	Hypolaetin 7-O-allosyl-(1→2)-[6″-O-acetyl]-glucoside	32.03	276 ; 298 ; 340	667	669
7	Leucoseptoside A	33.47	330	637	
8	Unknown	35.38	335	649	651
9	Isoscutellarein 7-O-allosyl-(1→2)-[6″-O-acetyl]-glucoside	36.36	277 ; 306 ; 326	651	287
10	3'-O-Methylhypolaetin 7-O-[6'''-O-acetyl]-allosyl (1→2) glucoside	36.75	277 ; 338	681	
11	4'-O-Methylhypolaetin 7-O-[6'''-O-acetyl]-allosyl (1→2) glucoside	37.59	277 ; 338	681	
12	Hypolaetin 7-O-[2''', 6'''-di-O-acetyl]-allosyl (1→2) glucoside	41.22	277 ; 336	709	711

13	4'-O-MethylIsoscutellarein 7-O-[6'''-O-acetyl]-allosyl (1→2) glucoside	43.25	277 ; 325	665	667
14	Isoscutellarein 7-O-[6'''-O-acetyl]-allosyl (1→2) [6'''-O-acetyl] glucoside	43.68	277 ; 307 ; 325	693	695
15	Unknown	44.94	314	313	315

Table S5.6. Characterization of phenolic compounds in *T. zygis* extract by HPLC-PDA-MS.

Peak	Compound (Tentative identification)	t_R (min)	UV max (nm)	$[M-H]^-$ *m/z*	$[M+H]^+$ *m/z*
1	Quinic acid	1.99		191	193
2	Unknown	8.70	301	455	
3	Unknown	8.78	301	455	
4	Danshensu	10.71	281	197	
5	Salvianolic acid A-O-hexoside	13.66	282	359	383
6	Caffeic Acid	17.01	323	179	181
7	Naringenin-O-glucoside	17.42	274	433	611
8	5'-Hydroxyjasmonic acid-O-hexoside	17.85	278	387	
9	Unknown	18.25	325	437	
10	Dihydroxy-tetramethoxyflavone	18.75	283	373	
11	Apigenin-(6,8)-C-diglucoside	18.93	271 ; 335	593 ; 269	595
12	Unknown	19.05	282	377	
13	6.8-Di-C-hexosylapigenin	19.37	324	593 ; 503	
14	Eriodictyol-7-O-glucoside	19.58	282	449 ; 287	
15	Feruloylquinic acid	20.13	286 ; 324	367	317
16	Salvianolic acid F derivative	20.40	286 ; 318	375	359
17	Eriodictyol-7-O-glucoside	20.73	283	449	289
18	Luteolin acetyl pentosyl-hexoside	20.96	268 ; 319	621	623
19	5'-Hydroxyjasmonic acid-O-hexoside isomer	21.83	286	387	
20	Unknown	22.60	282	421	
21	Quercetin-O-hexoside	23.06	282 ; 345	463 ; 301	
22	Luteolin-7-O-glucoside	24.23	339	447 ; 285	
23	Unknown	25.89	288	303	
24	Luteolin-(6,8)-C-diglucoside	26.70	269 ; 344	593	595
25	Unknown	27.40	269 ; 344	415	
26	Luteolin-5-β-O-glucoside	27.78	252 ; 347	447	449
27	Luteolin-7-O-glucuronide	28.13	252 ; 347	461	463
28	Unknown	29.90	283	471	495
29	Chrysoeriol-7-β-O-glucoside	32.58	338	461	301
30	Apigenin-7-β-O-glucuronide	34.15	267 ; 335	445	
31	Rosmarinic acid	35.27	329	359 ; 197	181
32	Salvianolic acid k	36.34	286 ; 324	555 ; 359	181
33	Luteolin-7-O-glucuronide isomer	36.44	269 ; 335	461 ; 285	

34	3'-O-(8"-z-caffeoyl)-rosmarinic acid	38.16	289 ; 324	537 ; 493 ; 357	
35	Unknown	39.37	286 ; 330	505	
36	Eriodictyol	40.01	286	287	289
37	Luteolin	41.38	346	285	287
38	Salvianolic acid B	42.13	287 ; 330	717 ; 519	521
39	Trihydroxy-dimethoxyflavone	43.26	283 ; 336	329	331
40	Naringenin	45.09	288	271	273
41	Apigenin	45.64	330	269	271
42	Hydroxy-trimethoxyflavone	45.85	325	327	
43	Hispidulin	46.86	329	299	301
44	Cirsimaritin	51.73	275 ; 334	313	
45	Unknown	52.66	275 ; 345	343	345
46	Unknown	54.78	330	343	345
47	Unknown	55.78	282 ; 344	373	375
48	Unknown	58.01	275	519	

La borsa di dottorato è stata cofinanziata con risorse del
Programma Operativo Nazionale Ricerca e Innovazione 2014-2020 (CCI 2014IT16M2OP005),
Fondo Sociale Europeo, Azione I.1 “Dottorati Innovativi con caratterizzazione Industriale”

UNIONE EUROPEA
Fondo Sociale Europeo